NTNU – Trondheim
Norwegian University of
Science and Technology

Dynamic Analysis of a Subsea Module During Splash-zone Transit

Min Wu

Marine Technology
Submission date: June 2013
Supervisor: Bernt Johan Leira, IMT

Norwegian University of Science and Technology
Department of Marine Technology

Dynamic Analysis of a Subsea Module During Splash-zone Transit

Dynamisk Analyse av Undervannsmodul ved gjennomgang av Bølgesonen

Design of subsea structural components should be based on a thorough analysis to ensure that these structures are able to withstand the relevant forces during installation, levelling and lowering, also including a safety margin. During installation, the lifted structure is exposed to dynamic loading due to both motion of the installation vessel and the direct action of waves. During lowering through the splash zone, significant loads are generally acting on the subsea module. These are typically of a transient nature and possibly have a significant magnitude.

The scope of the present thesis work is to review relevant design rules and guidelines for such operations. Furthermore, dynamic response analyses and associated parametric studies are to be performed for a particular subsea module during transition through the splash zone.

The following subjects are to be addressed as part of this work:

1. Give a general description of the main phases that are relevant during installation of subsea modules. Identify the particular challenges which are related to each of these phases. (Perform a review of technical literature related to this type of marine operations.)
2. Relevant design rule for the lifting operation are to be summarized.
3. Give a general description of the subsea module to be installed, the installation vessel, environmental characteristics and some background in relation to the specific field development.
4. Particularities associated with the complete installation procedure with respect to critical phases and importand design parameters are to be elaborated upon. A numerical model of the structure based on beam elements is to be established.
5. A dynamic response analysis is to be performed by application of the beam model and loading based on the relevant formulations in the rules. Parametric variations are performed to the extent that time allows. If it is found to be relevant, a more refined structural model comprising both beam and shell elements is to be applied.

The work scope may prove to be larger than initially anticipated. Subject to approval from the supervisor, topics may be deleted from the list above or reduced in extent.

In the thesis the candidate shall present his personal contribution to the resolution of problems within the scope of the thesis work.

Theories and conclusions should be based on mathematical derivations and/or logic reasoning identifying the various steps in the deduction.

The candidate should utilise the existing possibilities for obtaining relevant literature.

The thesis should be organised in a rational manner to give a clear exposition of results, assessments, and conclusions. The text should be brief and to the point, with a clear language. Telegraphic language should be avoided.

The thesis shall contain the following elements: A text defining the scope, preface, list of contents, summary, main body of thesis, conclusions with recommendations for further work, list of symbols and acronyms, references and (optional) appendices. All figures, tables and equations shall be numbered.

The supervisor may require that the candidate, in an early stage of the work, presents a written plan for the completion of the work. The plan should include a budget for the use of computer and laboratory resources which will be charged to the department. Overruns shall be reported to the supervisor.

The original contribution of the candidate and material taken from other sources shall be clearly defined. Work from other sources shall be properly referenced using an acknowledged referencing system.

The thesis shall be submitted as an electronic version:

- Signed by the candidate
- The text defining the scope included
- Drawings and/or computer prints which cannot be bound should be organised in a separate folder.

Supervisor: Professor Bernt J. Leira

Deadline: June 8th 2013

Trondheim, January 14th, 2013

Bernt J. Leira

Preface

The basis for this master thesis lies with the understanding and well command of the SIMA program. Besides, this thesis is a new start for the analysis of the template lifting operation. Thus, there are many problems and difficulties exist and there remain a lot unsolved problems that are highly recommended for the further research. This master thesis has been carried out at the Department of Marine Technology, Faculty of Engineering Science and Technology at the Norwegian University of Science and Technology.

The guidance from Professor Bernt J. Leira is gratefully acknowledged.

Trondheim, June 5, 2013

Min Wu

Min Wu

Abstract

This thesis carries out a research on the dynamic performance of the template during the lowing operation through splash-zone. During the lifting operation, especially under harsh environment, the waves, winds as well as the currents will leave significant influences on the template. Hence, to study how the template performed under such environmental conditions is the main purpose of this thesis.

A brief introduction to the marine operation industry as well as the lifting operation is presented first. During the installation, template is exposed to the magnificent dynamic loads from the environment. So during the lifting process, the forces acting on the template as well as the displacement of the template should be inspected and controlled.

Thus, the wave description and an introduction to the different dynamic loads due to the wave movement are performed. In addition, the methodology and the theory background of SIMA program is also included in this thesis.

After building up the model of the lifting system in SIMA, the static and dynamic analysis of the lifting operation is performed. The results of the static and dynamic analysis are all listed in the thesis as figures or tables. The finding of the studies shows that the template experiences a significant drift in the wave induced direction for all sea-states. Besides, the dynamic load of the lifting lines can be more than twice than the static load. This will lead to a huge challenge to the capacity of the lifting wires. Additionally, the vertical motion of the template is sufficient large during the lifting operation and may lead to potential risk.

Overall, the environmental conditions have magnificent influences on the lifting structures. In particular, lifting operations must not take place once the significant wave height exceeds an up-limitation. On the meantime, the lifting action needs to be paused if the wave peak period is approaching a critical value.

Content

List of Figures

List of Tables

1 Introduction

Design of subsea structural components should be based on a thorough analysis to ensure that these structures are able to withstand the relevant forces during installation, levelling and lowering, also including a safety margin. This applied for the particular situations in which the lifted structure will be exposed to both static and dynamic load from the environment, including wave, wind and current. During lowering through slash zone, the dynamic loads will be sufficient large to leave a significant influence on the structure.
During the lifting operation, the vessel or the jack-up rig is required to be kept within a certain position. The wire forces during the lifting are of the most concern. On the meantime, the position, the velocity as well as the acceleration of both the structure and hook are also important for the safety and efficiency of the operation.

This thesis presents a further research on the dynamic and static response of the template under harsh environment (slash-zone) during lifting operation. This thesis work is organized as follows: ***Part 1***(Chapter 2) gives a brief introduction to the marine operation and installation industry. ***Part 2***(Chapter 3 and Chapter 4) mainly discusses the basic theories and rules applied in the lifting operation. Besides, the guidelines used in the SIMA program is also includes in this part. ***Part 3***(Chapter 5) performs the method for modeling different components in the SIMA program, while ***part 4***(Chapter 6 and Chapter 8) carries out the static and dynamic analysis of the lifting system. The final conclusions as well as the prospect for future work are drawn in ***part 5***(Chapter 8).

2 Marine Operation

In the oil and gas industry, there are various kinds of work related to operation, maintenance, and modifications of offshore and onshore facilities. The consequences of insufficient maintenance and safety can be catastrophic, both in terms of loss of human lives, environmental impact, and damage to assets. Therefore, Marine operation and maintenance engineering covers important activities needed to ensure a well-functioning, safe and environmental friendly system.

During the last few decades, with the dramatic development of the oil and gas industry, the requirements for the marine operation and installation industry is getting higher and higher.

As the oil and gas industry is moving into deeper water, subsea solutions are becoming more common. Important equipment placed on the seabed makes great demands on the operation, in terms of maintenance of the equipment and ensuring control over the technical condition.

Thus, a brief introduction to the marine operation industry, mainly about the lifting operation is performed in this chapter.

2.1 Introduction to Marine Operation

Marine operation is a summary of all the onshore and offshore activities performed by vessels, platforms and onshore or other floating structures, for the purpose of transferring objects or energy between structures. Marine operations in this thesis are characterized by: [1]

- The operation has a short duration.
- The operation may be interrupted.
- The system considered is not in stationary condition.

Examples of the most typical marine operations are listed as below:

- Towing: The transfer at sea from one location to another of a self-floating structure or a structure resting on a barge by pushing/pulling by tugs.
- Positioning: The activities necessary to position a structure at s certain predetermined location.
- Upending: The activities necessary to upend a floating structure
- Lifting: The activities necessary to lift or assist a structure by crane
- Lift off: The activities necessary for transfer (a deck) structure positioned on construction pillars onto the transportation barges.
- Transit and positioning of semisubmersibles: The activities necessary to move a semisubmersible rig from one location to another and mooring on new location.
- Transit and positioning of jack-up rigs: The activities necessary to move a jac-up rig from one location to another and jacking up on the new location.

Apart from the operations mentioned above, there are also a lot of other activities

included in the marine operation category.

The figures below show some cases of the marine operation discussed above.

Figure 2.1 Example of the towing operation

Figure 2.2 Vessel under dynamic positioning system

Figure 2.3 Lifting off operation Figure 2.4 Transit and positioning of jack-up rigs

Traditionally, marine operations have relied mostly on practical marine experience. This is still a very important aspect in planning and execution of marine operations.

However, as new kinds of operations are to be performed, there will be a strong need to the response (forces, motions) and safety level. The realization of these purposes will strongly depend on the improving in physical insights and the computational methods.

Generally, marine operations represent the intermediate phases for a structure. As a marine operation takes place over a limited period of time, or may be interrupted during unsuitable weather or sea states (E.g. drilling & lifting), one may take the duration into consideration in the design process and safety considerations.

2.2 Lifting operation

Lifting Operation is usually phrased as crane operation as well, thus in the section some aspects related to the offshore crane operation are addressed. Offshore crane operations have become more and more important due to the increased water depth as well as the demand for lower field development costs. [1]

Examples of common lifting operations are:

i) Crane assisted installation of jacket structure.
ii) Installation of deck modules
iii) Installation of subsea equipment e.g. template, manifolds, spool pieces protection structures, anchors etc.
iv) Intervention in subsea wells, maintenance of subsea equipment.

Figure 2.5 Example on installation a subsea module

The lifting operations are usually divided into two main categories:

Light lifts: The light lifts are defined if the load of the structure is very small compared to the vessel. It may be assumed that the motion characteristics of the vessel (at the top of the crane) is unaffected by the presence of the load. The order of magnitude of the load will be less than 1-2% of the vessel displacement and less than a few hundred tons. For such loads heave compensation is possible.

Heavy lifts: For such lifts the coupled dynamic of the vessel-load system must be considered as there will be mutual interaction. The structural interaction is due to e.g. mooring lines between crane vessel and barge, and hoisting wire and tugger lines

between load and crane vessels. Order of magnitude of the load is more than 1-2% of the vessel displacement and typically more than 1000 tons. Heave compensation is normally impossible in such situations.

If the load is to be lifted through the splash zone, considerations must be made to ensure that the wave induced forces and the corresponding dynamic response are within acceptable limits.

2.2.1 Template lifting

A subsea template is a large steel structure which is used as a base for various subsea structures such as wells and subsea trees and manifolds.

The size of a template mainly depends on the number of structures attached to it. Many will have protective structures covering them, as does the template pictured right. This helps prevent damage from fishing activities and also improves fishing safety by reducing the likelihood of nets becoming snagged on the equipment.

The template was designed to meet the following requirements: [2]

1) To accommodate four subsea wellheads
2) To allow possible subsea completions
3) To accommodate conventional platform well spacing and geometry
4) To allow either platform jacket stab-over or docking pile alignment
5) To allow for diverless template installation by a semi submersible rig
6) To restrict total costs for template design, fabrication, and installation to $500,000.

The image below shows the template that is used in this thesis:

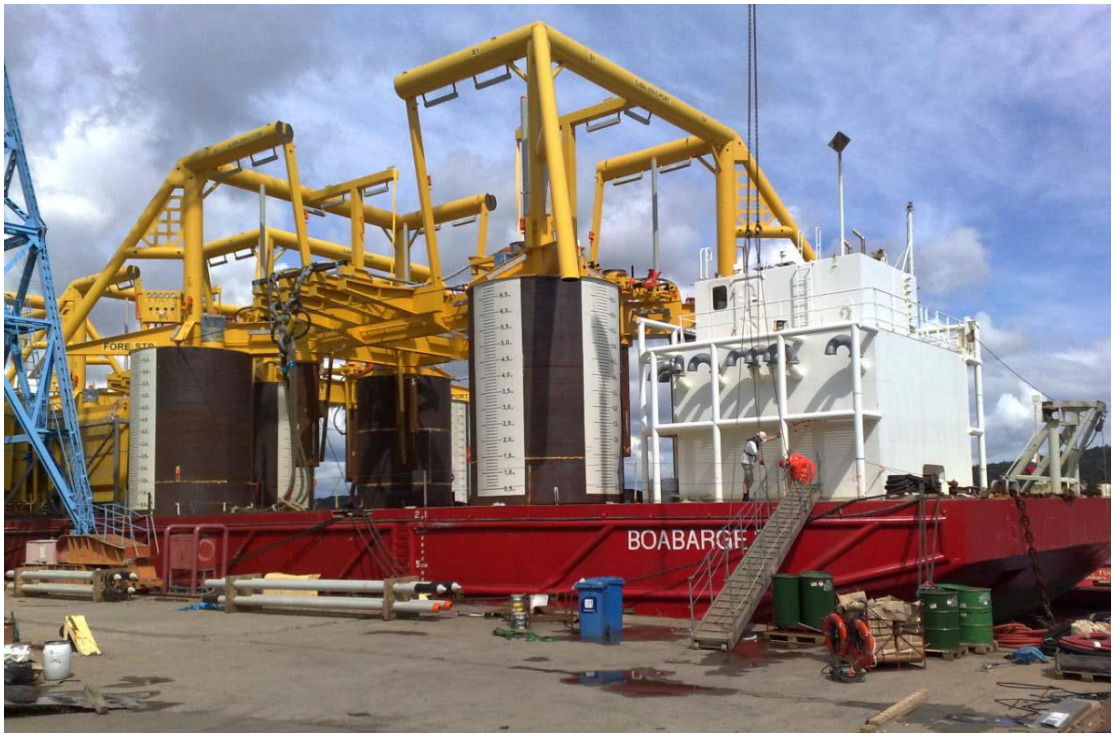

Figure 2.6 The 4 off Integrated Template Structure used in this thesis

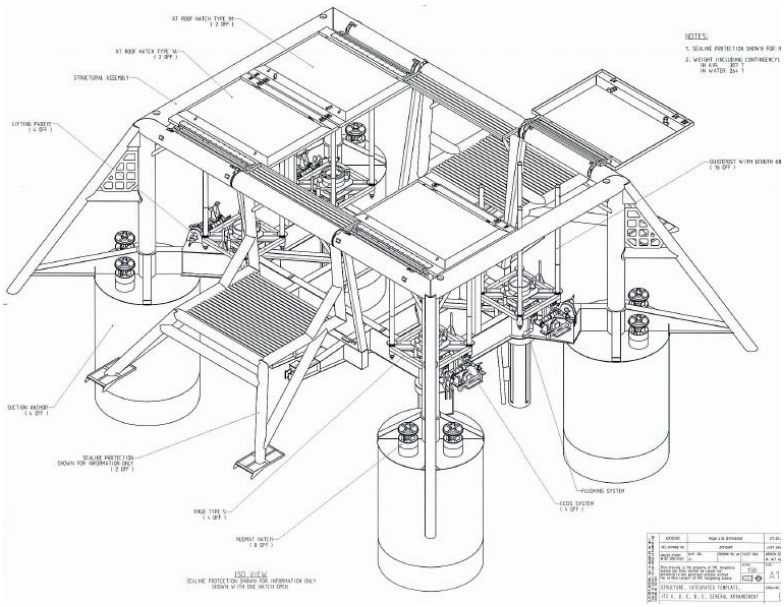

Figure 2.7 Sketch of the template used in this thesis

Subsea templates are traditionally transported to the relevant location either on the deck of a crane vessel or a barge, depending on their size and shape. In both cases the template has to be lifted off from deck and lowered through the splash zone. The lift-off operation is a very critical marine operation that may lead to a large magnitude dynamic load and potential risk for the collision between the lifting structure and the vessels. During immersion, significant wave impact forces (slamming) may also occur. Hence, to study the dynamic response of the template under such harsh environment and to find out possible proper methods to avoid the hazards and to reduce the potential risk is the main purpose of this thesis. [3]

3 Rules and guidelines of Marine Operation

The safety and risk control of marine operations have been increasingly important since the operations is moving to increased water depth and the scale of the operation objects tends to growing larger. Thus, in order to perform the marine operations safely and efficiently, there will be various kinds of rules and guidelines need to be obeyed and followed.
Thus, this chapter mainly presents the relative rules and guidelines that are highly involved in the lifting operations.

3.1 Description of waves

All of the offshore activities are highly influenced by the wave performances. Thus, to study the wave characteristics is the first priority to do analysis on the marine operations.
Basically, waves can be divided into two aspects: regular waves and irregular waves. Ocean waves are irregular and random in shape, height, length and speed of propagation. A real sea state is best described by a random wave model.
Usually, wave states for analysis are classified into different categories. Like for instance, the wave conditions in a sea state can be divided into two classes: *wind seas* and *swell*. Wind seas are generated by local wind, while swell have no relationship to the local wind. Swells are waves that have travelled out of the areas where they were generated. Moderate and low sea states in open sea areas are often composed of both wind sea and swell. [4]

3.1.1 Regular wave

A regular travelling wave is propagating with permanent form. It has a distinct wave length, wave period, wave height.
A regular wave is described by the following main characteristics;
— *Wave length*: The wave length λ is the distance between successive crests.
— *Wave period:* The wave period T is the time interval between successive crests passing a particular point.
— *Phase velocity:* The propagation velocity of the wave form is called phase velocity, wave speed or wave celerity and is denoted by $c = \lambda / T = \omega / k$
— *Wave frequency* is the inverse of wave period: $f = 1/T$
— *Wave angular frequency:* $\omega = 2\pi / T$
— *Wave number*: $k = 2\pi / \lambda$
— *Surface elevation*: The surface elevation $z = \eta(x,y,t)$ is the distance between the still water level and the wave surface.
— *Wave crest height* A_C is the distance from the still water level to the crest.

— *Wave trough depth* A_H is the distance from the still water level to the trough.
— *Wave height*: The wave height H is the vertical distance from trough to crest. $H = A_C + A_T$.
All of these characteristics are illustrated in the following image:

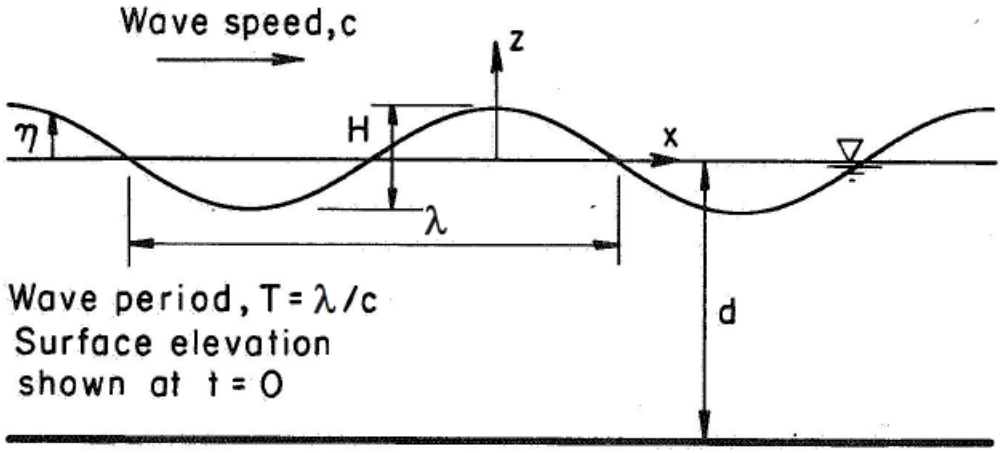

Figure 3.1 Example of the regular wave properties

3.1.2 Irregular waves

In reality, the waves in real sea-states are always the irregular waves. Mostly, the irregular waves can be modeled as a summation of sinusoidal wave components.
The simplest random wave model is the linear long crested wave model given by;

$$\eta_1(t) = \sum_{k=1}^{N} A_k \cos(\omega_k t + \varepsilon_k) \tag{3.1}$$

Where ε_k is a random phase between 0 and 2π. As for the amplitude for each component, they are taken to be Rayleigh distributed with mean square value of:

$$\mathrm{E}\left({A_k}^2\right) = 2S(\omega_k)\Delta\omega_k \equiv {\sigma_k}^2 \tag{3.2}$$

In which,

$S(\omega_k)$ is the wave spectrum

$$\Delta\omega_k = {(\omega_{k+1} - \omega_{k-1})}/{2}$$

Use of deterministic amplitudes $A_k = \sigma_k$ can give non-conservative estimates.
The lowest frequency interval $\Delta\omega$ is governed by the total duration of the simulation t, $\Delta\omega = {2\pi}/{t}$. The number of frequencies to simulate a typical short term sea state is governed by the length of the simulation, but should be at least 1000 in order to capture the properties of extreme waves.

3.1.3 Wave spectrum

In reality, it is very difficult to define the exact sea state, so a wave spectrum should be adopted to describe the sea state. Currently, three main wave spectrums are widely used in the dynamic analysis. One is Pierson-Moskowitz(PM) spectrum, one is the ITTC spectrum and the other one is the JONSWAP spectrum.
This section will perform the construction of each spectrum and discuss the relationship between the three spectrums. [5]

Pierson-Moskowitz(PM) spectrum

This spectrum is based on data from the North Atlantic, and the basic formula for this spectrum is described as:

$$S(\omega) = \frac{A}{\omega^5} \exp\left[-\frac{B}{\omega^4}\right] \tag{3.3}$$

All the spectra matched to this equation will experience one peak and have a steep front at low frequencies.
As for the PM spectrum, the A and B in Eq.(3.3) are given by:

$$A = 0.0081g^2$$
$$B = 0.74\left(\frac{g}{V}\right)^4 \tag{3.4}$$

In which V is the wind speed at 19.5m altitude.
This is a one-parameter spectrum with the wind speed V as a parameter. The acceleration of gravity g is given in $\left[\frac{m}{s^2}\right]$ and the angular frequency ω has dimension of $\left[\frac{rad}{s}\right]$.

This spectrum is based on the presumption that it will approach the curve ω^{-5} for $\omega \to \infty$, such that for increasing wind speed V, the numerical value of the maximum will increase and move to the left.

ITTC spectrum

The ITTC spectrum is equal to the ISSC (International Ship Structure Congress) spectrum for fully developed sea states on open sea. [5]

ITTC spectrum is used to simulate the 1st order wave force, given by Eq. (3.3).

The significant wave height H_s=average of the 1/3 highest waves is introduced and then mean frequency ω_1 is added as parameters instead of the wind speed V in the PM spectrum. Then the following relationships are achieved:

$$A = 0.11{H_s}^2{\omega_1}^4$$
$$B = 0.44{\omega_1}^4 \tag{3.5}$$

The mean frequency ω_1 corresponds to the centre of gravity of the spectrum. This gives the following relations between H_s, ω_1 and V:

$$H_s = 0.21\frac{V^2}{g}$$

$$\omega_1 = 1.14\frac{g}{V} \tag{3.6}$$

Increasing wind speed V implies increasing H_s and decreasing ω_1, i.e. increasing mean period $T_1 = 2\pi/\omega_1$. This is in accordance with what is expect. The ISSC spectrum is a two-parameter spectrum with H_s and ω_1 as parameters.

The following figure gives a example for the ITTC spectrum with the peak frequency of $\omega \approx 0.65$ rad/s.

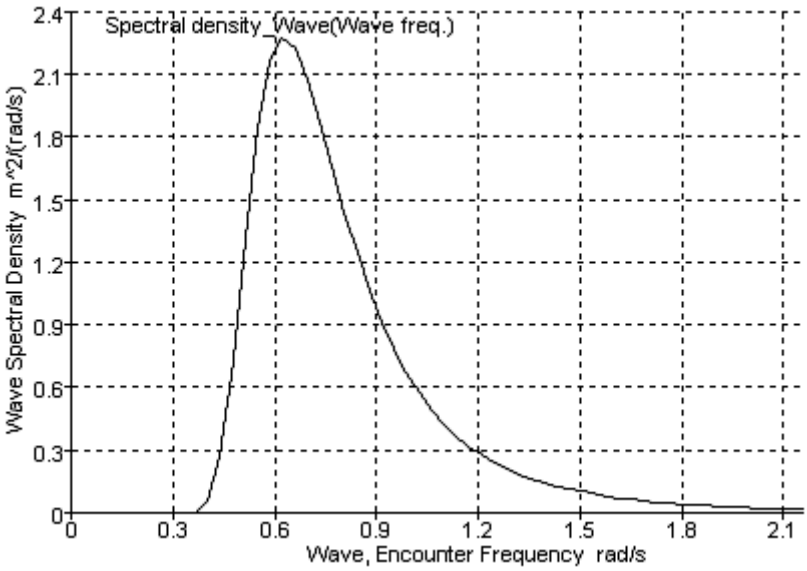

Figure 3.2 Example of ITTC spectrum

The JONSWAP spectrum ("Joint North Sea Wave Project")

This spectrum is a result of a multinational measuring project in the south-east part of the North Sea in 1968-1969. At the location where the measurements took place one found that the spectrum had a rather sharp peak. [5]

The construction of the JONSWAP spectrum is as follows:

1. One starts by taking the PM spectrum and the introducing the peak frequency ω_p, instead of the wind speed V, the parameters are given as;

$$A = \alpha g^2$$

$$B = \frac{5}{4}\omega_p{}^4 \tag{3.7}$$

Which gives the following relation between ω_p and the wind speed:

$$\omega_p = 0.87\frac{g}{V} \tag{3.8}$$

By inserting Eq.(3.7) into Eq.(3.3) the JONSWAP spectrum is obtained:

$$S(\omega) = \alpha \frac{g^2}{\omega^4} \exp\left[-\frac{5}{4}\left(\frac{\omega_p}{\omega}\right)^4\right] \tag{3.9}$$

2. The spectrum is created by multiplying by the factor

$$\gamma^{exp\left[-\frac{1}{2}\left(\frac{\omega-\omega_p}{\sigma\omega_p}\right)^2\right]}$$

γ= peakedness parameter

$$\sigma = \begin{cases} \sigma_a & for \ \ \omega \leq \omega_p \\ \sigma_b & for \ \ \omega > \omega_p \end{cases}$$

α= parameter which determines the spectrum shape in the high frequency range

The peakedness parameter is proportional to the ratio between maximum energy in the JONSWAP spectrum and the maximum energy in the PM energy, which is to say that:

$$\gamma = \frac{S_{JONSWAP,max}}{S_{PM,max}} \cdot constant \tag{3.10}$$

γ is a value between 1 and 7. The following figure shows the influence from the value γ on the shape of the JONSWAP spectrum.

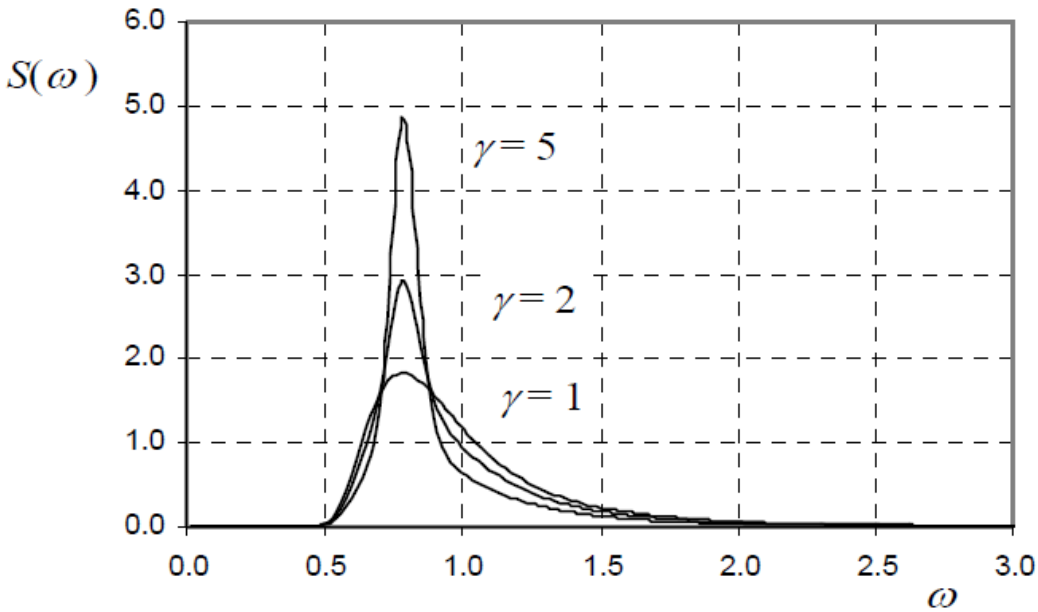

Figure 3.3 Example of the JONSWAP spectrum for Hs = 4.0 m, Tp = 8.0s

1.2 Wave loads and loads effect

An object lowered into or lifted out of water will be exposed to a number of different forces acting on the structure.

In general the following forces should be taken into account when assessing the response of the object;

F_{line} = force in hoisting line/cable

W_0 = weight of object (in air)

F_B = buoyancy force
F_c = steady force due to current
F_I = inertia force
F_{wd} = wave damping force
F_d = drag force
F_w = wave excitation force
F_s = slamming force
F_e = water exit force

The following sections will present a detailed introduction to those force components that is most relative to the lifting operations.

3.2.1 Slamming force

The slamming force on an object lowered through the free surface with a *constant* slamming velocity v_s (assumed positive) in *still water* can be expressed as the rate of change of fluid momentum: [6]

$$F_s(t) = \frac{d(A_{33}^{\infty} v_s)}{dt} = v_s \frac{dA_{33}^{\infty}(t)}{dt} \quad [N] \tag{3.11}$$

Where A_{33}^{∞} is the instantaneous high-frequency limit heave added mass.
Using the high-frequency limit of the added mass is based on the assumption that the local fluid accelerations due to water entry of the object are much larger than the acceleration of gravity g. This corresponds to the high frequency limit for a body oscillating with a free surface.
The slamming force can also be written in the term of the slamming coefficient, which is given as:

$$F_s(t) = \frac{1}{2}\rho C_s A_p v_s^2 \quad [N] \tag{3.12}$$

Where C_s is the slamming coefficient and is defined as:

$$C_s = \frac{2}{\rho A_p v_s} \cdot \frac{dA_{33}^{\infty}}{dt} = \frac{2}{\rho A_p} \cdot \frac{dA_{33}^{\infty}}{dh} \tag{3.13}$$

In which,

$\frac{dA_{33}^{\infty}}{dh}$ is the rate of change of added mass with submergence.

ρ is the mass density of water [kg/m3]
A_p is the horizontal projected area of object [m2]
h is the submergence relative to surface elevation [m]

For water entry in waves the relative velocity between lowered object and sea surface must be applied, so that the slamming force can be taken as

$$F_s(t) = \frac{1}{2}\rho C_s A_p (\dot{\zeta} - \dot{\eta}) \tag{3.14}$$

In which,
$\dot{\zeta}$ is the vertical velocity of sea surface [m/s]
$\dot{\eta}$ is the vertical motion of the object [m/s]

3.2.2 Hydrodynamic loads on slender elements

The hydrodynamic force exerted on a slender object can be estimated by summing up sectional forces acting on each strip of the structure. For slender structural members having cross-sectional dimensions considerably smaller than the wave length, wave loads may be calculated using Morison's load formula being a sum of an inertia force proportional to acceleration and a drag force proportional to the square of the velocity. Normally, Morison's load formula is applicable when the wave length is more than 5 times the characteristic cross-sectional dimension. [4]
The following sketch shows how the wave load acting on a slender element.

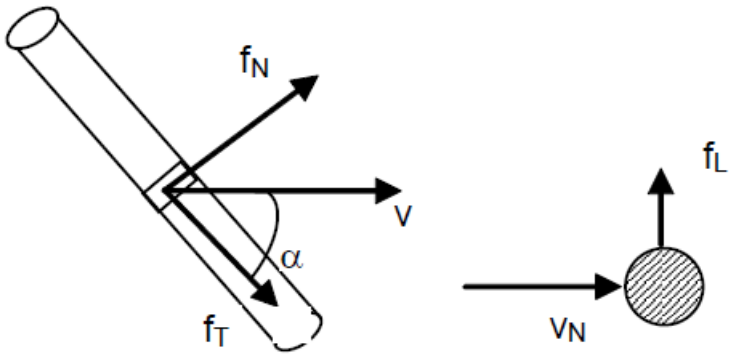

Figure 3.4 Hydrodynamic forces on a slender element

The sectional normal force on a slender structure is written as:

$$f_N = -\rho C_A A \ddot{X}_N + \rho(1 + C_A)\dot{v}_N + \frac{1}{2}\rho C_D D v_{rN}|v_{rN}| \qquad (3.15)$$

Where
ρ = mass density of water [kg/m3]
A = cross-sectional area [m2]
C_A = added mass coefficient [-]
C_D = drag coefficient in oscillatory flow [-]
D = diameter or characteristic cross-sectional dimension [m]
$\ddot{X}_N$ = acceleration of element normal to element [m/s2]
v_{rN} = relative velocity normal to element [m/s]
$\dot{v}_N$ = water particle acceleration in normal dir. [m/s2]

Added mass of slender elements
The sectional (2D) added mass for a slender element is $a_{ij} = \rho C_A A_R$, i,j = 1,2 where A_R is a reference area, usually taken as the cross-sectional area. The added mass coefficient is listed in the table in APPENDIX B.
Drag Force of slender elements
For bare cylinders the tangential drag force f_t is mainly due to skin friction and is small compared to the normal drag force. However for long slender elements with a predominantly tangential velocity component, the tangential drag force may be important. More information will be listed in APPENDIX C.

Lifting Force of slender elements

The lift force f_L, in the normal direction to the direction of the relative velocity vector may be due to unsymmetrical cross-section, wake effects, close proximity to a large structure (wall effects) and vortex shedding.

Slamming force on slender element

The sectional slamming force on a horizontal cylinder can be written in terms of a slamming coefficient C_s as:

$$f_s(t) = \frac{1}{2}\rho C_s D v_s^2 \quad [N \cdot m] \tag{3.16}$$

And the slamming coefficient is defined as:

$$C_s = \frac{2}{\rho D} \cdot \frac{da_{33}^{\infty}}{dh} \tag{3.17}$$

Where

ρ is the mass density of water [kg/m^3]

D is the diameter of cylinder [m]

h is the submergence relative to surface elevation [m]

da_{33}^{∞}/dh is the rate of change of sectional added mass with submergence [kg/m2]

3.2.3 Linear and nonlinear Drag force

Drag forces from waves are important for the design of many types of marine structures. Hence, it is needed to know how to include such forces in dynamic analysis in a correct way. [7]

Drag forces are normally calculated by use of Morison's equation if the vibration amplitudes of the pile are small relative to wave induced water particle motions. Thus, under this assumption the drag force acting on a cylinder element can be written as:

$$F_{d1} = \frac{1}{2}\rho C_D D \Delta l u(t)|u(t)| \tag{3.18}$$

If the pile response becomes significant, then the relative velocity between pile and water must be considered:

$$F_{d2} = \frac{1}{2}\rho C_D D \Delta l [u(t) - \dot{r}]|u(t) - \dot{r}(t)| \tag{3.19}$$

In which,

ρ is the density of the water

C_D is the non-dimensional drag coefficient

D is the diameter of the cylinder pipe

$u(t)$ is the wave induced velocity

$\dot{r}$ is the velocity of the pipe motion

If the wave induced motions are harmonic, the follow relation is obtained:

$$u(t) = u_0 \sin \omega t \tag{3.20}$$

By inserting Eq. (3.20) into Eq. (3.18) and (3.19), the drag force can be rewritten as:

$$F_{d1} = C_D^* u_0^2 \sin \omega t \, |\sin \omega t| \tag{3.21}$$

$$F_{d2} = C_D^* (u_0 \sin \omega t - \dot{r}) |u_0 \sin \omega t - \dot{r}| \tag{3.22}$$

Where:

$$C_D^* = \frac{1}{2} \rho C_D D \Delta l \tag{3.23}$$

Consider a rigid pipe, which is shown in figure 3.5, so the pipe velocity can be neglected, this is to say:

$$\begin{aligned} \mathrm{F(t)} &= \frac{1}{2} \rho C_D D \Delta l u_0^2 \sin \omega t \, |\sin \omega t| \\ &= F_0 \sin^2 \omega t \cdot sign(\sin \omega t) \end{aligned} \tag{3.24}$$

In which $F_0 = C_D^* \cdot u_0^2 = \frac{1}{2} \rho C_D D \Delta l u_0^2$.

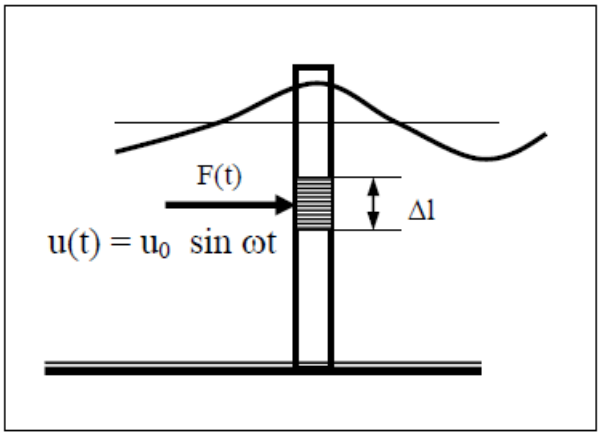

Figure 3.5 A rigid pipe with drag load

Express the drag force as Fourier series and the following result will be given:

$$\mathrm{F(t)} = \sum_{i=1}^{N} b_n \sin n\omega t \tag{3.25}$$

The Fourier coefficient b_n can be found as:

$$b_n = \frac{2}{T} \int_0^{\frac{T}{2}} F(t) \cdot \sin n\omega t \, dt = \frac{2F_0}{T} \int_0^{\frac{T}{2}} \sin^2 \omega t \cdot \sin n\omega t \, dt \;:\; \omega = \frac{2\pi}{T} \tag{3.26}$$

The integral can be found in standard mathematical handbooks:

$$\frac{2}{T} \int_0^{\frac{T}{2}} \sin^2 \omega t \cdot \sin n\omega t \, dt = \begin{cases} \frac{8}{3\pi} \; for \; n = 1 \\ 0 \; for \; even \; value \; of \; n \\ -\frac{8}{15\pi} \; for \; n = 3 \\ -\frac{8}{105\pi} \; for \; n = 5 \end{cases} \tag{3.27}$$

The force time function can now be written:

$$\mathrm{F(t)} = F_0 [\frac{8}{3\pi} \sin \omega t - \frac{8}{15\pi} \sin 3\omega t - \frac{8}{105\pi} \sin 5\omega t + \cdots] \tag{3.28}$$

This equation shows that the drag force will have higher order frequency components than the wave frequency. It can be shown in a similar way that in the case of current in combination with wave there will be even frequency components (2, 4, 6 etc) as

well.

The following figure illustrates the true drag load time history and the first Fourier component. It is easy to realize from this figure that there must be a significant load component at the third order frequency by inspecting the difference between the total load and the first component.

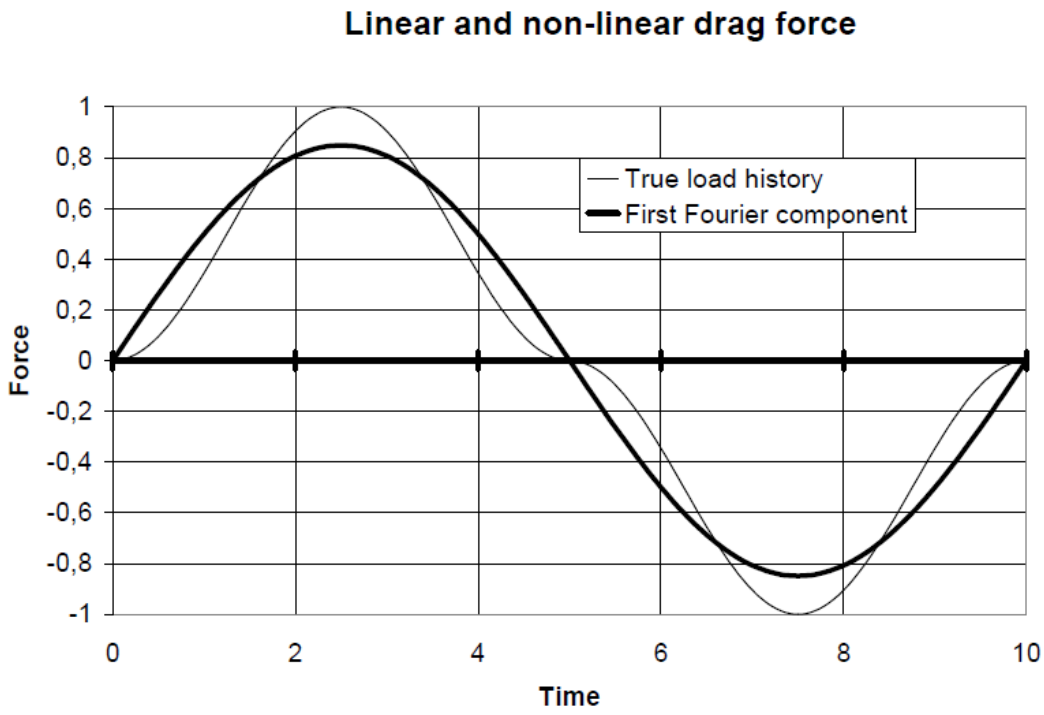

Figure 3.6 Comparison between the true drag force and first Fourier component

These coefficients and parameters in the nonlinear drag force terms are obtained under the regular wave conditions. While in real situation, all the structures are exposed to irregular waves, which means that these coefficients will be different from those in Eq. (3.28).

3.2.4 Dynamic Amplitude Factor (DAF)

The Dynamic Amplitude Factor states the ration between the dynamic and static response for the relevant load. The value of DAF can be both larger or less than 1.0, depending on the frequency ratio β. [8]

The Dynamic Amplitude Factor is then defined as:

$$\mathrm{DAF} = \frac{u_{dynamic}}{u_{static}} \tag{3.29}$$

In which $u_{dynamic}$ is the dynamic response and u_{static} is the static response.

However, the DAF can also be presented as a function of the damping ratio ξ and the frequency ratio β. This can be written as:

$$\mathrm{DAF} = \frac{1}{[(1-\beta^2)^2+(2\xi\beta)^2]^2} \tag{3.30}$$

The following figures give out the relations between the DAF as well as the phase angle and the frequency ratio.

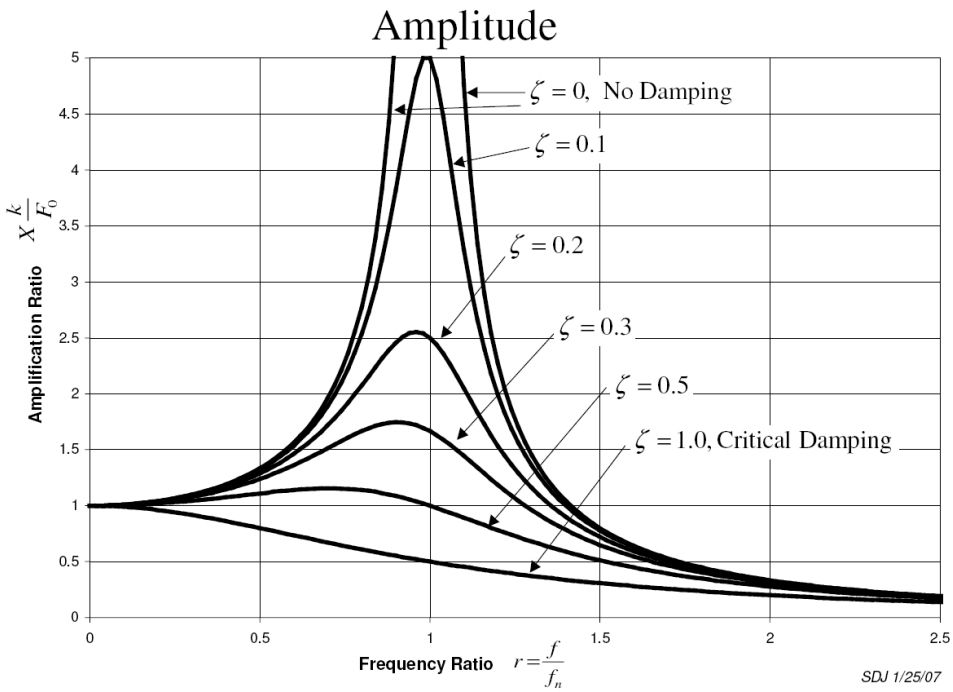

Figure 3.7 Dynamic Amplitude factor as function of the frequency ratio for given values of damping ratio

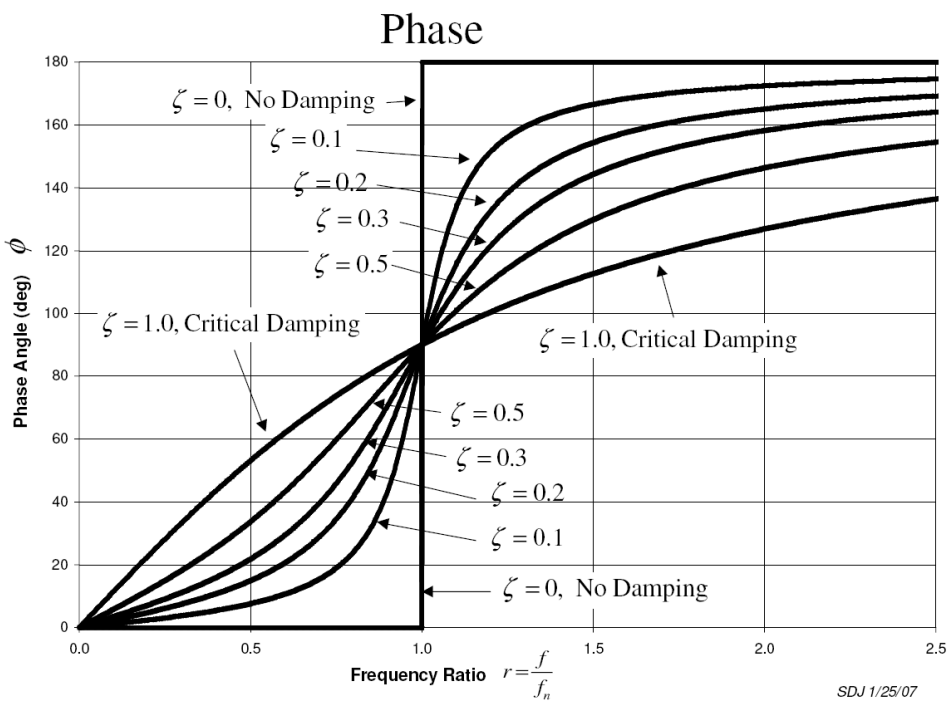

Figure 3.8 Phase angle between load and response as function of the frequency ratio for given values of damping ratio

Figure 3.7 illustrates that the maximum response for lightly damped system will increase dramatically when the enforced frequency approaches the natural frequency ω_0 for $\beta = 1$. For load frequency $\omega > \omega_0$, the response will decrease with increasing β, and for $\beta > 1.41$ the dynamic response will be less than the static response.

3.3 Equation of Motion for operating vessels

First of all, the vibration for single degree of freedom is under analysis, the dynamic equation can be expressed as: [9]

$$M\ddot{r} + C\dot{r} + Kr = F_{ext} \tag{3.31}$$

In which, M is the mass for the sway, surge and heave, while for roll, pitch and yaw, M should be replaced with I, which means the moment of inertia. C is the damping coefficient and K is the stiffness of the system. F_{ext} is the excitation force for this motion.

This is the uncoupled motion for the vessel motion. However, in the real motion for the vessel, it needs to take the influence from other degree of freedoms into consideration. Besides, the nonlinear effect is also need to the accounted for.

The 3-degree-of-freedom (DOF) nonlinear LF body-fixed coupled equation of motion in surge, sway and yaw of the DP vessel can be formulated in a vectorial setting according to [8]:

$$M_{RB}\dot{\nu} + C_{RB}(\nu)\nu + g(\eta) + M_A\dot{\nu} + C_A(\nu_r)\nu_r + D(\nu_r)\nu_r = \tau_{env} + \tau_{thr} \tag{3.32}$$

The first three terms of the left hand is the rigid-body terms, while the last three terms of the left hand is the hydrodynamic terms.

The effect of the current can be modeled into the relative velocity term $\upsilon_r = \upsilon - \upsilon_c$, where υ_c is the fixed-body current velocity vector.

For most motion control problems the vessel can be consider as a rigid body, i.e. the relative motion of the different parts of the hull structure is negligible [10].

The mass matrix for the rigid-body part can be expressed as:

$$\mathbf{M_{RB}} = \begin{bmatrix} m & 0 & 0 \\ 0 & m & mx_g \\ 0 & mx_g & I_z \end{bmatrix} \tag{3.33}$$

Where m is the mass and I_z is the moment of inertia about z-axis. The added mass matrix can be written as:

$$\mathbf{M_A} = \begin{bmatrix} -X_{\dot{u}} & 0 & 0 \\ 0 & -Y_{\dot{v}} & -Y_{\dot{r}} \\ 0 & -Y_{\dot{r}} & -N_{\dot{r}} \end{bmatrix} \tag{3.34}$$

The terms $-X_{\dot{u}}, -Y_{\dot{v}}, -N_{\dot{r}}$ are the zero-frequency added mass in surge, sway and yaw.

The skew-symmetric Coriolis and Centripetal Matrix of the template can be formulated as:

$$\mathbf{C_{RB}}(\nu) = \begin{pmatrix} 0 & 0 & -m(x_g r + v) \\ 0 & 0 & mu \\ m(x_g r + v) & -mu & 0 \end{pmatrix} \tag{3.35}$$

The skew-symmetric Coriolis matrix due to the potential part of the current is modeled as:

$$\mathbf{C_A}(\nu_r) = \begin{pmatrix} 0 & 0 & Y_{\dot{v}} v + Y r_{\dot{r}} \\ 0 & 0 & -X_{\dot{u}} u \\ -(Y_{\dot{v}} v + Y r_{\dot{r}}) & X_{\dot{u}} u & 0 \end{pmatrix} \tag{3.36}$$

The linear damping matrix due to the surface friction can be formulated as:

$$\mathbf{D} = \begin{pmatrix} -X_u & 0 & 0 \\ 0 & -Y_v & -Y_r \\ 0 & -N_v & -N_r \end{pmatrix} \tag{3.37}$$

Although the nonlinear damping will give a more accurate result, it may lead to a more complicated calculation. So in this thesis, the linear damping is applied instead.

4 Theory and methodology of SIMA

4.1 SIMA Introduction

SIMA program is a powerful tool for modeling and analysis of tasks within the field of marine technology. In this chapter, a brief introduction for this program will be carried out.

SIMA is an improved version based on the program SIMO. SIMA program realizes the function of 3-D visualization and transfers the input pattern from text file into windows input, which has brought two main advantages:

1) Creating a tool for beginners that shorten the time it takes to become proficient in modeling and analysis
2) Creating a tool for experts that shorten the time from project initiation to conclusion.

Currently SIMA supports the following programs:

- *SIMO* - Used to model marine operations.
- *RIFLEX* - Used to model a system consisting of slender elements, e.g. a riser system.
- *RIFLEX Coupled* - SIMO and RIFLEX coupled. Used to model slender, elastic structure(s) within a marine operation.
- *MULDIF2* - Used to model input to hydrodynamical software package MULDIF2.
- *SIMLA JLay* - Used to model laying of pipe lines.
- *HLA* - Used to set up an interactive HLA simulation.

SIMA is very easy and efficient for beginners to use. However, in order to achieve a well handle of the program, it is necessary to understand the basic theoretical background of SIMA. Thus, in this section, one introduction of the most frequently used functions will be carried out.

4.2 Coupling specifications

There are varieties kinds of coupling types that are available in SIMA, the “Simple wire coupling” as well as the “Force-elongation characteristic” are applied in the thesis. The parameters FLEXC and DAMPSW may be given.

FLEXC (inverse of stiffness) is the flexibility in the wire attachment point. DAMPSW is the material damping in the line. The value can normally be set to 1-2% of E*A.

Simple wire coupling

The simply wire coupling is modeled as a linear spring according to: [11]

$$\Delta \boldsymbol{l} = \frac{\mathbf{T}}{\boldsymbol{k}} \tag{4.1}$$

In which:

$\Delta \boldsymbol{l}$=elongation

T=wire tension

$\boldsymbol{k}$=effective axial stiffness

The effective axial stiffness is given as:

$$\frac{1}{k} = \frac{l}{\boldsymbol{EA}} + \frac{1}{k_0} \tag{4.2}$$

Where:

$\boldsymbol{E}$=modulus of elasticity

$\boldsymbol{A}$=cross-section area

l= unstretched wire length (may be variable with respect to time)

$1/k_0$=connection flexibility (crane flexibility)

Knowing the position of each line end, the elongation and thereby the tension may be determined.

Besides, material damping, which is another very important parameter, is included as:

$$\mathrm{F} = \frac{\mathrm{C_w} * l}{\Delta l * \Delta t} \tag{4.3}$$

Force-elongation characteristic

The model is identical to that described as station-keeping force. As a coupling force, any force elongation relationship may be specified. The curves for increasing and decreasing elongation may be different in order to model hysteresis effects. Damping may be specified as a force proportional to any exponent of the relative velocity of the end points. This model is also used for passive motion compensators.

4.3 Distributed element force

4.3.1Physical relevance

The distributed element force model is applicable to two different modeling features:

- Long, slender elements
- Concentrated, fixed elements (with zero extension)

Long, slender elements can be used to model jacket legs and bracings or spool pieces. A slender object such as a spool piece will normally have a 3-D geometry consisting of a number of straight elements with different orientation, and can be modeled by a set of slender elements. End connectors can be modeled either by a short element or by a concentrated, fixed element.

4.3.2 Element Definition

Small-body theory is used to calculate forces both for the slender element and the concentrated fixed element. Stiff connection implies that all the 'sub-body' (slender element or fixed, concentrated element) forces are calculated and transferred to the

'main' body. Each slender element specified by the user is divided into NSTRIP strips with equal length.

4.3.3 Coordinate system

In SIMA program, three coordinate systems are mainly used:
`XG`, global coordinate system, `XG(1)`, `XG(2)`, `XG(3)`
`XB`, local body fixed coordinate system, `XB(1)`, `XB(2)`, `XB(3)`
`XS`, local strip coordinate system, `XS(1)`, `XS(2)`, `XS(3)`
All coordinate systems are orthogonal and right-handed.
Figure 4.1 illustrates a single strip, introducing the local strip coordinate system.

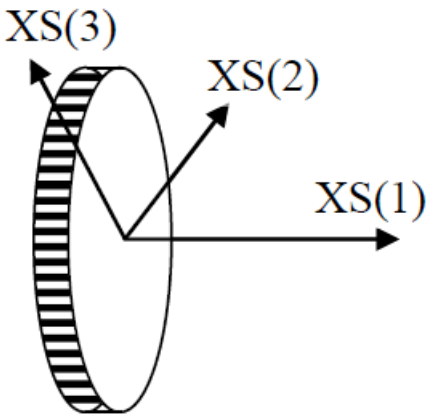

Figure 4.1 Definition of local strip coordinate system

The `XS(1)`-axis is directed along the longitudinal axis of the strip, and hence also the element, the `XS(2)`-axis is placed perpendicular to the `XS(1)` axis in the local strip xy-plane and the `XS(3)` axis is then defined from the definition of orthogonal right-handed coordinate systems.
In addition, the local coordinate system of the slender element is also of much concern. The axial direction of the slender element is set to be the x-axis, which means the start point and the end point of the slender elements are located on the x-axis. In order to define of the Y-Z plane, the concept of “Reference Point” is brought in. As shown in figure 4.2, the X-Y plane contains both of the two end points of the element and the reference point, while the Y-Z plane is perpendicular to the X-Y plane.

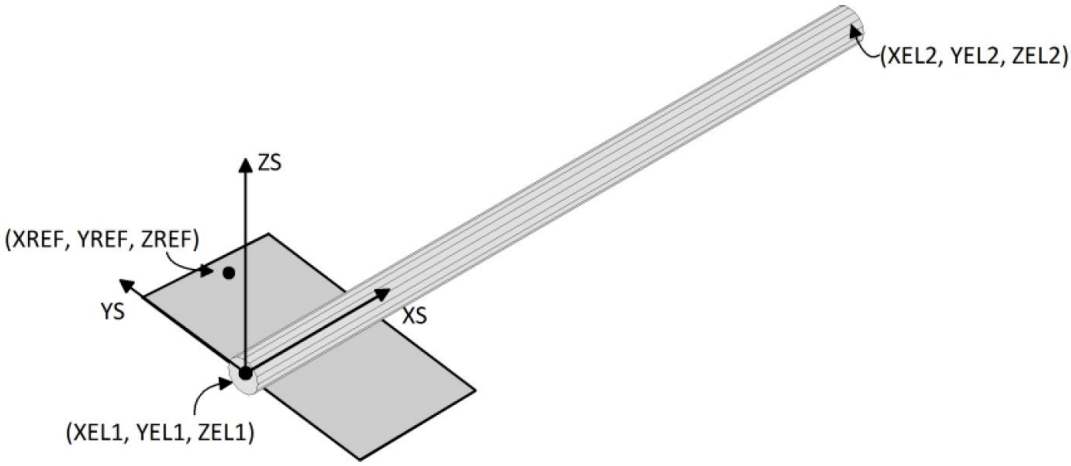

Figure 4.2 Coordinate system [XS,YS,ZS] of the slender element

4.3.4 Calculation of the mass matrix, M

The mass matrix of the element is made up of two components: the structural mass matrix and the added mass matrix. Therefore this section will mainly present how these two components will contribute to the total mass matrix.

i) Contribution from structural mass

The contribution from each of the slender elements to the mass matrix of the main body is calculated and added, in local body coordinates. The contribution from each element is calculated by adding the contributions from each strip, which has length L, mass per unit length, m, and coordinates (x,y,z) in the local body coordinate system. The contribution from each strip within each element to the total mass matrix of the body will be:

$$\Delta\mathbf{M} = \begin{pmatrix} 1 & 0 & 0 & 0 & z & -y \\ 0 & 1 & 0 & -z & 0 & x \\ 0 & 0 & 1 & y & -x & 0 \\ 0 & -z & y & y^2+z^2 & -xy & -zx \\ z & 0 & -x & -xy & z^2+x^2 & -yz \\ -y & x & 0 & -zx & -yz & x^2+y^2 \end{pmatrix} \cdot mL$$

$$= \begin{pmatrix} \mathbf{I} & \mathbf{A}^{\mathbf{T}} \\ \mathbf{A} & \mathbf{A} \times \mathbf{A}^{\mathbf{T}} \end{pmatrix} \cdot mL \tag{4.4}$$

Where **I** is a 3×3unity matrix and

$$\mathbf{A} = \begin{pmatrix} 0 & -z & y \\ z & 0 & x \\ -y & x & 0 \end{pmatrix} \tag{4.5}$$

The mandatory specified `'BODY MASS DATA'` for the main body can be zero (but not necessarily), and will be added to the contributions from the slender elements.

ii) Contribution from added mass

The contribution from the added mass will be an extension to the above, since the

added mass of each strip is different in the 3 directions.

Assume the following parameters:

Linear acceleration vector (main body) **V**

Rotation acceleration vector (main body) **W**

Radius vector to the strip **R**

Added mass matrix for the strip $\mathbf{M_a}$

$$\mathbf{V} = \begin{pmatrix} e \\ f \\ g \end{pmatrix} \quad \mathbf{W} = \begin{pmatrix} p \\ q \\ r \end{pmatrix} \quad \mathbf{R} = \begin{pmatrix} x \\ y \\ z \end{pmatrix} \quad \mathbf{M}_{\boldsymbol{a}} = \begin{pmatrix} a_x & 0 & 0 \\ 0 & a_y & 0 \\ 0 & 0 & a_z \end{pmatrix} \tag{4.6}$$

The local acceleration of the strip will be:

$$\mathbf{V_L} = \mathbf{V} + \mathbf{W} \times \mathbf{R} \tag{4.7}$$

The local force and moment can be expressed by:

$$\mathbf{F_L} = \mathbf{M}_{\boldsymbol{a}} \cdot \mathbf{V} + \mathbf{M}_{\boldsymbol{a}} \cdot (\mathbf{W} \times \mathbf{R})$$

$$\mathbf{M_L} = \mathbf{R} \times \mathbf{F_L} = \mathbf{R} \times (\mathbf{M}_{\boldsymbol{a}} \cdot \mathbf{V}) + \mathbf{R} \times (\mathbf{M}_{\boldsymbol{a}} \cdot (\mathbf{W} \times \mathbf{R})) \tag{4.8}$$

Further expansion yields:

$$\mathbf{A} \cdot \mathbf{V} = \mathbf{R} \times (\mathbf{M}_{\boldsymbol{a}} \cdot \mathbf{V}) = \begin{bmatrix} -a_y zf + a_z yg \\ a_x ze - a_z xg \\ -a_z ye + a_y xf \end{bmatrix} = \begin{bmatrix} 0 & -a_y z & a_z y \\ a_x z & 0 & -a_z x \\ -a_x y & a_y x & 0 \end{bmatrix} \cdot \begin{bmatrix} e \\ f \\ g \end{bmatrix}$$

$$\mathbf{B} \cdot \mathbf{W} = \mathbf{R} \times \left(\mathbf{M}_{\boldsymbol{a}} \cdot (\mathbf{W} \times \mathbf{R})\right)$$

$$= \begin{bmatrix} (a_z y^2 + a_y z^2) & -a_z xy & -a_y xz \\ -a_z xy & (a_x z^2 + a_z x^2) & -a_x yz \\ -a_y xz & -a_x yz & (a_x y^2 + a_y x^2) \end{bmatrix} \begin{bmatrix} p \\ q \\ r \end{bmatrix} \tag{4.9}$$

The resulting added mass contribution is:

$$\Delta \mathbf{M}_{\boldsymbol{a}} = \begin{pmatrix} \mathbf{M}_{\boldsymbol{a}} & \mathbf{A}^{\mathbf{T}} \\ \mathbf{A} & \mathbf{B} \end{pmatrix} \tag{4.10}$$

The contribution from all strips will be added to the body mass matrix.

Depth dependent hydrodynamic coefficient corrections may be specified for both slender and fixed elements. Added mass data for the main body may be zero (but not necessarily), and will be added to the contributions from the slender elements.

4.3.5 Calculation of external load, F

The model for external load on a slender element strip consists of three contributions:

- buoyancy forces, F_B
- wave forces, F_W
- slamming forces, F_S

The resulting force on a slender element is accumulated force contribution from each strip. The body force is the sum of contributions from all elements.

Gravity Force

The gravity force acts in global Z-direction and is written:

$$\mathbf{F}_G = \begin{bmatrix} 0 \\ 0 \\ -mgds \end{bmatrix} \tag{4.11}$$

Buoyancy Force

The buoyancy force acts in the global z-direction, through the center of buoyancy. Load vector for a strip, expressed in the global coordinate system can be written:

$$\mathbf{F}_{Buoy,G} = \begin{bmatrix} 0 \\ 0 \\ \rho \cdot V_s \cdot g \cdot dS \end{bmatrix} \tag{4.12}$$

Wave Force

The wave force on a strip acts through the center of buoyancy. Load vector for a strip, expressed in the local strip coordinate system can be written:

$$\boldsymbol{F}_{W,S} = (\rho V_s + \mathbf{m}_h) \cdot \boldsymbol{a_s} + \boldsymbol{C}_q \cdot \left\{ \left(\dot{\boldsymbol{X}}_\mathrm{S} - \mathbf{U}_\mathrm{s} - \mathbf{v}_\mathrm{s} \right) \cdot \left| \dot{\boldsymbol{X}}_\mathrm{S} - \mathbf{U}_\mathrm{s} - \mathbf{v}_\mathrm{s} \right| \right\}$$

$$+\boldsymbol{C}_1 \cdot \left(\dot{\boldsymbol{X}}_\mathrm{S} - \mathbf{U}_\mathrm{s} - \mathbf{v}_\mathrm{s} \right) \tag{4.13}$$

Where,

V_s is submerged volume per length unit, calculated to z=0

$\boldsymbol{a_s} = (a_{sx} \quad a_{sy} \quad a_{sz})^\mathrm{T}$ is water particle acceleration in local strip coordinate system

$\mathbf{v_s} = (\mathrm{v}_{sx} \quad \mathrm{v}_{sy} \quad \mathrm{v}_{sz})^\mathrm{T}$ is water particle velocity in local strip coordinate system

$\dot{\boldsymbol{X}}_\mathrm{S}$ is strip velocity in local strip coordinate system

$\mathbf{U}_\mathrm{s} = (U_{sx} \quad U_{sy} \quad U_{sz})^\mathrm{T}$ is current flow velocity in local strip coordinate system

The first term contains the Froude-Krylov and diffrection forces. The second term is the quadratic drag term of Morison formula. The third term represents linear drag.

Slamming Force

The slamming force on a strip, which is moving around can be related to the change in (added) mass with time.

Expressed in local strip coordinates, the slamming force can be expressed by:

$$\mathbf{F}_{\mathrm{S,S}} = -\frac{\partial \mathbf{m}_\mathrm{s}}{\partial \mathrm{t}} \dot{\boldsymbol{X}}_\mathrm{S} = -\frac{\partial \mathbf{m}_\mathrm{s}}{\partial \mathrm{t}} \frac{\partial \mathrm{h}}{\partial \mathrm{t}} \dot{\boldsymbol{X}}_\mathrm{S} = -\frac{\partial}{\partial \mathrm{t}} \begin{bmatrix} m_{h,x(h)} & 0 & 0 \\ 0 & m_{h,x(h)} & 0 \\ 0 & 0 & m_{h,x(h)} \end{bmatrix} \frac{\partial \mathrm{h}}{\partial \mathrm{t}} \dot{\boldsymbol{X}}_\mathrm{S} \tag{4.14}$$

In which,

h: distance between instantaneous surface elevation and strip origin in global Z-direction.

4.4 Dynamic Positioning

The Dynamic Positioning (DP) system is widely used in the marine operation industry. Most of the operation and supply vessels are equipped with the DP system. However, since the Jack-up model is applied in this thesis instead of the operating vessel, only a brief introduction to the existing dynamic positioning theories is presented in this section.

The dynamic positioning module is a control module with the following input and output:

Input:

- Position measurement
- Wind measurement
- Anchor line force measurement
- Thrust measurement

Output:

- Desired resultant forces and moment from the thrusters

Currently, there is a PID controller and a Kalman filter-based controller exists.

PID Controller

The controller converts position and velocity errors into a demand for thrust forces to correct the errors. A decoupling approach allows PID control parameters to be specified separately for surge,

sway and yaw. However, the PID theory is much more complicated and difficulty for beginner to use, thus in this thesis the Kalman-filter controller is finally applied.

Kalman filter

The Kalman filter module was originally developed at SINTEF, division of Automatic Control during the period 1975-77, and has later been maintained and slightly modified by MARINTEK.

4.5 Forces due to propulsion units

The propulsion units are used to serve the DP system and gain the controlling of the vessel in different sea-states. The available propulsion units used for positioning in SIMA are listed:

- **tunnel** thrusters, the thrusters are installed in a tunnel (fixed direction).
- **nozzle (**ducted) thruster. The nozzle increases the thrust compared to a conventional propeller at low vessel speed, and is often used where the performance in bollard pull condition is important. The thruster may be rotatable, partly rotatable or fixed.
- **conventional** propellers. They are designed mainly for propulsion, but may also be used for positioning. Combined with a rudder, the system can produce forces in transverse direction to the propeller axis.

5. Method of modeling components in SIMA

In order to carry out the analysis, a model in SIMA needs to be built. In this chapter, the method for modeling different components in SIMA will be presented.
First of all, a brief introduction for the subject used in this thesis will be carried out. The lifting object in this thesis is a template installed by the company Acergy in 2008. The basic information of the template lifting is stated in table 5.1, and figure 5.1 is a sketch of the template.

Table 5.1 Basic information of the template lifting

Parameters	Values	Unit
Mass	285	Te
Length	29	m
Width	24	m
Height	16	m
Water depth	360	m
SWL	300	Te
Hook height	40	m
Crane radius	17	m
Maximum DHL	390	Te

5.1 Modeling method for structures equipped with cranes

Generally, there will be two kinds of structures that can be equipped with cranes. One is floating structure such as crane vessels, the other one is the fixed-position structures like jack-up rigs.

5.1.1 Modeling for Jack-up rigs

For jack-up rigs, both of the crane and the rig will be fixed at one position, which will leave out the influence of the movement of the crane. This can be done by selecting “Prescribed” mode for the body type, which is shown in Figure 5.1.

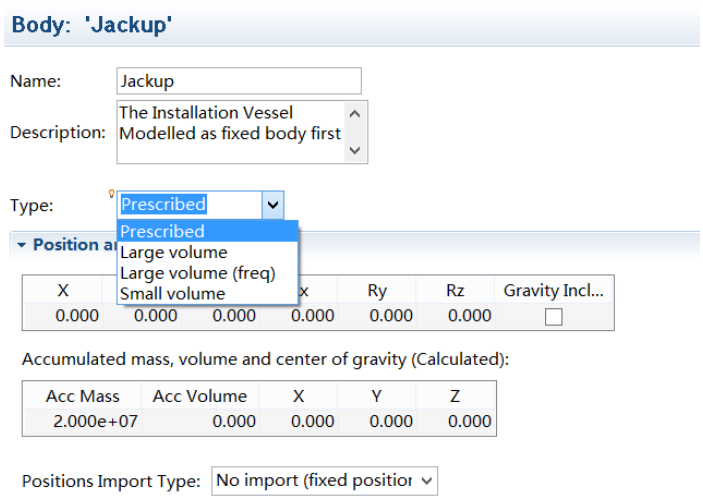

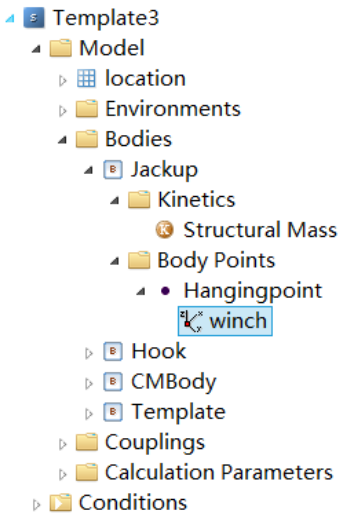

Figure 5.1 Body type settling **Figure 5.2 Jack-up model in SIMA**

In addition, the body mass and related parameter will be carried out by the term "Strucure Mass" under the "Kinetics" option.
After all, the function of the crane is realized by creating one body point to the jack-up body. One winch is added to this body point to lower the lifting structure. Figure 5.2 represents the details of these two functions.

5.1.2 Modeling for vessels

The method of modeling vessels in SIMA is very difficult and complicated. For example, the Kinetics function contains more than 8 term, which is shown in figure 5.3

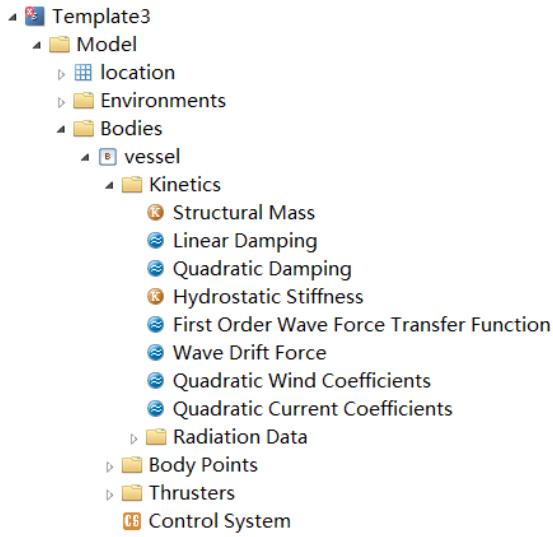

Figure 5.3 Vessel Model in SIMA

Because of the lack of the detail information about the operation vessel, which makes

the modeling work extremely difficult, thus the jack-up model is applied in this thesis. However, more attention should be paid to the water depth issue. The water depth in this thesis is 360m, while the maximum depth for the application of a Jack-up rig is around 200m. Thus, a discussion concerning the influence of the water depth on the dynamic performance of the template is carried out. The figures are listed in the Appendix A. The result shows that the water depth has very limited influence on the dynamic performance of the template. This means that when using the jack-up model in the water depth of 360m, the result of the dynamic analysis is still acceptable.

5.2 Modeling method for lifting system

The lifting system consists of the hook, the crane master and the lifting wires.

5.2.1 Modeling for hook structure

Hook is the structure that connects the crane and the lifting structure. Since the mass of the hook is considered small in comparison to the template, the movement of the hook won't cause any significant influence on the movement of the template. So the mass of the hook is the only parameter needs to be taken into consideration. Thus, the hook is modeled as body mass with two body points to attach the lifting wire, which is shown in figure 5.4.

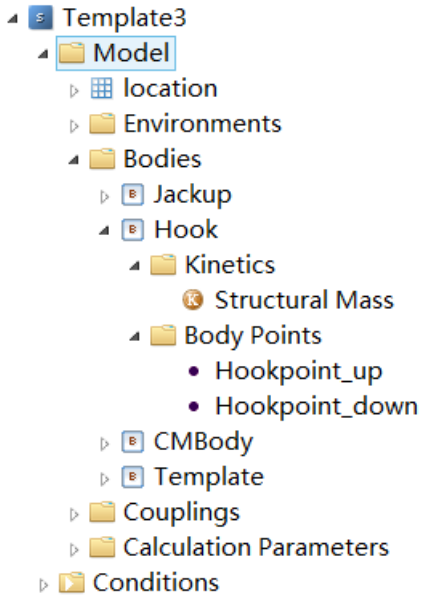

Figure 5.4 Hook model in SIMA

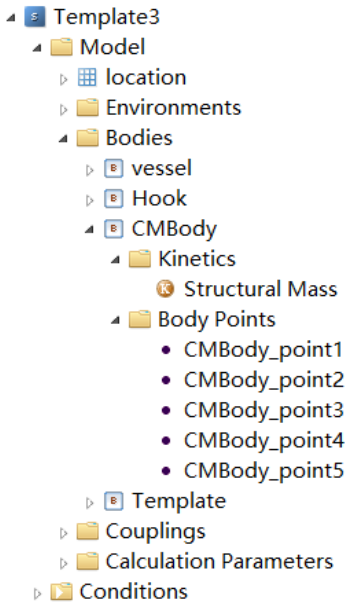

Figure 5.5 Crane Master Model in SIMA

5.2.2 Modeling for crane master

The crane master is widely used in marginal lift, especially for large scale structure. In

the lifting case of this thesis, in order to obtain the balance of the template during the lifting, there will be 4 lifting wires connect to each corner of the template. Therefore, the crane master is applied as transition between the hook and the template. As the same reason as the hook, the vibration of the crane master won't contribute to the movement of the template. Thus the crane master can be modeled as a body with structure mass and 5 body points. The details are illustrated in figure 5.5.

5.2.3 Modeling for lifting wires

Lifting wires are the key element in the whole lifting system. The selection of the right type of the wires and the proper settling of the wire properties will eventually determine the efficiency and the safety level of the lifting operation.
SIMA program provide several types of coupling force to meet different kind of demands in particular circumstances. Table 5.2 presents all the coupling specification for wires involved in SIMA.

Table 5.2 Coupling specification for wires

Number	Coupling specification
1	Simple wire coupling
2	Multiple wire coupling
3	Lift line coupling
4	Force-elongation with fixed attack points

The simply wire coupling and force-elongation coupling will be applied in the case of this thesis.
There are totally six lifting wires included in the lifting system. The following table illustrates the position and the type of all the wires.

Table 5.3 Wire types and positions

Wire number	Position	Wire type
1	Between the hook and the crane	Simply wire coupling
2	Between the took and the crane master	Force-elongation with fixed attack points
3	Wire 1 from the CM to the template	Simply wire coupling
4	Wire 2 from the CM to the template	Simply wire coupling
5	Wire 3 from the CM to the template	Simply wire coupling
6	Wire 4 from the CM to the template	Simply wire coupling

(CM stands for the crane master in this table)

The next step is to determine all the properties for the lifting wires. First of all, it is assumed that all the wires won't have failure or break. And the connection flexibility is set as zero, which will leave out the effect of the other unnecessary factors. This will leave only three characteristics of the wires to be decided, the length, the material damping and the wire cross section stiffness (Ea).

For wire 3,4,5 and 6, they are symmetric line system from the crane master to the template. Thus, all the properties of these wires will be exactly the same. These wires will only undertake the loads from the template, The details are shown in figure 5.5.

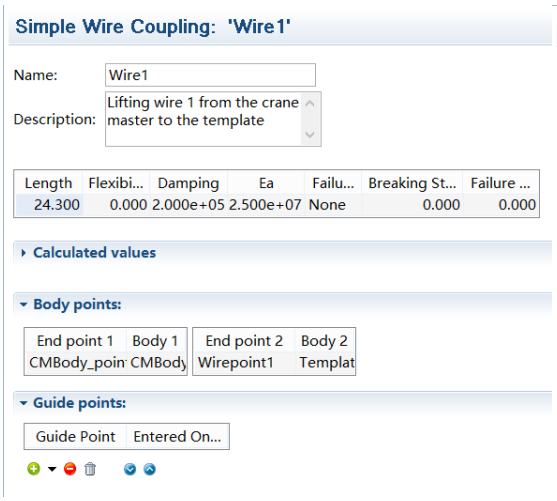

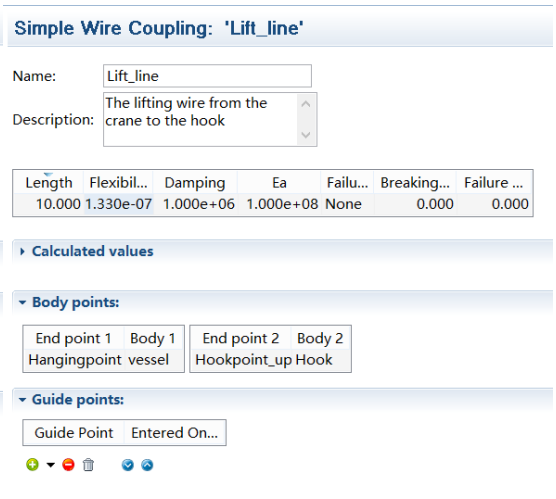

Figure 5.6 Wire model in SIMA (Wire from the crane master to the template) **Figure 5.7 Wire model in SIMA (Wire from the crane to the hook)**

Wire 1 is the lifting wire connecting the crane to the hook, which undertakes all the loads and forces from the whole system, for this reason, there should be an increase in both the material damping and the stiffness (Ea) in order to the meet the higher demands. These changes are all presented in figure 5.6 and 5.7.

Finally, it comes to the wire which is modeled as force-elongation with fixed attack point, the wire between the hook and the crane master. The model is identical to that described as station-keeping force, which is to say that the relations between the elongation and the tension force will be pre-described. In order to simplify the problem, both of the damping and force interpolation are linear. Figure 5.8 and 5.9 will state the relationships for the force and damping.

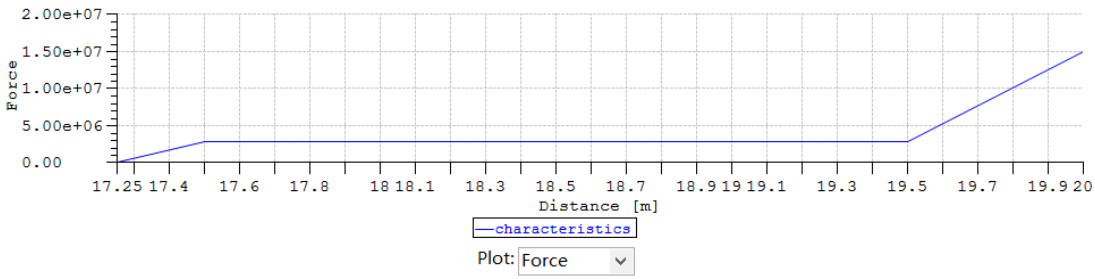

Figure 5.8 Relationship of the wire force against the wire elongation

The wire force is zero while the wire length is below 17.25m, then it increases to a certain number within a small elongation (0.25m). After that the tension force will

witness a gradual increase within the range from 17.5m to 19.2m. As can be seen from the figure, the slope of this line is almost zero, which is to say, the tension force will stay in a steady level in this range. Once the wire is tensioned and the wire length surpasses 19.5m, the tension force will experience a dramatic increase against the elongation.

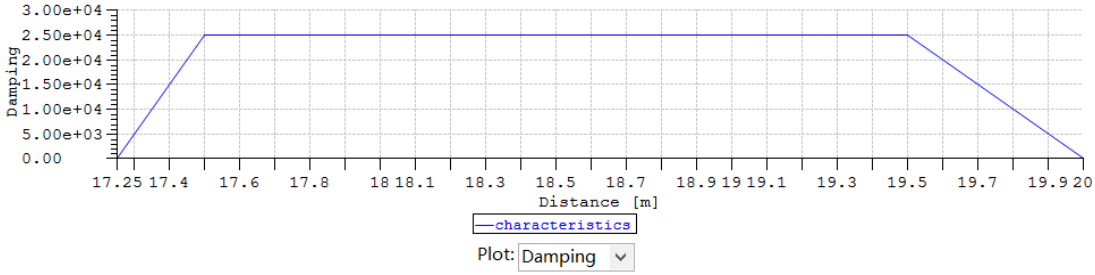

Figure 5.9 Relationship of the wire damping against the wire elongation

The material damping, just like the tension force, experiences a stable range between 17.5m and 19.5m, while the damping will decrease until zero for any wire length below 17.25m or over 20m.

Since the wire force and damping are pre-described, it is necessary to predict the wire force during static analysis. The tension force in this wire is the summary of the gravity of the template and the crane master, which is given as:

$$\mathrm{T} = \mathrm{M_{CM}} + \mathrm{M_T} = (800 + 284000) \cdot 9.81 = 2.794 \cdot 10^6 (N) \tag{5.3}$$

And the distance between the hook and the crane master is 19.5m, so the wire force should be approximate 2794KN when the wire length is around 19.5m. During the real lifting operation, the tension of the wire will lead to the change of the relative position of each structures, this phenomenon will be presented in the static analysis in chapter 6.

5.3 Modeling method for the template

The template is the most complicated and difficult structure to model in the program. First of all, the template used in this thesis is 285tons and it consists of dozens of beams and pipes. Secondly, due to the existence of the horizontal beams, the added mass and the drag coefficient will normally depend on the vertical position of the beam, thus it will bring new challenges to the determination of these coefficients.

5.3.1 Kinetic model of the template

The weight of the template is carried out by the beam elements, so the structure mass is set to zero. But, one linear damping and a hydrostatic stiffness are added to the template. The linear damping term presents the damping of the template in air, which is different from the dynamic damping of the template in water that is defined in the

beam elements, while the hydrostatic stiffness is added only in yaw direction to prevent the template from the unrealistic rotation in yaw. All of the information are shown in the following figures.

Linear Damping on Template

Description: Added damping in air

	Surge	Sway	Heave	Roll	Pitch	Yaw
Surge	1.000e+	0.000	0.000	0.000	0.000	0.000
Sway	0.000	1.000e+	0.000	0.000	0.000	0.000
Heave	0.000	0.000	1.000e+	0.000	0.000	0.000
Roll	0.000	0.000	0.000	1.000e+	0.000	0.000
Pitch	0.000	0.000	0.000	0.000	1.000e+	0.000
Yaw	0.000	0.000	0.000	0.000	0.000	1.000e+

Figure 5.10 Linear damping in air

Hydrostatic Stiffness on Template

Description: Added yaw stiffness, to prevent numerical rotation to prevent numerical

Stiffness Reference:

X	Y	Z	Rx	Ry	Rz
0.000	0.000	0.000	0.000	0.000	0.000

Stiffness Matrix:

	Surge	Sway	Heave	Roll	Pitch	Yaw
Surge	0.000	0.000	0.000	0.000	0.000	0.000
Sway	0.000	0.000	0.000	0.000	0.000	0.000
Heave	0.000	0.000	0.000	0.000	0.000	0.000
Roll	0.000	0.000	0.000	0.000	0.000	0.000
Pitch	0.000	0.000	0.000	0.000	0.000	0.000
Yaw	0.000	0.000	0.000	0.000	0.000	2.000e+

Figure 5.11 Hydrostatic Stiffness in yaw

In addition, there are 4 body points in the template model for connecting the lifting wires.

5.3.2 Beam model of the template

The template consists of several beam elements and four vertical tanks, and all of these components will contribute to the dynamic performance of the template. Each beam has its own dimensions and makes its own contribution to the whole system with the gravity, the added mass as well as the drag force. Thus, slender element seems to be a suitable option for modeling the template.

Since there are dozens of beam elements included in the template model, it is not possible to describe the modeling method for all the elements. Thus the modeling methods for 2 typical beams are to the presented.

i) Vertical beam

Vertical beam is easier and more convenient to build in the SIMA program. Take one of the vertical tanks for instance, the diameter is 2m and the distributed mass is 7500kg/m. With reference to appendix B, the added mass, linear drag force and quadratic drag force can be found and calculated. The result is shown in figure 5.11

Hydrodynamic coefficients

Quadratic drag:

C2x	C2y	C2z
100.000	2.050e+0	2.050e+0

Linear drag:

C1x	C1y	C1z
0.000	150.000	150.000

Added mass:

Amx	Amy	Amz
0.000	1.287e+0	1.287e+0

Figure 5.12 Hydrodynamic Coefficient in SIMA

ii) Horizontal beam

The horizontal beam is part of the frame structure to fixate the tanks, the diameter is 0.2m and the distributed mass is set as 62kg/m. With the same method of the vertical beams, the added mass and drag force of the horizontal beams can be calculated. However, the most important problem for the horizontal beams is that the dynamic coefficients will vary with the change of the vertical position. To seek a solution to this situation, it is necessary to bring in the function of the depth-dependent hydrodynamic coefficients

The depth-dependent hydrodynamic coefficients function is based on the linear interpolation assumption of the values at several particular positions. In this thesis, the values of 5 different vertical positions are used, which is illustrated in the following figure.

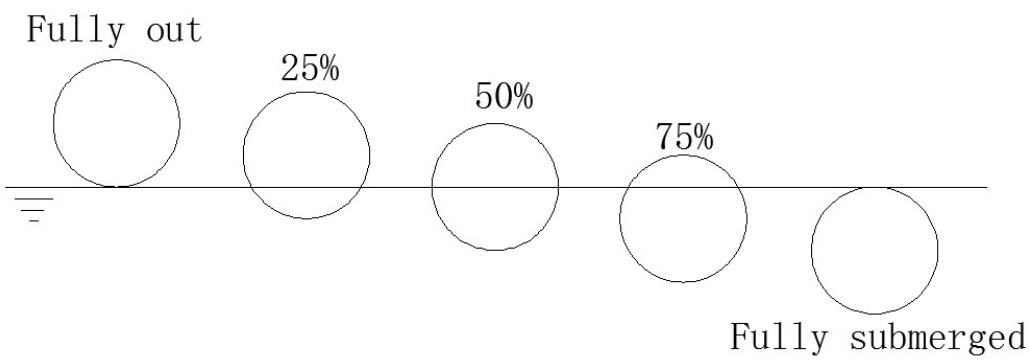

Figure 5.13 The sketch of the lowing process

All the relative values and information are contained in figure 5.14.

Depth-dependent hydrodynamic coefficients

Vertical position: 0.000

Vert. pos...	Rel. vol.	RQx	RQy	RQz	RLx	RLy	RLz	RAMx	RAMy	RAMz
0.100	0.000	0.000	0.000	0.000	0.000	0.000	0.000	0.000	0.000	0.000
0.050	0.227	0.350	0.350	0.350	0.350	0.350	0.350	0.227	0.227	0.227
0.000	0.500	0.600	0.600	0.600	0.600	0.600	0.600	0.500	0.500	0.500
-0.050	0.773	0.850	0.850	0.850	0.850	0.850	0.850	0.773	0.773	0.773
-0.100	1.000	1.000	1.000	1.000	1.000	1.000	1.000	1.000	1.000	1.000

Figure 5.14 The Depth-dependent hydrodynamic coefficients

5.3.3 Specified Force of the template

The slender element is modeled as a sealed pipe in SIMA program. However the valves on the vertical tanks of the template are opened during the lowing procedure, which means there is redundant buoyancy on the template in the program. Thus, in order to balance the redundant buoyancy of the template, the concept of specified force is brought in.

Specified Force: 'specifiedForce'

Name: specifiedForce

Description:

Load Type: Constant force

Constant force component

Activation ...	Deactivatio...	Magnitu...
80.000	300.000	-3.028e+06

Position / Direction

Attack point (local coordinates):

X	Y	Z
0.000	0.000	-3.000

Reference frame and direction vector:

Reference ...	Vx	Vy	Vz
Local	0.000	0.000	1.000

Figure 5.15 Specified Force Model in SIMA

In modeling the specified force, the following parameters are of most attention:
Activation: Time for switching component on
Deactivation: Time for switching component off
Magnitude: Force component magnitude
Attack point: The coordinate of the point that the specified force is acting on
The detailed information of the specific force are all presented in figure 5.15.

6 Calculation settings and Static Analysis

As soon as the modeling work in SIMA is finished, the static and dynamic analysis of the lifting operation will be carried out. This chapter mainly presents the calculation parameters as well as the result of the static analysis

6.1 Calculation Parameters

The calculation parameter is mainly used to define the calculation procedure and the related parameters. The calculation parameter consists of two parts, the static calculation parameters and the dynamic calculation parameters. The details of each part will be presented in the following sections.

6.1.1 Static Calculation Parameters

There are five main parameters involved in the static calculation parameters:

- Maximum natural Period
- Position Tolerance
- Direction Tolerance
- Equilibrium Time step
- Maximum numbers of time steps

Among all the five parameters, the maximum natural period and the equilibrium time steps are of most concern. The influence of these two parameters will be discussed respectively.

Maximum natural Period

The maximum natural period is used to find the natural period of the template in the static analysis. During the static analysis, the program will first try to find out the natural period of the structure, based on the range from 0 to the maximum natural period.

If the selected value is too small, it is impossible to find the natural period of the structure within the range. Thus the result of the static analysis will be incorrect or inaccurate.

On the other hand, if the maximum natural period is too large, this means that it might take the program too much time to achieve the natural period. If the time demands is larger than the total calculation time (the total calculation time is the product of the equilibrium time step and the maximum number of the time steps), the program will not be able to get access to the correct static analysis result.

Equilibrium Time step

All the calculation of the program is carried out step by step, thus choosing the proper length of the time step is very important for a quick and accurate calculation.

If the time step length is too large, this may lead to a radiation effect and the

equilibrium positions will not be able to be found out.
If the time step length is too small, the program can not find the equilibrium positions within the total calculation time.
Thus as soon as one of the situations above occurs, the program is not able to obtain the accurate static analysis. Therefore, all these parameters should be chosen with fully considerations and elaborate practices. The chosen parameters used in this thesis are shown in the following figure.

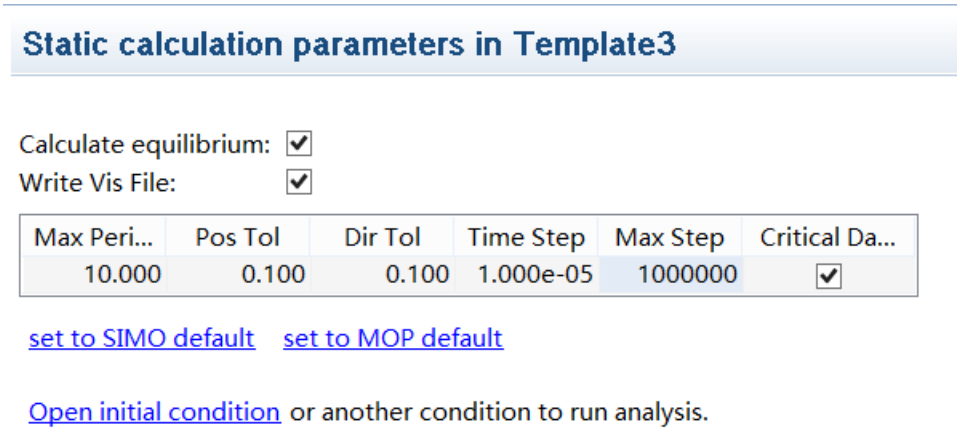

Figure 6.1 Static Calculation parameters

6.1.2 Dynamic Calculation Parameters

Since the dynamic analysis is more complex than the static analysis, there will be more parameters involved in the dynamic calculation parameters.
The first step is to select the integration method. The Runge Kutta method is finally chosen instead of Euler method because of the high accuracy and highly convenience.
Among all the parameters, the following three factors are drawing most attention:

- Time step for pregeneration/Storage
- Number of steps in fft is 2^N.(This value must be equal to or lager tan the number of the simulation steps)
- Number of simulation steps

Both of the time step length and the simulation steps are following the same discipline applied for the static calculation parameters. The only different is that more attention should be paid to the number of steps in fft, the value of N might be changed in order to meet the certain requirements.
Moreover, there is a storage function included in the dynamic calculation parameters. This function provides the user with an access to display all the demanded information about the dynamic analysis.
The following figures, figure 6.2 &6.3 illustrate the details of the dynamic calculation parameters used in this thesis.

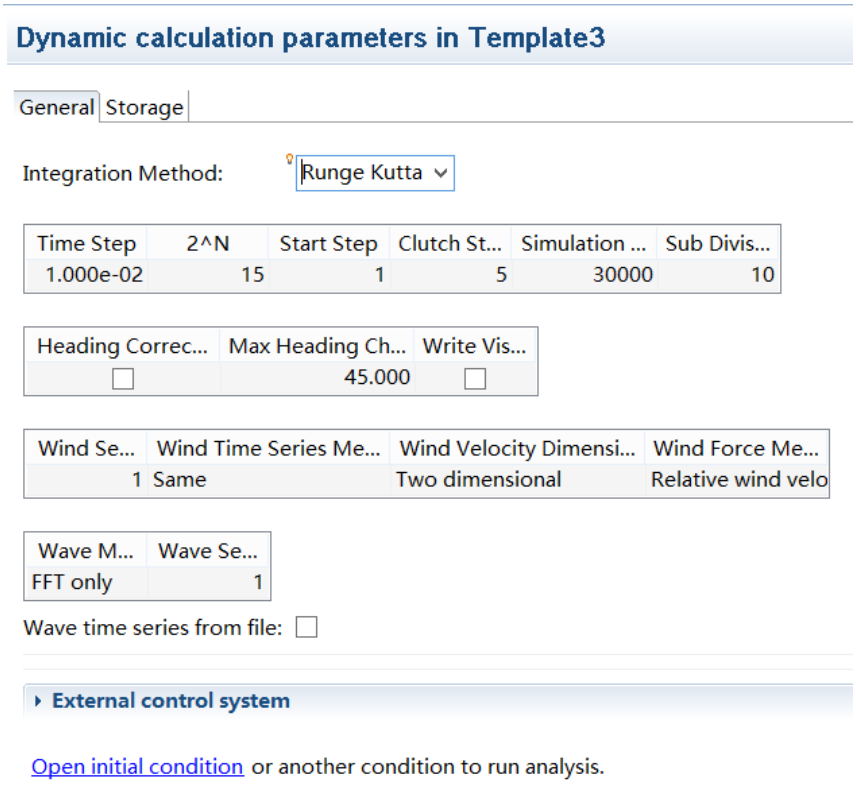

Figure 6.2 Dynamic Calculation Parameters

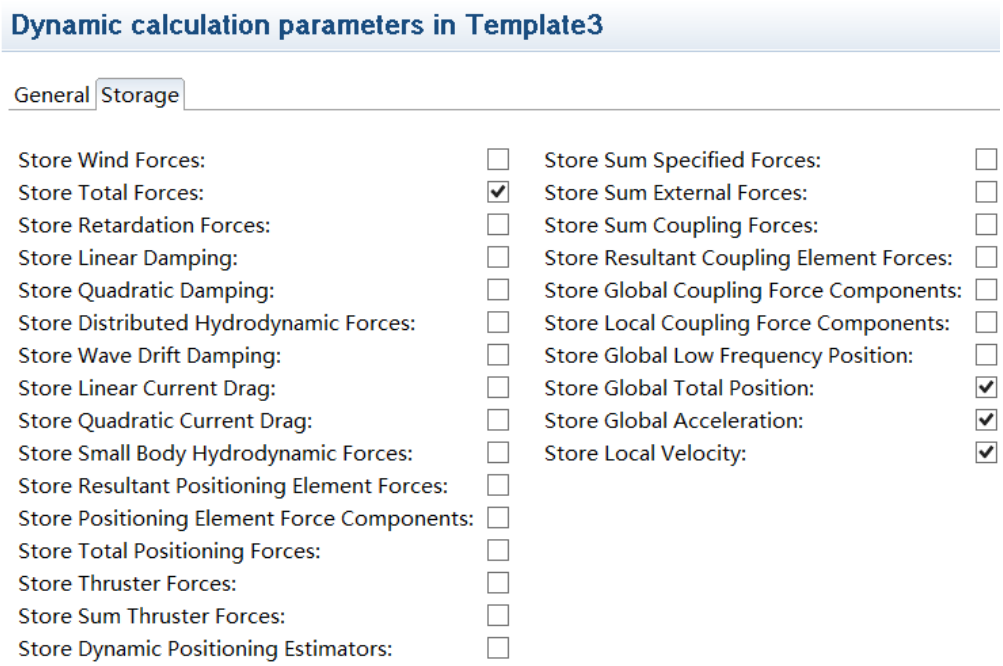

Figure 6.3 Storage information of the Dynamic Calculation

6.2 Result of the static analysis

The static analysis mainly gives out the static force and the equilibrium positions of each component involved in the lifting operation.
In figure 6.4 the body position result of all the structures are presented.

Body Results

Body positions. Select a body to display its force components:

Body	X	Y	Z	Rx	Ry	Rz
Jackup	0.00 (0.00)	0.00 (0.00)	0.00 (0.00)	0.00 (0.00)	0.00 (0.00)	0.00 (0.00)
Hook	30.0 (0.00)	0.00 (0.00)	49.3 (-0.67)	0.00 (0.00)	0.00 (0.00)	0.00 (0.00)
CMBody	30.0 (0.00)	0.00 (0.00)	30.3 (0.32)	0.00 (0.00)	0.00 (0.00)	0.00 (0.00)
Template	30.0 (0.00)	0.00 (0.00)	9.24 (-0.76)	0.00 (0.00)	0.00 (0.00)	0.00 (0.00)

Filter Forces: ☑ Apply positions

Figure 6.4 Body position of each component from static analysis

From figure 6.4, it can be seen that the hook and the template has a negative displacement while the crane master witness a positive displacement. All of these three components have a small move under the static analysis.
As for the force components, the static analysis result will be shown respectively in the rest of the section.

Jack-up model

Static forces and moments on Jackup

Name	Fx	Fy	Fz	Ftotal	Accelera...	Mx	My	Mz
Coupling forces	0.000	-6.989	-2.872e+06	2.872e+06	1.436e-04	419.320	8.616e+07	-209.660
Total	0.000	-6.989	-2.872e+06	2.872e+06	1.436e-04	419.320	8.616e+07	-209.660

Coupling element forces on Jackup

Coupling	Connec...	Ftotal	Fx	Fy	Fz	Mx	My	Mz
Lift_line	Hook	2.872e+06	0.000	-6.989	-2.872e+06	419.320	8.616e+07	-209.660

Figure 6.5 Force components of the Jack-up

Since the Jack-up rig is fixed at the location, it will only experience the coupling force from the lifting line, the value of which is the total weight of the whole lifting system.

Hook model

Static forces and moments on Hook

Name	Fx	Fy	Fz	Ftotal	Accelera...	Mx	My	Mz
Gravity	0.000	0.000	-7.848e+04	7.848e+04	9.810e-03	0.000	0.000	0.000
Coupling forces	0.000	4.678	7.801e+04	7.801e+04	9.751e-03	0.000	0.000	0.000
Gravity+buoyancy	0.000	0.000	-7.848e+04	7.848e+04	9.810e-03	0.000	0.000	0.000
Total	0.000	4.678	-471.490	471.513	5.894e-05	0.000	0.000	0.000

Coupling element forces on Hook

Coupling	Connec...	Ftotal	Fx	Fy	Fz	Mx	My	Mz
Lift_line	Jackup	2.872e+06	0.000	6.989	2.872e+06	0.000	0.000	0.000
Crane	CMBody	2.794e+06	0.000	-2.310	-2.794e+06	0.000	0.000	0.000

Figure 6.6 Force components of the Hook

The hook body takes the load from the crane master and the template, and balanced to the force from the lifting line with its own weight.

Crane Master model

Static forces and moments on CMBody

Name	Fx	Fy	Fz	Ftotal	Accelera...	Mx	My	Mz
Gravity	0.000	0.000	-7.848e+03	7.848e+03	9.810e-03	0.000	0.000	0.000
Coupling forces	0.000	2.611	7.836e+03	7.836e+03	9.795e-03	-1.005	0.000	0.000
Gravity+buoyancy	0.000	0.000	-7.848e+03	7.848e+03	9.810e-03	0.000	0.000	0.000
Total	0.000	2.611	-11.753	12.039	1.505e-05	0.000	0.000	0.000

Coupling element forces on CMBody

Coupling	Connec...	Ftotal	Fx	Fy	Fz	Mx	My	Mz
Wire1	Template	8.506e+05	-4.062e+05	2.708e+05	-6.965e+05	0.000	0.000	0.000
Wire2	Template	8.506e+05	4.062e+05	2.708e+05	-6.965e+05	0.000	0.000	0.000
Wire3	Template	8.506e+05	4.062e+05	-2.708e+05	-6.966e+05	0.000	0.000	0.000
Wire4	Template	8.506e+05	-4.062e+05	-2.708e+05	-6.966e+05	0.000	0.000	0.000
Crane	Hook	2.794e+06	0.000	2.310	2.794e+06	0.000	0.000	0.000

Figure 6.7 Force components of the Jack-up

The crane master is used to connect with the template, thus it will mainly undertake the weight of the template through four lifting wires, which is shown in figure 6.7.

Template model

Static forces and moments on Template

Name	Fx	Fy	Fz	Ftotal	Accelera...	Mx	My	Mz
Distributed forces,vol	0.000	-8.165	-2.786e+06	2.786e+06	9.810e-03	-15.625	0.000	0.000
Coupling forces	0.000	7.866	2.786e+06	2.786e+06	9.812e-03	-121.180	0.000	0.000
Total	0.000	-0.299	523.620	523.620	1.844e-06	-136.810	0.000	0.000

Coupling element forces on Template

Coupling	Connec...	Ftotal	Fx	Fy	Fz	Mx	My	Mz
Wire1	CMBody	8.506e+05	4.062e+05	-2.708e+05	6.965e+05	5.572e+06	8.358e+06	-5.931
Wire2	CMBody	8.506e+05	-4.062e+05	-2.708e+05	6.965e+05	5.572e+06	-8.358e+06	5.931
Wire3	CMBody	8.506e+05	-4.062e+05	2.708e+05	6.965e+05	-5.572e+06	-8.359e+06	5.931
Wire4	CMBody	8.506e+05	4.062e+05	2.708e+05	6.965e+05	-5.572e+06	8.359e+06	-5.931

Figure 6.8 Force components of the Template

The total coupling force from 4 lifting wires will balance the weight of the template in the vertical direction**.** However, due to the large weight of the template, there is some differences in the total vertical force of the template. But this difference is under the acceptable range.

7 Environment data and Dynamic Analysis

The dynamic analysis simulated the whole lifting operation process, thus the result of the dynamic analysis will contains the information and details concerned about the force components, the displacements of each structures and the local or global velocity as well as the acceleration. As discussed in section **6.1.2**, it is very convenient and sufficient to choose all the information needs to store and display. Based on the analysis requirements, the following information are stored for the further analysis:

- Total Force
- Summary Coupling Force
- Global Coupling Force Components
- Local Coupling Force Components
- Global Total Position
- Global Acceleration
- Local velocity

Therefore, this chapter will mainly discuss the dynamic performance of each component of the system based on the variables listed above.

7.1 Environment setting

The environment setting in SIMA is very convenient and direct. There are four kinds of input data available in SIMA:

- Wind wave
- Swell wave
- Wind
- Current

In this thesis, only the wind wave is taken into consideration, the related parameters are all illustrated in the following figure.

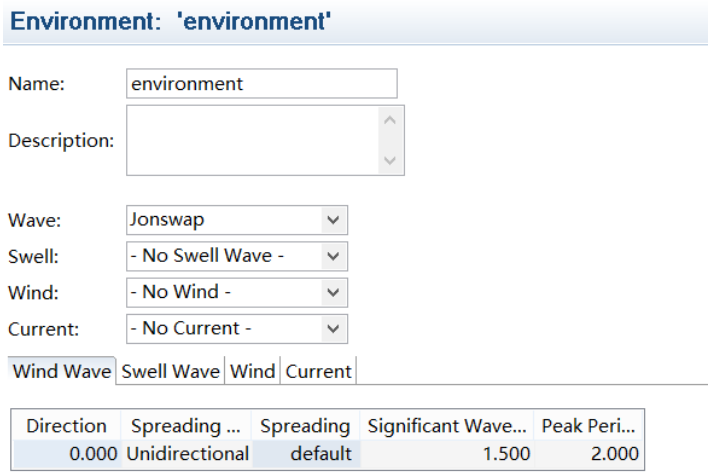

Figure 7.1 Environment setting in SIMA program

Since most lifting operations in Norway are carried out in the north sea, thus the Jonswap("Joint North Sea wave project") spectrum is chosen in the analysis.

To simplify the problem, the spreading characteristic is selected as unidirectional, and the exponent value in cos spreading function is the default value (which is "1").

Therefore, there are three parameters left to be determined: the wave direction, the significant wave height and the peak period.

The template is a symmetric structure and the jack-up is fixed at a certain position, so the wave direction won't produce a significant influence on the final result. Thus the problem remains is to decide the significant wave height and the peak period.

Significant wave height

In order to decide the significant wave height, a comparison between the dynamic performances under different wave heights will be presented.

To compare the dynamic performance under different wave heights, the wave period should be maintained the same. Under this assumption, a comparison between two circumstances concerning the vertical position and the total coupling force in the Z-axis will be carried out.

Case 1: Hs=4.5m&Tp=5s

Case 2: Hs=1.5m&Tp=5s

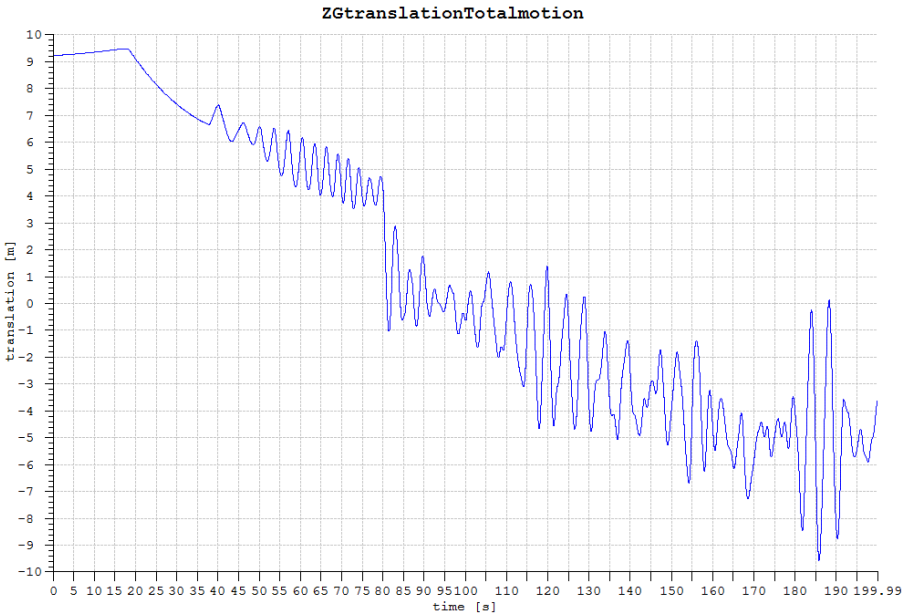

Figure 7.2 Vertical translation of the template (Case 1)
(max= 9.489, min=-7.883, mean= 1.148, dev= 5.183)

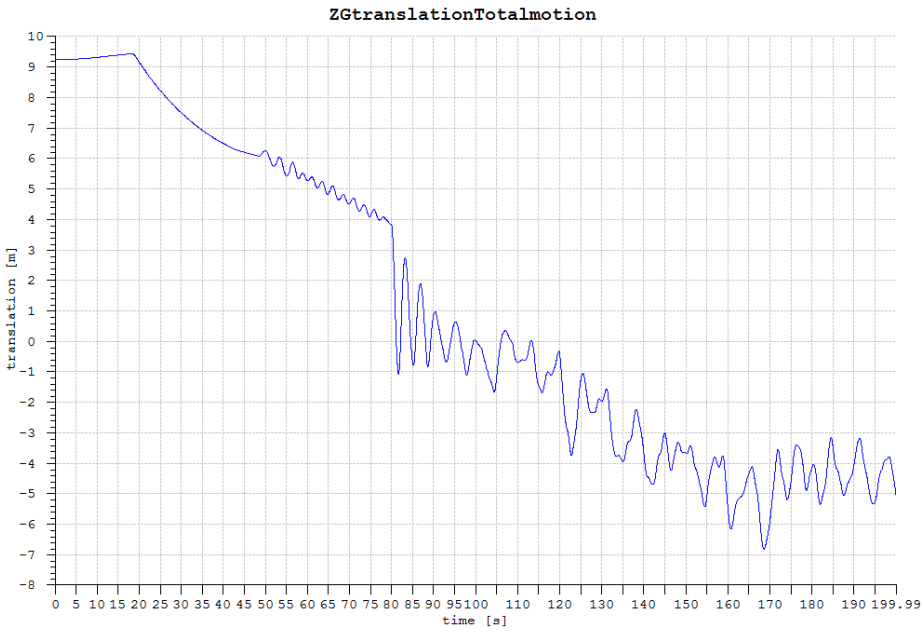

Figure 7.3 Vertical translation of the template (Case2)
(max= 9.438, min=-5.741, mean= 1.446, dev= 4.789)

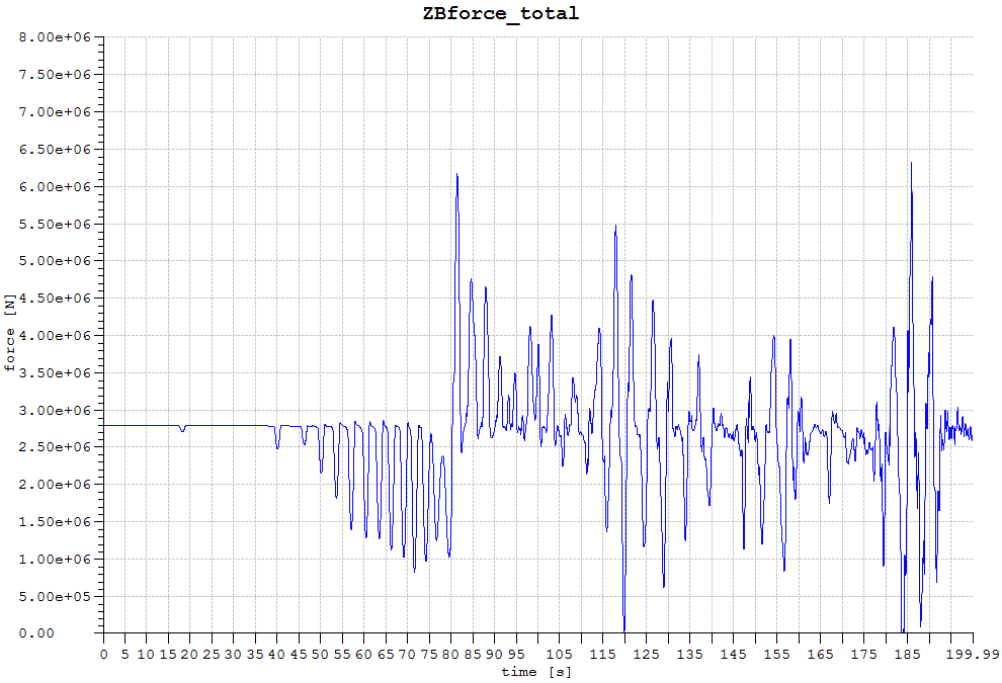

Figure 7.4 Total vertical coupling force on template (Case1)
(max=6.278e+06, min= 0.000, mean=2.677e+06, dev=7.214e+05)

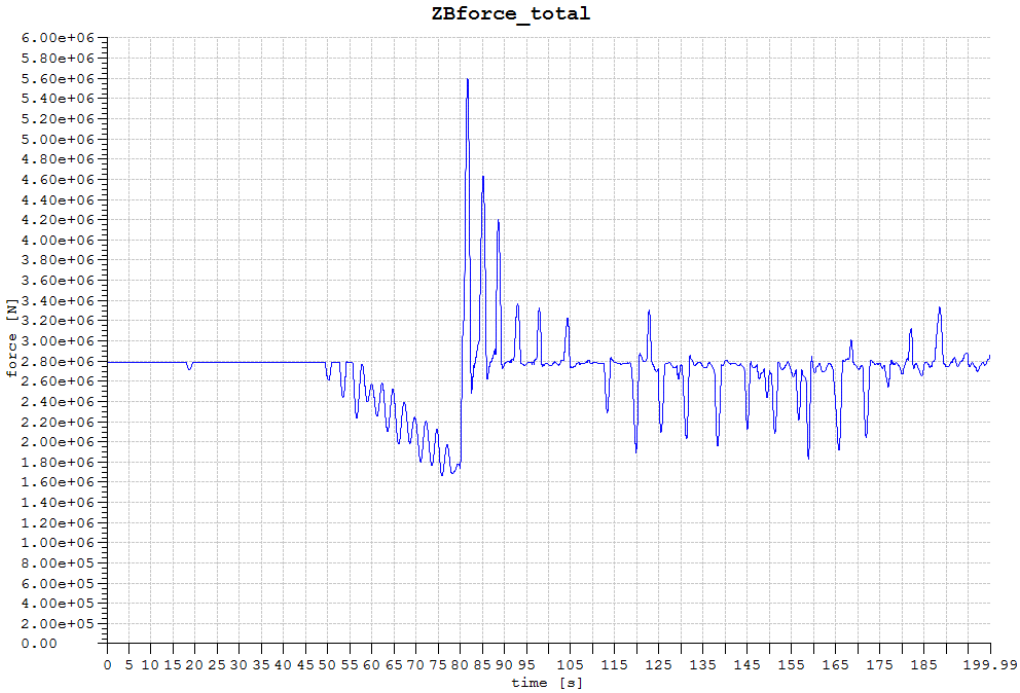

Figure 7.5 Total vertical coupling force on template (Case2)
(max=5.662e+06, min=1.659e+06, mean=2.730e+06, dev=3.678e+05)

Based on the information from figure 7.2 to figure 7.5, it is obvious that with the increase of the significant wave height, both of the amplitude of the vertical motion of the template during the lowing operation as well as the total coupling force acting on the template witness a dramatic increase. Since the original purpose of this thesis is to do the analysis of the lifting operation under harsh environment, thus the significant wave height will be 4.5m instead of 1.5m.

Peak Period

As for the wave peak period, the variables controlling method is applied as well. However, since the effect of the wave period on the performance is more complicated, more cases will be required to obtain the comparison. Thus there will be 5 cases involved in the determination of the wave peak period.

Case 1: Hs=4.5m&Tp=2.5s
Case 2: Hs=4.5m&Tp=5s
Case 3: Hs=4.5m&Tp=7.5s
Case 4: Hs=4.5m&Tp=10s
Case 5: Hs=4.5m&Tp=15s

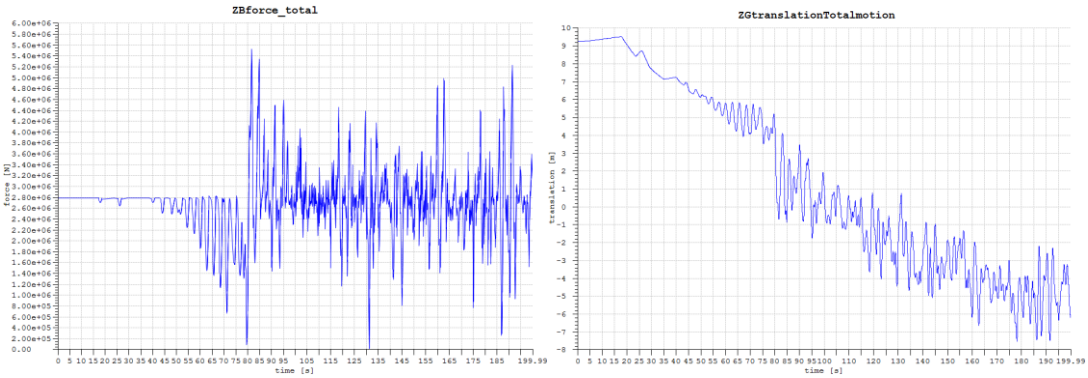

Figure 7.6 Vertical total force and vertical motion of the template, Case 1

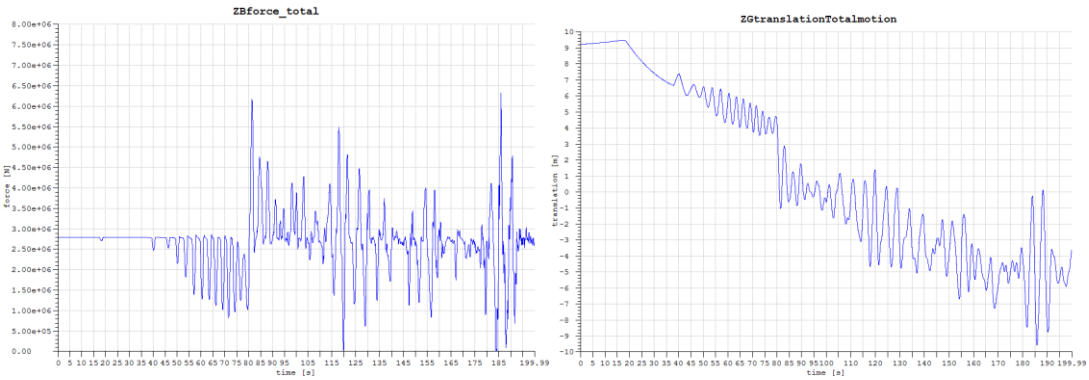

Figure 7.7 Vertical total force and vertical motion of the template, Case 2

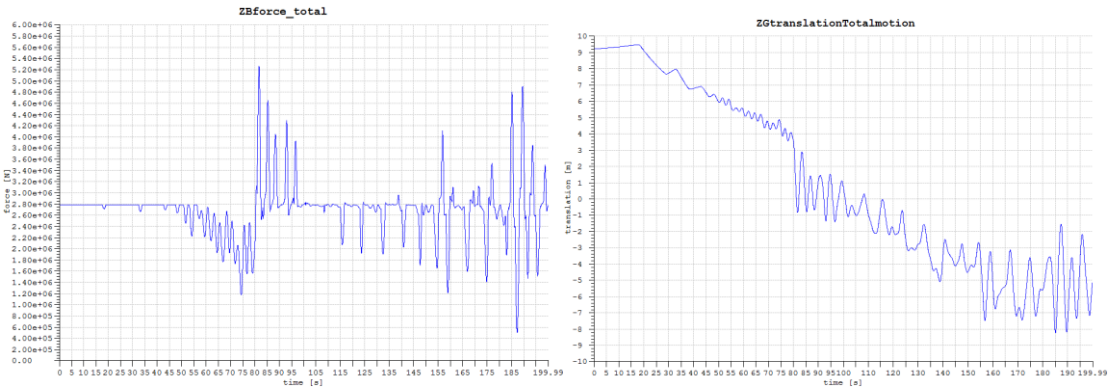

Figure 7.8 Vertical total force and vertical motion of the template, Case 3

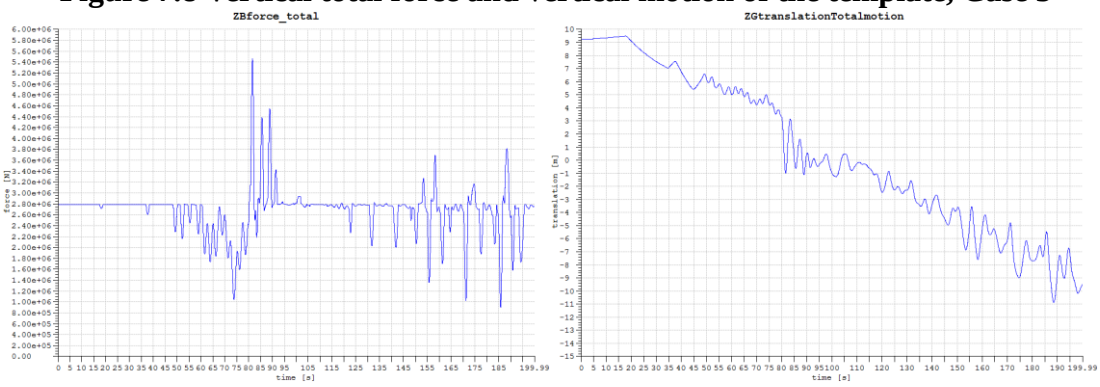

Figure 7.9 Vertical total force and vertical motion of the template, Case 4

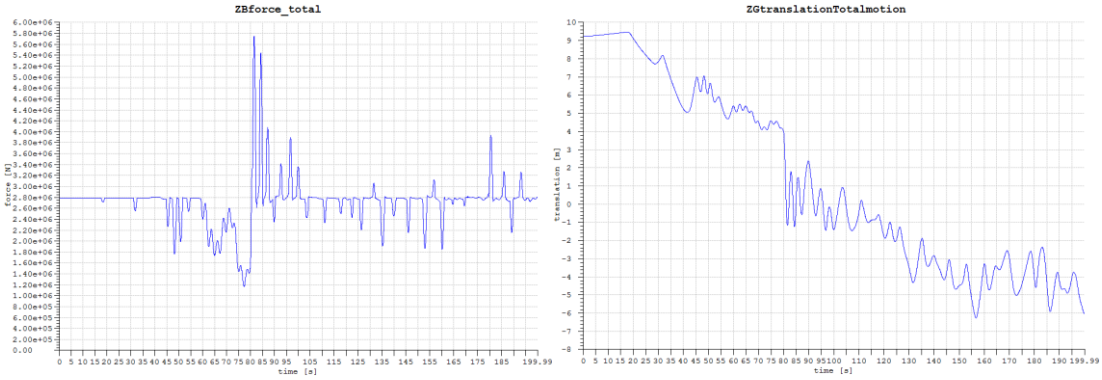

Figure 7.10 Vertical total force and vertical motion of the template, Case 1

Figure 7.6 to 7.10 shows that both the vertical coupling force and the vertical template motion experience a soft increace while the Tp increase from 2.5s to 5s. After that, two variables tend to decrease immediately once the peak period exceed 5s. Therefore, for the purpose of undertaking the anaylysis in harsh-zone, the wave peak period is finally chosen as 5s.

To summarize, the significant wave height applied in this thesis is 4.5m while the peak period is 5s.

7.2 Dynamic analysis of the template

The template is the heaviest and the most complicated structure in the lifting system, which makes the dynamic performance of the template is of most concern and attention.

Before the analysis is carried out, a brief study on the procedure of lowing the template with the winch should take place.

The winch starts to work at time point t=10s with a velocity of v=0.1m/s.

With reference to the static analysis, the vertical position of the template is 9.24m, which is to say that the distance between bottom of vertical tank element and the water surface is 3.24m, and the top point of the template is 17.24m away from the water surface. So it will take 33s for the template to have contact with the water surface, and the time node when the template is fully submerged is t=10+173=183s.

Table 7.1 Lowing procedure of the lifting operation

Time node	Events
0s	The dynamic analysis starts
10s	The winch starts to work
43s	The template starts to have contact with the water surface
80s	The specified force is added in the program to balance the redundant buoyancy
103s	Vertical tank of the template is fully submerged
183s	The template is fully submerged

7.2.1 Analysis on Total Force

Total force records the resultant force loaded on the template, containing six components: XRforce, YRforce, ZRforce, Moment_XRaxis, Moment_YRaxis and Moment_ZRaxis.

The following figures show the all the force and moment components of the total force.

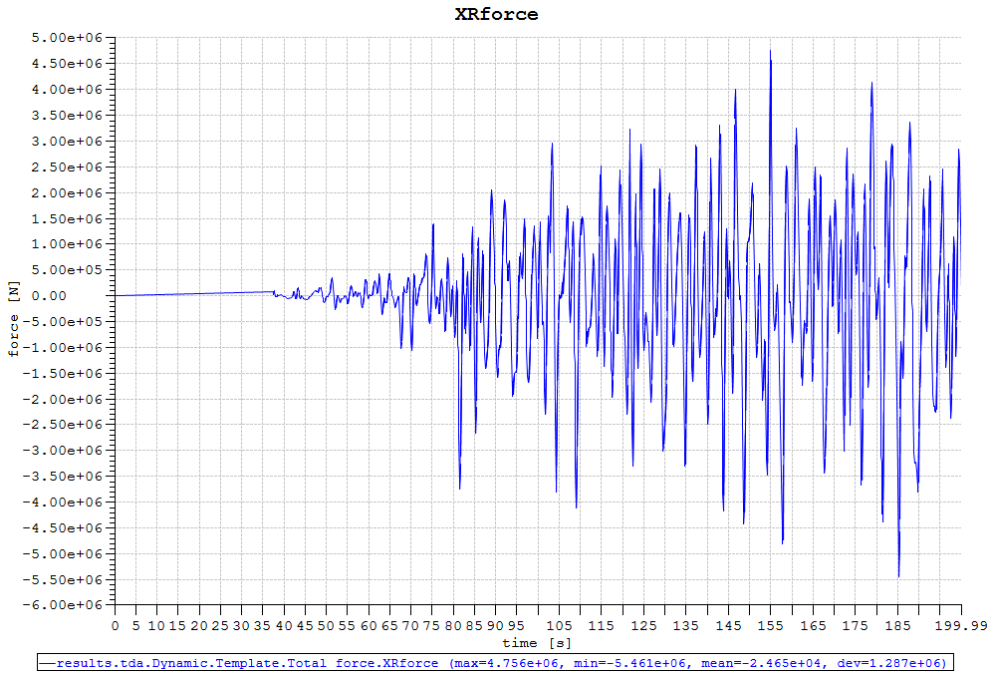

Figure 7.11 Force component of the total force, X-axis.
(max=4.756e+06, min=-5.461e+06, mean=-2.465e+04, dev=1.287e+06)

From the time period from 0s to 35s, the total force in the X direction is around zero, this is because that during this period, the template is still above the water surface. After that, the XRforce experience a smooth growth within the time range [35, 80]. And eventually the XRforce witness a harmonic force with a mean value around 0.

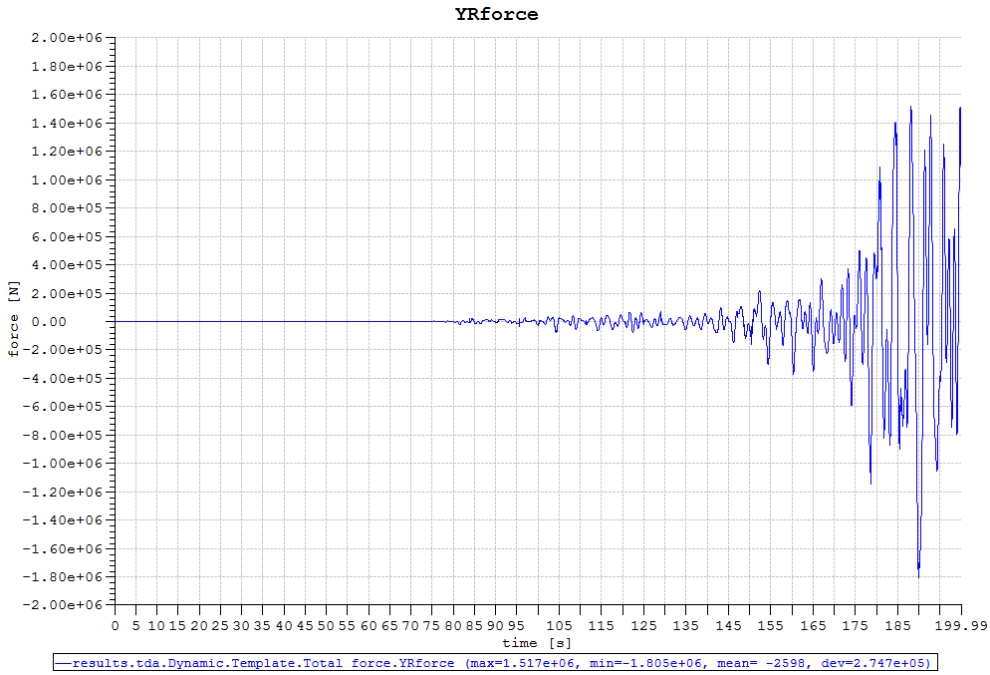

Figure 7.12 Force component of the total force, Y-axis.
(max=1.517e+06, min=-1.805e+06, mean= -2598, dev=2.747e+05)

The total force in the Y-direction is kept within a small level during a long range from 0s to almost 160s. However, it increases up to 7.00e+05N after the template is fully submerged.

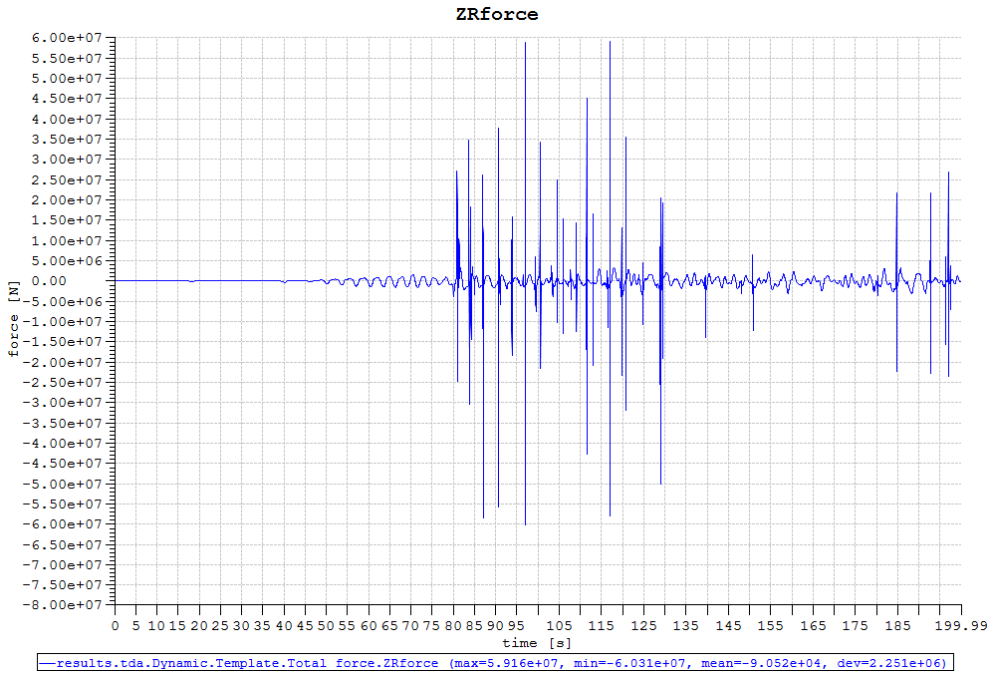

Figure 7.13 Force component of the total force, Z-axis.
(max=5.916e+07, min=-6.031e+07, mean=-9.052e+04, dev=2.251e+06)

Generally, the total force in the vertical direction is fully balanced. However, there are

still several mutations take place at the certain time points, like for instance, t=80s while the specified force is added and t=185s when the template is fully submerged.

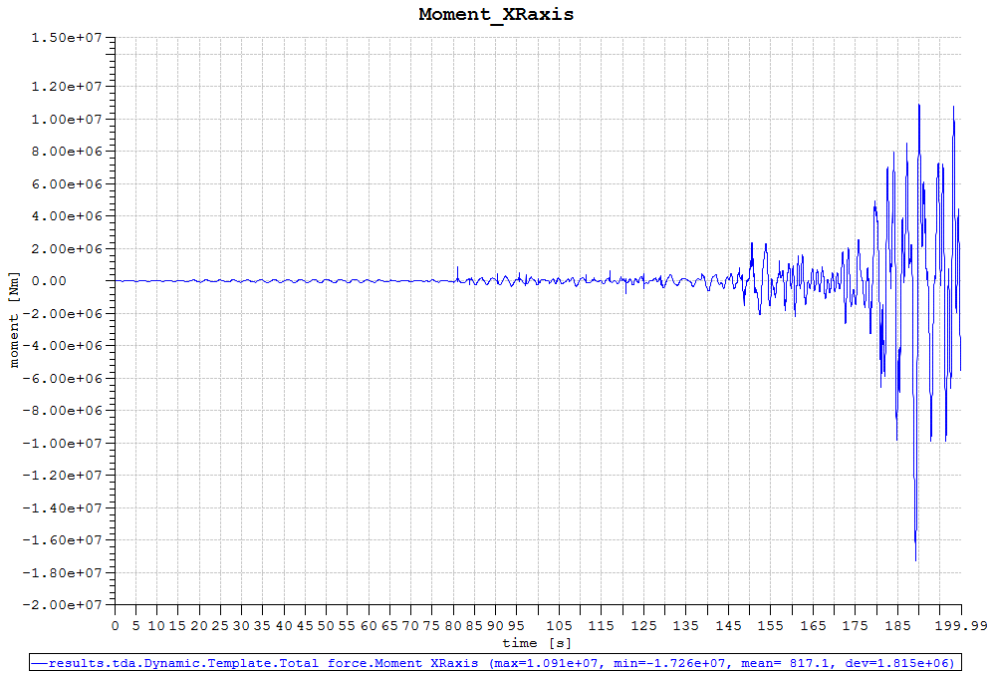

Figure 7.14 Moment component of the total force, X-axis.
(max=1.091e+07, min=-1.726e+07, mean= 817.1, dev=1.815e+06)

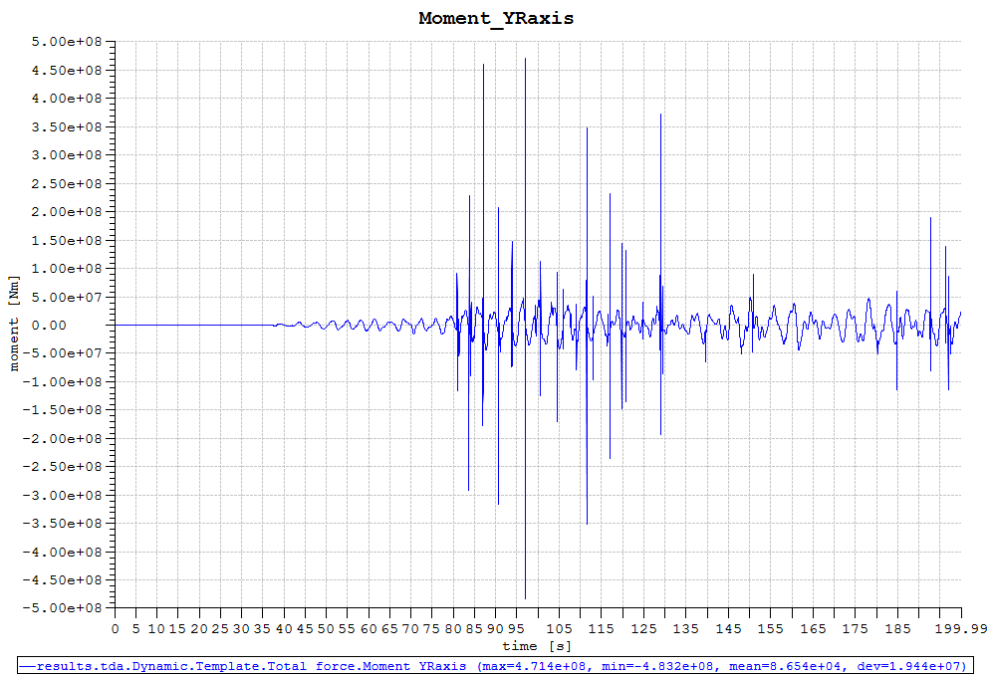

Figure7.15 Moment component of the total force, Y-axis.
(max=4.714e+08, min=-4.832e+08, mean=8.654e+04, dev=1.944e+07)

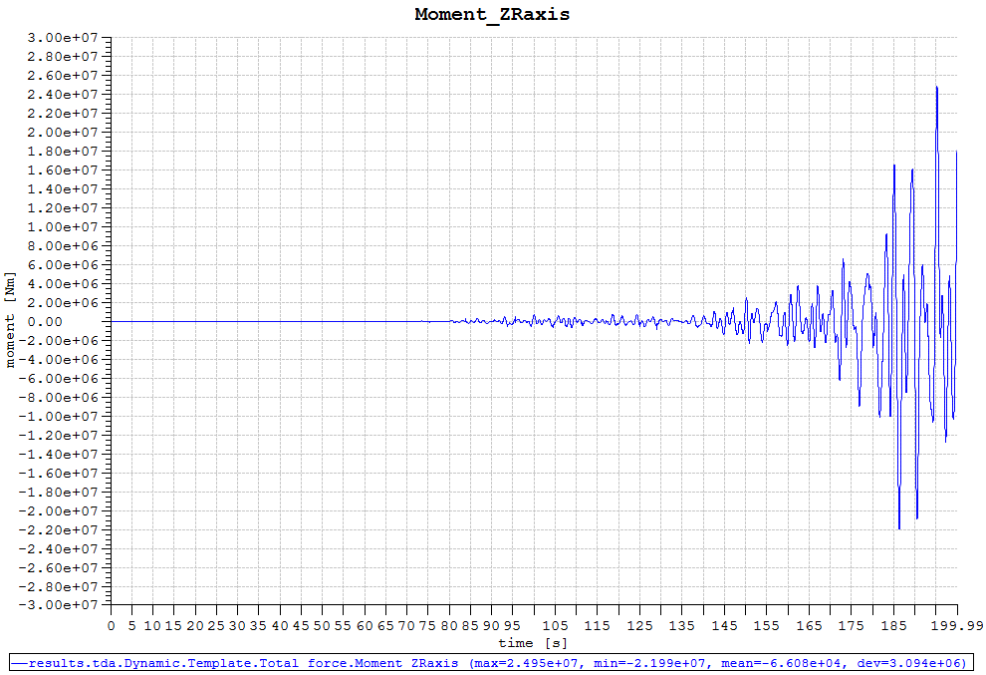

Figure7.16 Moment component of the total force, Z-axis.
(max=2.495e+07, min=-2.199e+07, mean=-6.608e+04, dev=3.094e+06)

Overall, the moment component is not of much concern in this thesis. From the figures it can tell that the moment component is varying within a small range around zero value at most of time. But it will increase up to a significant level at certain points.

In order to compare the different force components more directly, the maximum and minimum value as well as the mean value and the deviation of each components are listed in the following table.

Table 7.2 Comparison of the force components

Parameters / Component	Maximum Value	Minimum Value	Mean value	Deviation
XRforce	4.756e+06 (N)	-5.461e+06 (N)	2.465e+04 (N)	1.287e+06
YRforce	1.517e+06(N)	-1.805e+06 (N)	-2598 (N)	2.747e+05
ZRforce	5.916e+07(N)	-6.031e+07 (N)	-9.052e+04 (N)	2.251e+06
Moment-X	1.091e+07(Nm)	-1.726e+07(Nm)	817.1 (Nm)	1.815e+06
Moment-Y	4.714e+08(Nm)	-4.832e+08(Nm)	8.654e+04 (Nm)	1.944e+07
Moment-Z	2.495e+07(Nm)	-2.199e+07(Nm)	-6.608e+04(Nm)	3.094e+06

Based on the information from the table, more attention should be paid to the vertical force and the moment along the y-axis during the analysis of the lifting operation.
Take the ZRforce for instance, the weight of the template is

$$G = \mathrm{mg} = 285 \times 1000 \times 9.81 = 2.796 \times 10^6 (N)$$

This is to say that the maximum vertical force acting on the template is more than 20 times of its own weight, which will give an extreme challenge for the capacity of the lifting lines. So the analysis concerning the coupling force acting on the template is about to be carried out in the following section.

7.2.2 Analysis on Sum Coupling System Force

There are totally 4 lifting wires connected with the template, named as “wire 1”, “wire 2”, “wire 3” and “wire 4” in the program. The total coupling force as well as the force components for each wire will be discussed separately in this thesis.

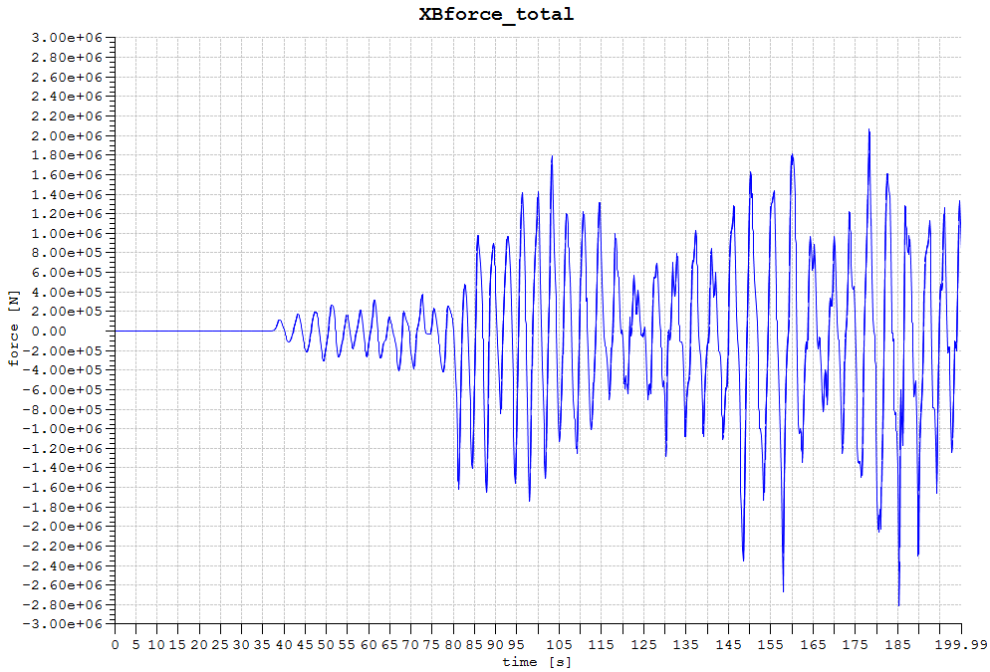

Figure 7.17 Total coupling force on the template, X-axis (max=2.069e+06, min=-2.816e+06, mean=-2.590e+04, dev=6.766e+05)

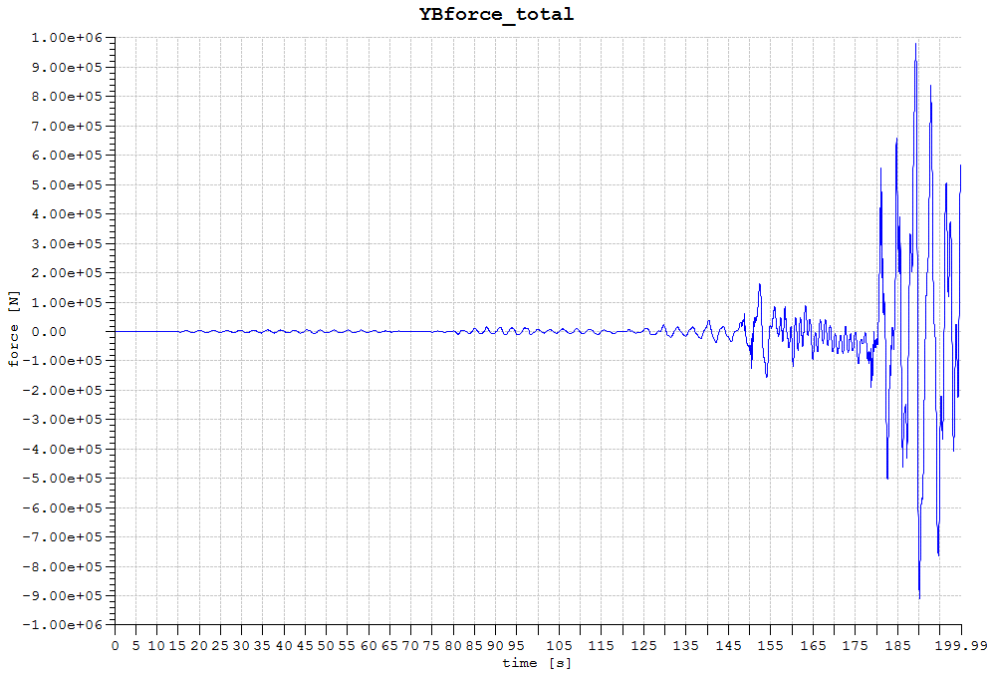

Figure 7.18 Total coupling force on the template, Y-axis (max=9.798e+05, min=-9.110e+05, mean=-1053, dev=1.271e+05)

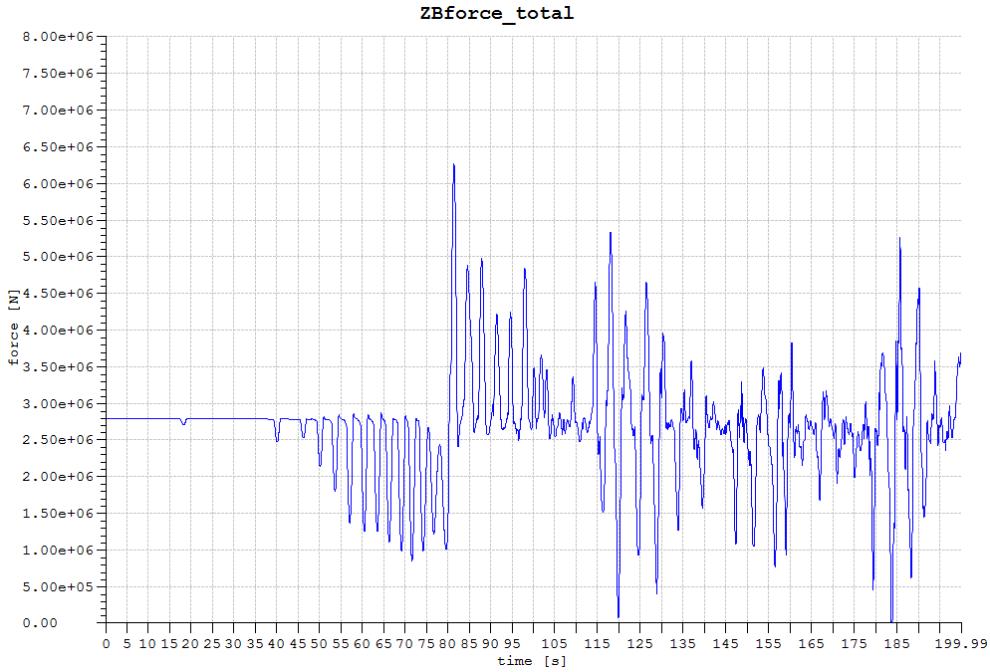

Figure 7.19 Total coupling force on the template, Z-axis (max=6.278e+06, min= 0.000, mean=2.677e+06, dev=7.214e+05)

Figure 7.17, 7.18, and 7.19 show the total coupling force acting on the template.
The total coupling force in X-axis is nearly a harmonic load with a mean value slightly over zero in the negative X-direction.
The total coupling force in Y-axis remain stable around zero value except there is a

mutation after t=180s, which is the time for the template to be fully submerged.

Finally it comes to the vertical coupling force component. First of all, the total coupling force is positive all the time. Secondly, the vertical force varies with the mean value of 2.677e+06(N), which is the weight of the template.

DAF Analysis

To do a further analysis on the template, the Dynamic Amplitude Factor (DAF) is brought in.

The Dynamic Amplitude Factor is defined as: [12]

$$\mathrm{DAF} = \frac{1}{\sqrt{\left[1-\left(\frac{T_n}{T}\right)^2\right]^2+\left[2\lambda\frac{T_n}{T}\right]^2}} \tag{7.1}$$

Where,

T_n = Natural period of the structure

T = Wave period

λ = Damping ratio

On the meantime the dynamic amplitude factor is also calculated as:

$$\mathrm{DAF} = \frac{Dynamic\ Response}{Static\ Response} = \frac{Dynamic\ Load}{Static\ Load} = \frac{6.278e+06}{2.786e+06} = 2.25 \tag{7.2}$$

The wave period is 5s. Assume the damping ration as 0.01, the natural period of the template can be solved by combing eq. (7.1) and (7.2). The result gives out that T_n =2.89s.

Coupling Force Component

As discussed before in chapter 5, in order to simply the problem, all the lifting wires are modeled as non-failure mode, which is impossible and unrealistic. So it needs to pay attention to the maximum tension force in the lifting wires, and save the related information to check or confirm with the real breaking strength for the further operations.

Additional, the compression in the lifting lines will also lead to serious operation accidents, which needs to be avoided in the real circumstances.

The tension force of the wires could be achieved by combining the vertical components of the tension force and the angle between the wire and the horizontal plane. The basic concept is illustrated in the figure below.

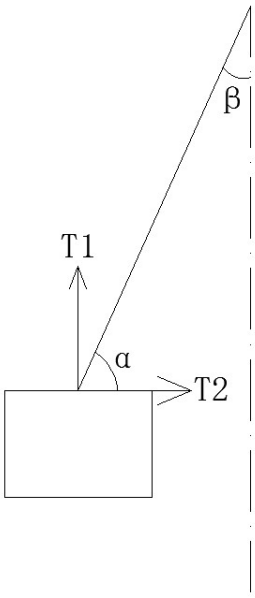

Figure 7.20 The sketch of the lifting wire of the template

Figure 7.20 tells very clear that the tension force of the wire can be calculated as:

$$\mathrm{T} = \frac{T_1}{\sin\alpha} = \frac{T_1}{\cos\beta} \tag{7.3}$$

$$\sin\alpha = 0.805 \tag{7.4}$$

Since the template and the lifting wires are both symmetric system, thus all the forces in the four wires are equal to each other, neglecting the influence of the force direction. Therefore wire 1 is taken out as an instance for the local coupling force analysis.

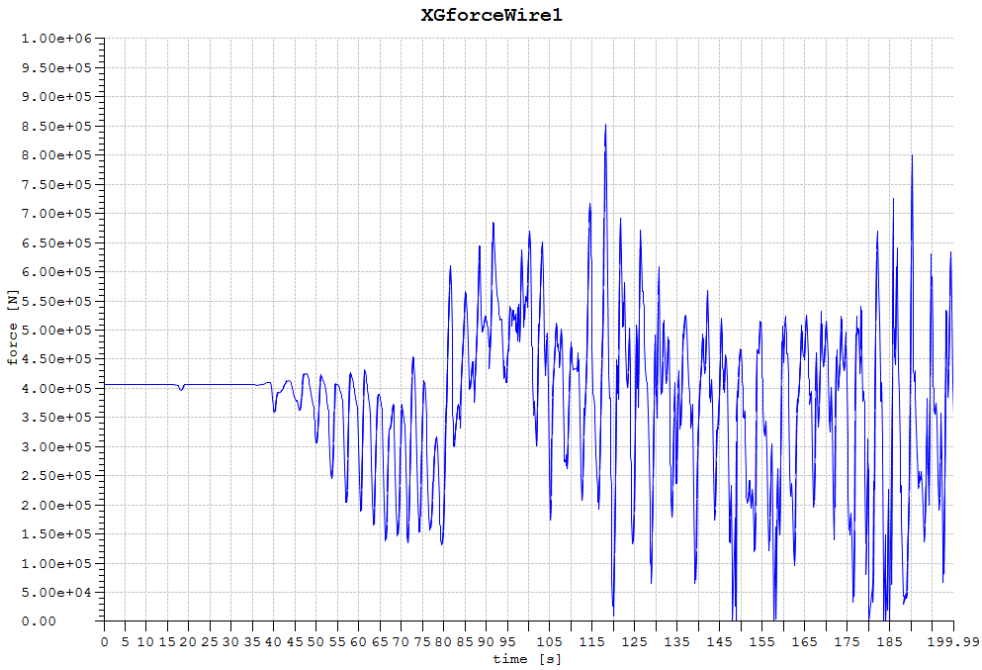

Figure 7.21 Local force component for wire 1, X-axis (max=8.537e+05, min= 0.000, mean=3.753e+05, dev=1.325e+05)

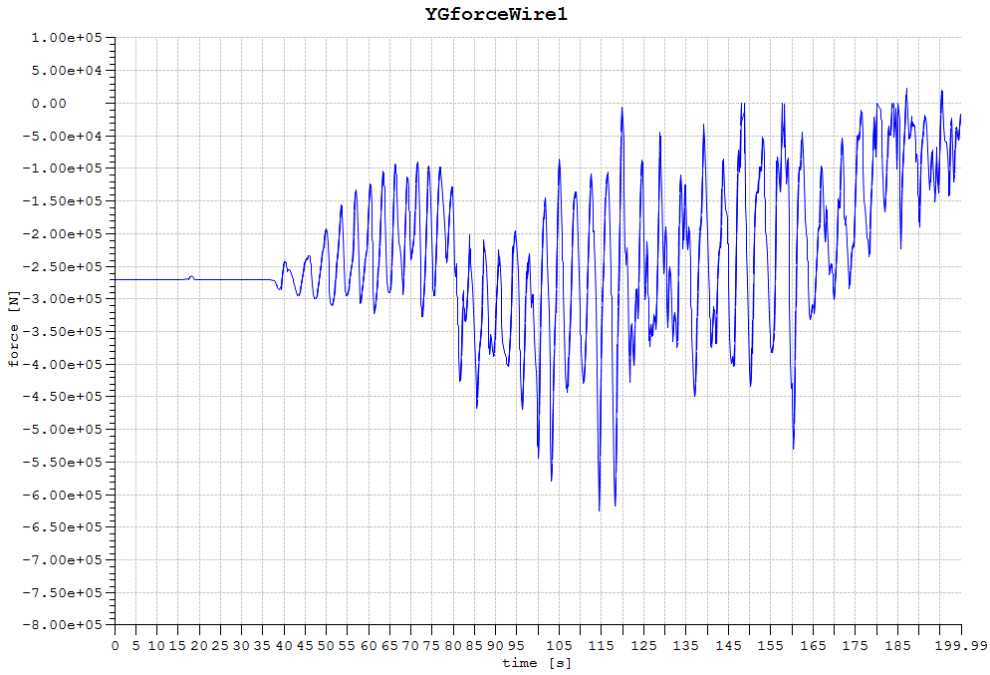

Figure 7.22 Local force component for wire 1, Y-axis (max=2.303e+04, min=-6.263e+05, mean=-2.332e+05, dev=1.102e+05)

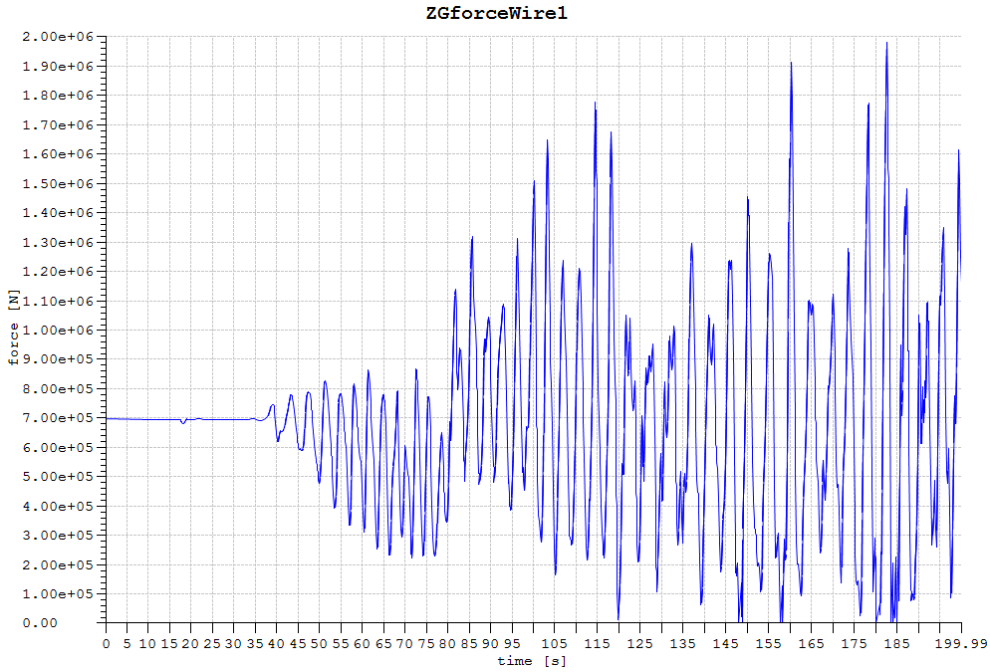

Figure 7.23 Local force component for wire 1, Z-axis (max=1.984e+06, min= 0.000, mean=6.722e+05, dev=3.294e+05)

From figure 7.23 it shows that the vertical coupling force in wire 1 is positive all the time, which is to say that there is no compression in the lines. However, it can be seen that the minimum value of the vertical coupling force is 0 and there are several points that the tension force in the lifting wires is approaching zero. The compression in the

lifting wire is very sensitive and extremely important for the safety of the lifting operation. Thus this critical situation may lead the potential risk to the operation. This is to say the operation under the wave height wave of 4.5m is very critical and has a relative high risk level.

The maximum vertical tension force is 1.984e+06, thus the maximum tension force in the lifting wires will be:

$$\mathrm{T} = \frac{T_1}{\sin\alpha} = \frac{1.984\times10^6}{0.805} = 2.465\times10^6(N) \tag{7.5}$$

7.2.3 Analysis on Global Position

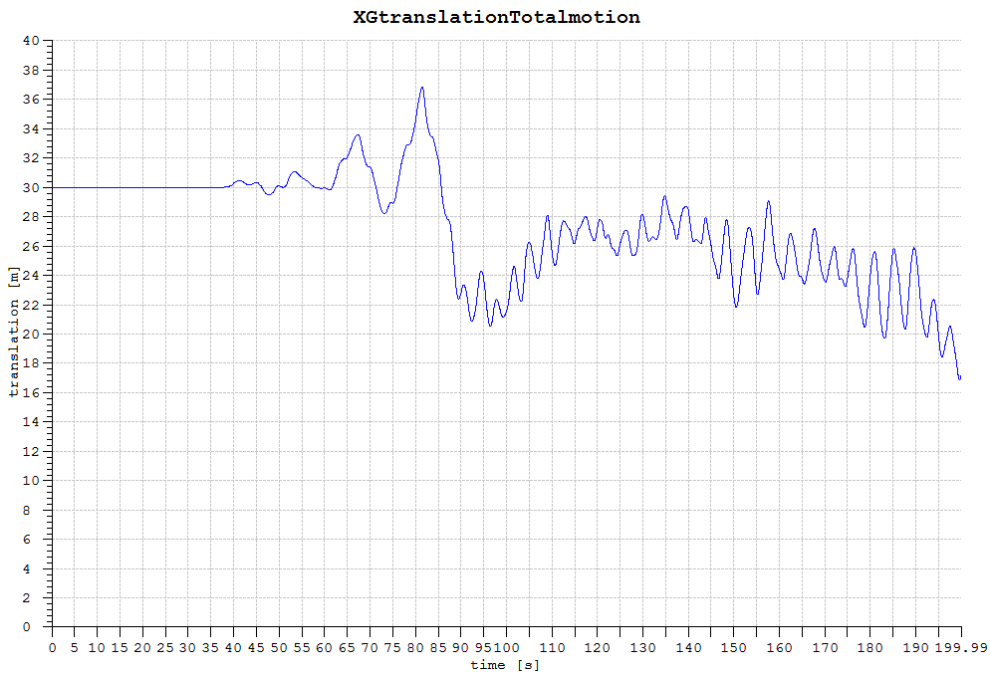

Figure 7.24 Global displacement of the template, X-axis (max= 36.87, min= 16.89, mean= 27.25, dev= 3.611)

The template experiences a large motion in the horizontal direction. The maximum displacement of the template is 6.87m in the positive direction and 13.11m in the negative direction. On this condition, there exists a potential danger that the template may hit the vessel during the lowing operation, which has to be avoided in reality.

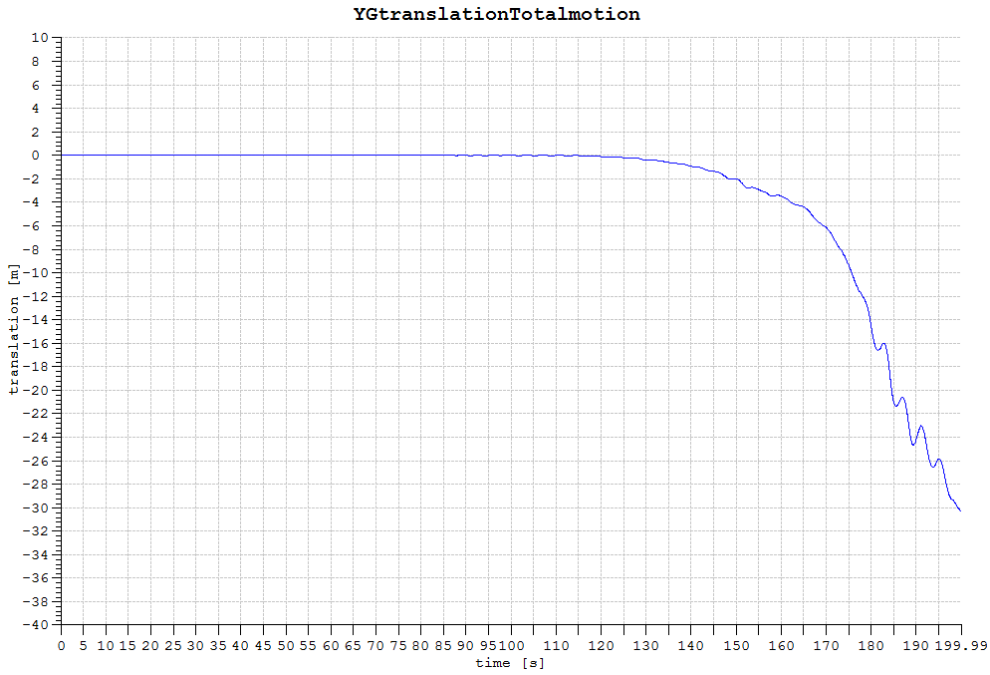

Figure 7.25 Global displacement of the template, Y-axis (max=0.02795, min=-30.30, mean=-3.284, dev= 7.154)

The template stays still at the original position in Y-direction for the quite a long time. However, it starts to drift to the negative direction in the Y-axis, the maximum displacement is around 30m. This phenomenon is unacceptable and may lead to a unsafe circumstance in the real operation.

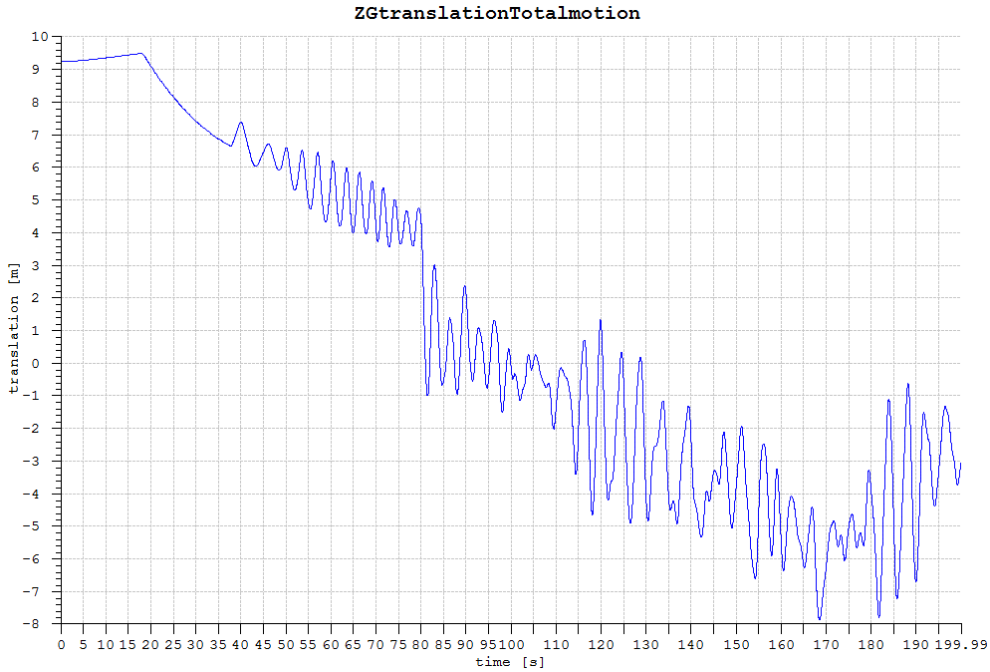

Figure 7.26 Global displacement of the template, Z-axis (max= 9.489, min=-7.883, mean= 1.148, dev= 5.183)

The template witnesses a significant vertical motion with the maximum amplitude is around 7m. This motion is extremely large and may also contribute to the potential risk and accidents.

Overall, the global position of the template under this sea-state may cause potential risk and danger to the vessel and the crews on board. Thus a research concerning the influence of sea-states on the global position of the template will be carried out in **section 7.5.**

7.2.4 Analysis on Local velocity

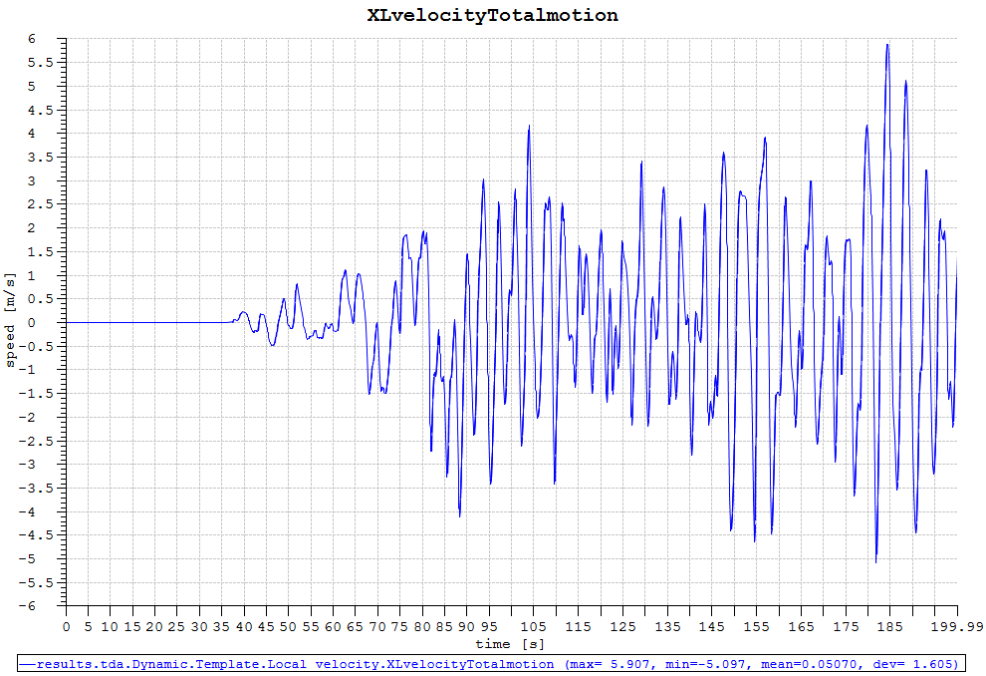

Figure 7.27 Local velocity of the template, X-axis.
(max= 5.907, min=-5.097, mean=0.05070, dev= 1.605)

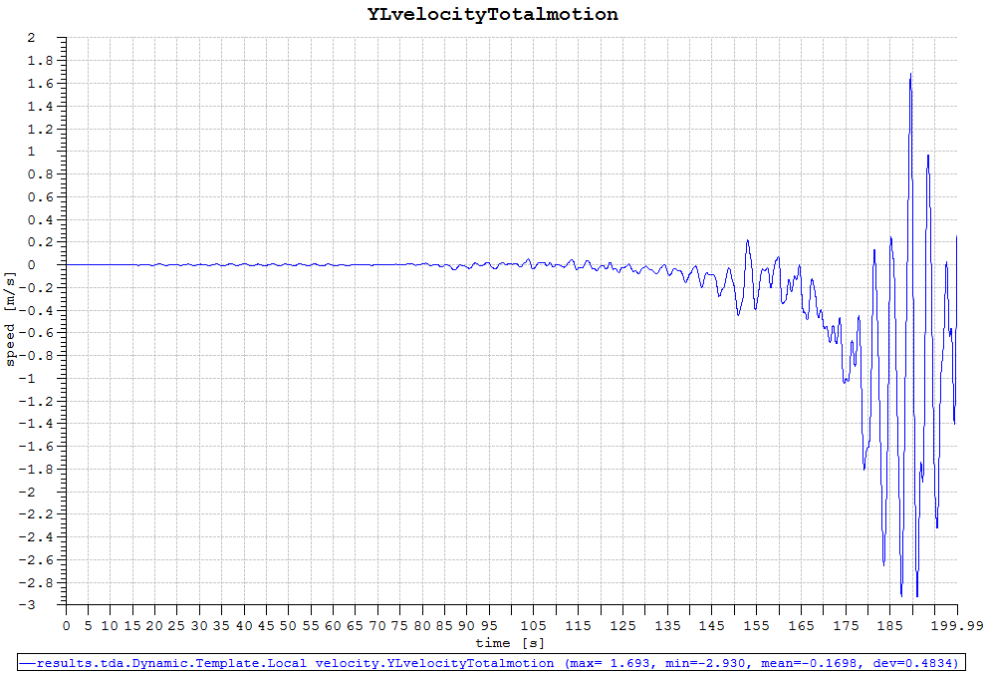

Figure 7.28 Local velocity of the template, Y-axis.
(max= 1.693, min=-2.930, mean=-0.1698, dev=0.4834)

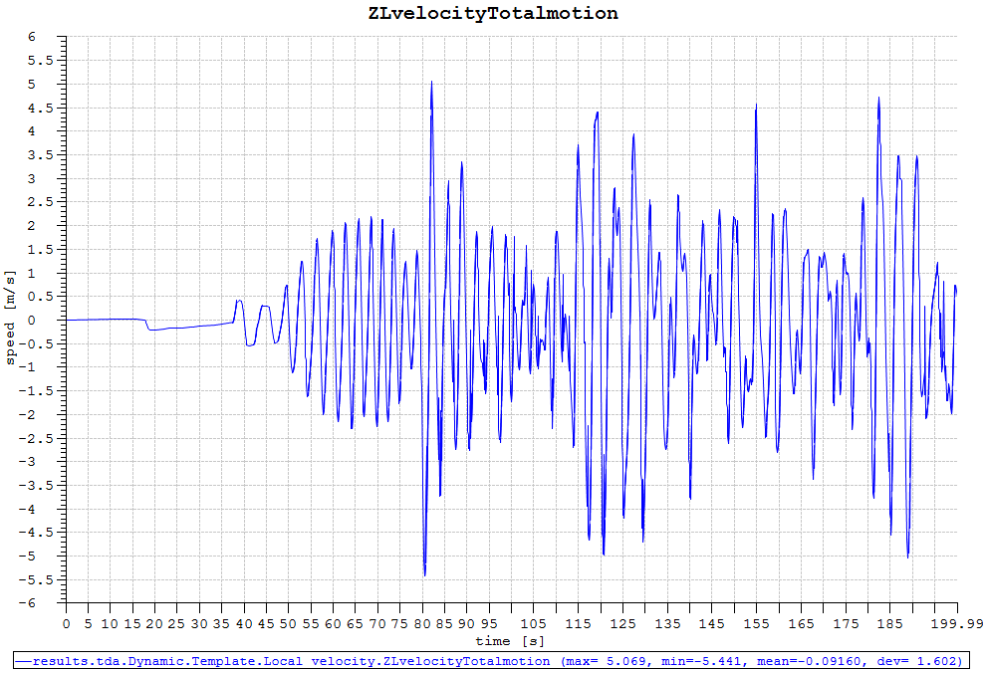

Figure 7.29 Local velocity of the template, Z-axis.
(max= 5.069, min=-5.441, mean=-0.09160, dev= 1.602)

The local velocity of the template is also of concern during the dynamic analysis. The horizontal and vertical velocity of the template is much larger than the transversal velocity. This might be caused by the direction of the incoming wave. The wave direction is 0 degree, which is exactly the X-axis direction, which explains the large

velocity in the X direction. Besides, the water partial motion leads to the large vertical velocity of the template.

7.2.5 Analysis on Local velocity Global Acceleration

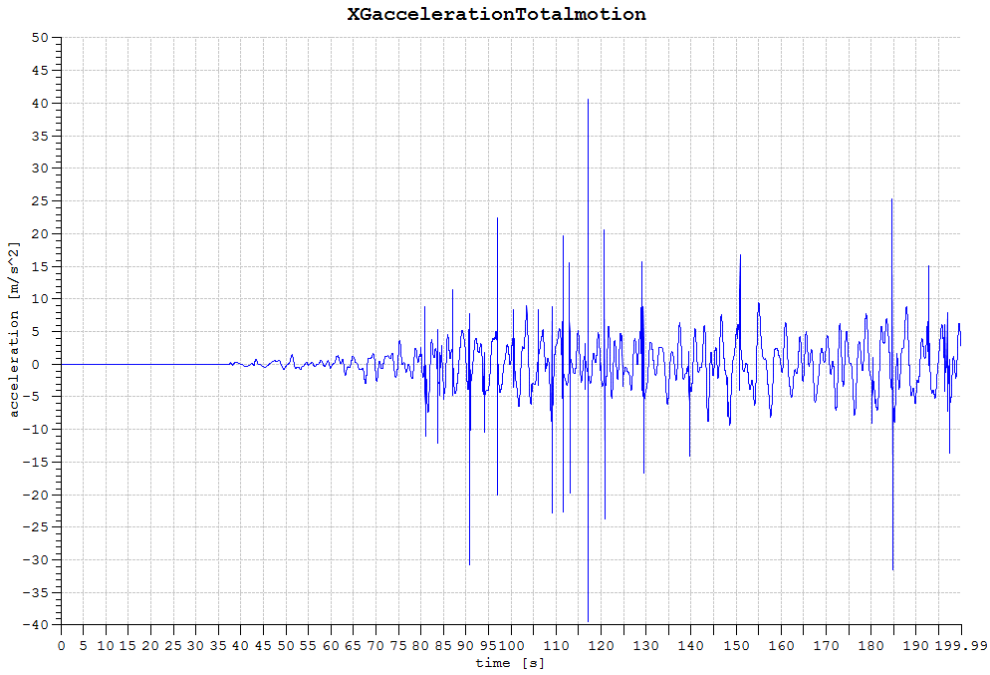

Figure 7.30 Global acceleration of the template, X-axis.
(max= 40.56, min=-39.49, mean=0.008792, dev= 2.860)

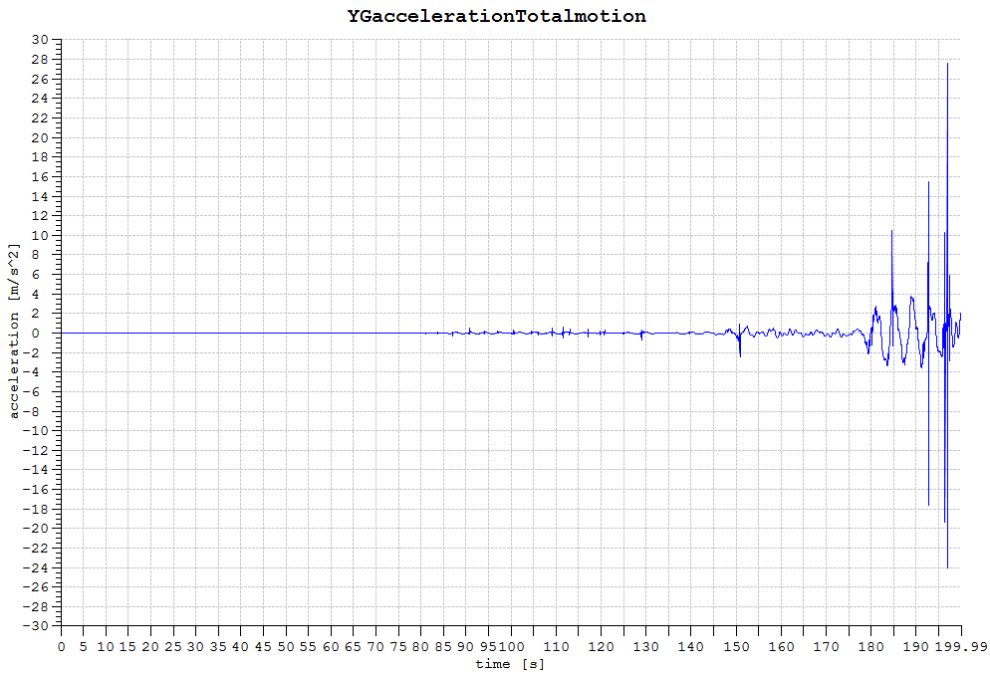

Figure 7.31 Global acceleration of the template, Y-axis.
(max= 27.62, min=-24.05, mean=0.001357, dev=0.7801)

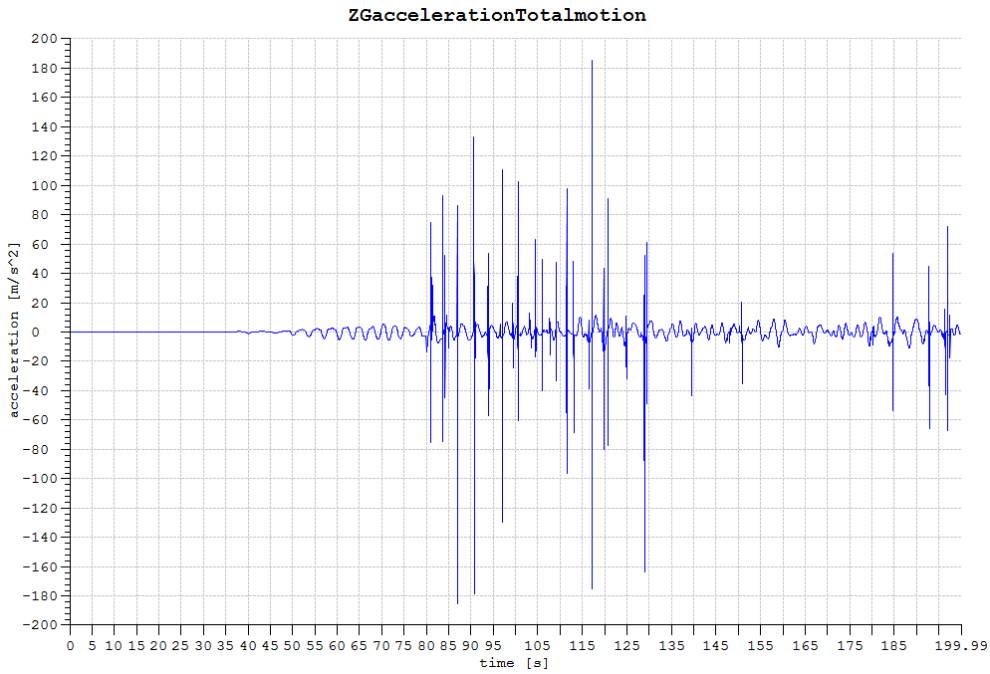

Figure 7.32 Global acceleration of the template, Z-axis.
(max= 185.3, min=-185.6, mean=0.002956, dev= 6.197)

Figure 7.30, 7.31 and 7.32 tell that the global acceleration of the templates in each direction remains within a small level, which is to say, the acceleration term is not a critical problem for the dynamic analysis.

7.3 Dynamic analysis of the Crane Master

The crane master is much lighter and more simply structure than the template, so the movement of the crane master won't affect the displacement or the loads of the template, which leaves out the effect of the velocity and acceleration term of the Crane Master. Thus this section mainly concentrates on the global position of the CM body and the coupling force of the "crane" line.
The dynamic analysis results concerning the global acceleration, local velocity as well as the total force of the crane master are all listed in Appendix A.

7.3.1 Analysis on Global Position

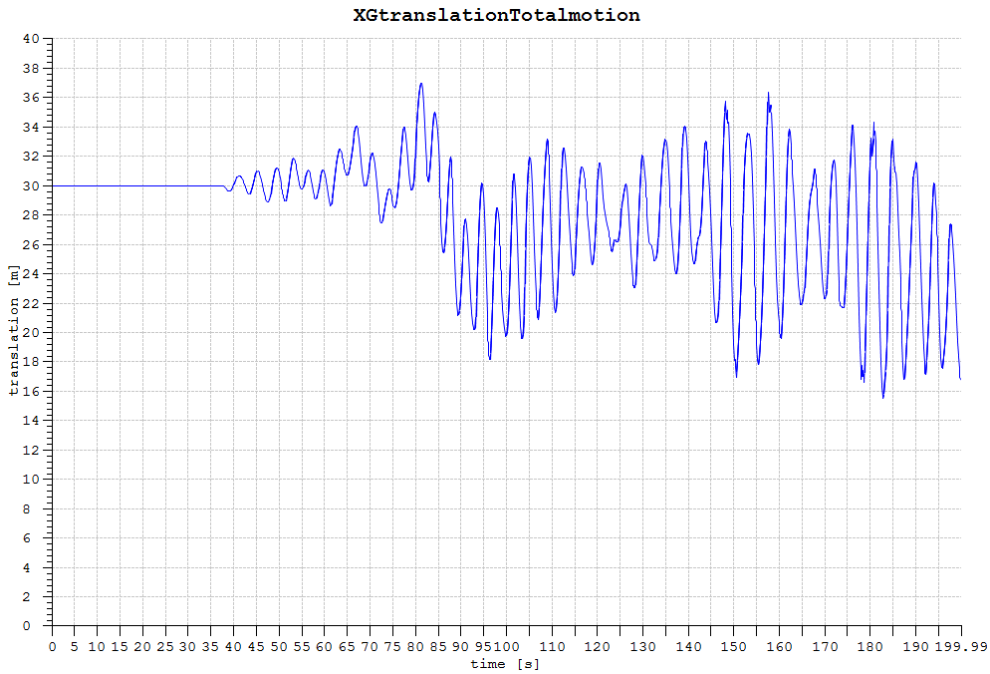

Figure 7.33 Global Position of the Crane Master, X-axis.
(max= 36.99, min= 15.50, mean= 28.10, dev= 4.141)

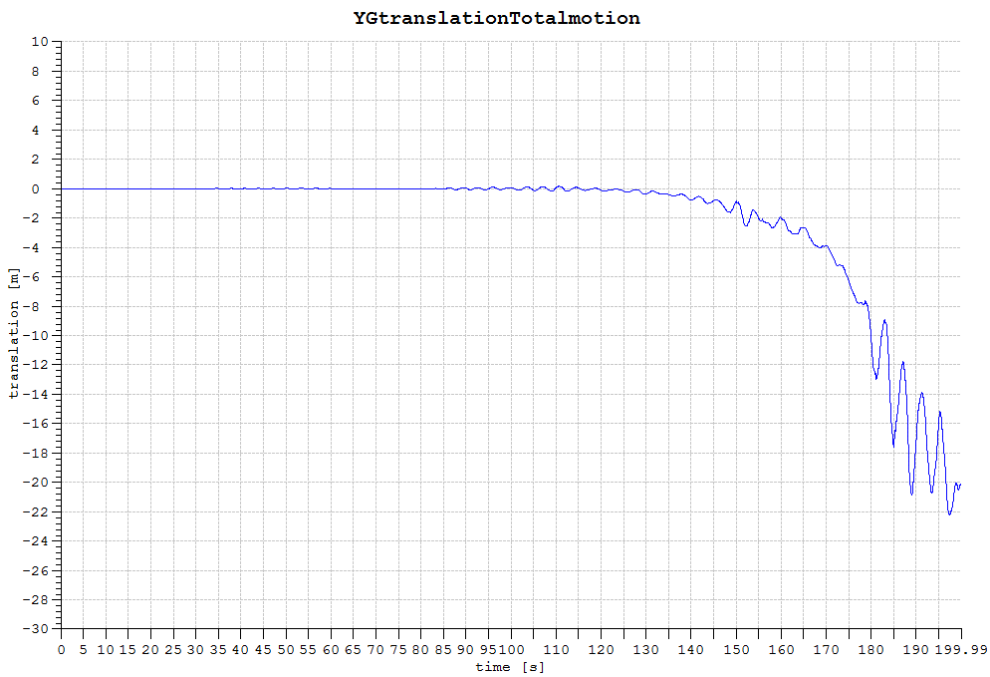

Figure 7.34 Global Position of the Crane Master, Y-axis.
(max=0.1636, min=-22.23, mean=-2.269, dev= 5.035)

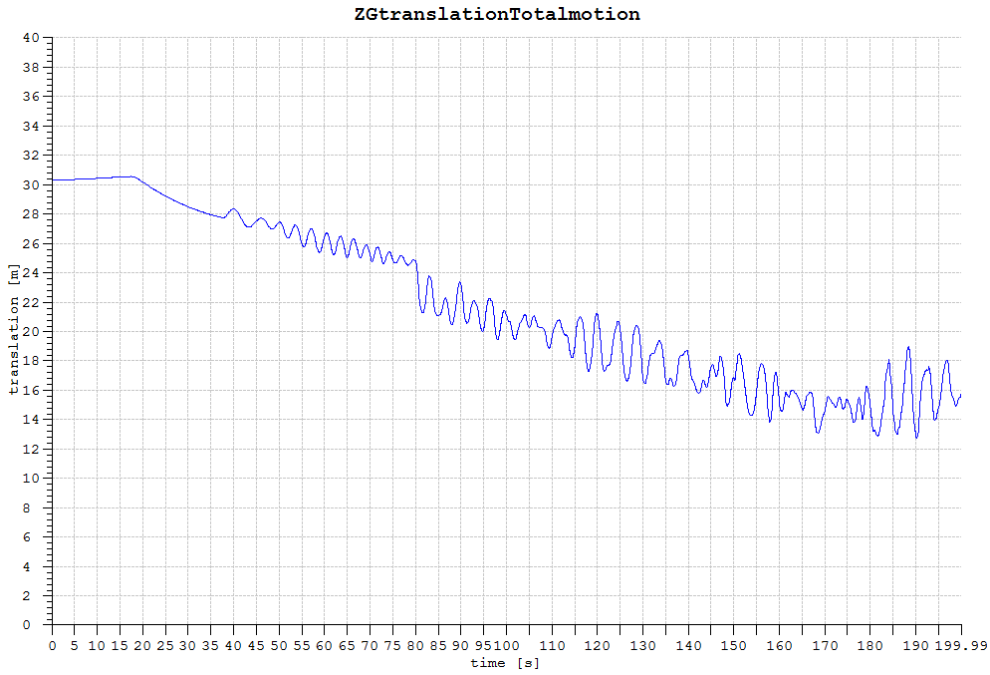

Figure 7.35 Global Position of the Crane Master, Z-axis.
(max= 30.56, min= 12.75, mean= 21.84, dev= 5.487)

Since the crane master is directly connected to the template, the global position of the CM body is very close-related to the motion of the template.
From figure 7.33 to 7.35, it can be seen that the motion of the Crane Master is similar to that of the template, except for the vertical motion. That is because the Crane Master is above the water during the operation, which leaves out the effect of the water partial motion. Therefore, the amplitude of the vertical motion of the crane master is much smaller than that of the template.

7.3.2 Analysis on Local Coupling Force

There all totally 5 wires attached to the crane master. Four of them are connected to the template, which has been analyzed in section 7.2. So only the lifting wire between the crane master and the hook remained to be check, named as “crane” in the program.
The following figures performed the analysis on the coupling force of the crane master, mainly on the “crane” wire.

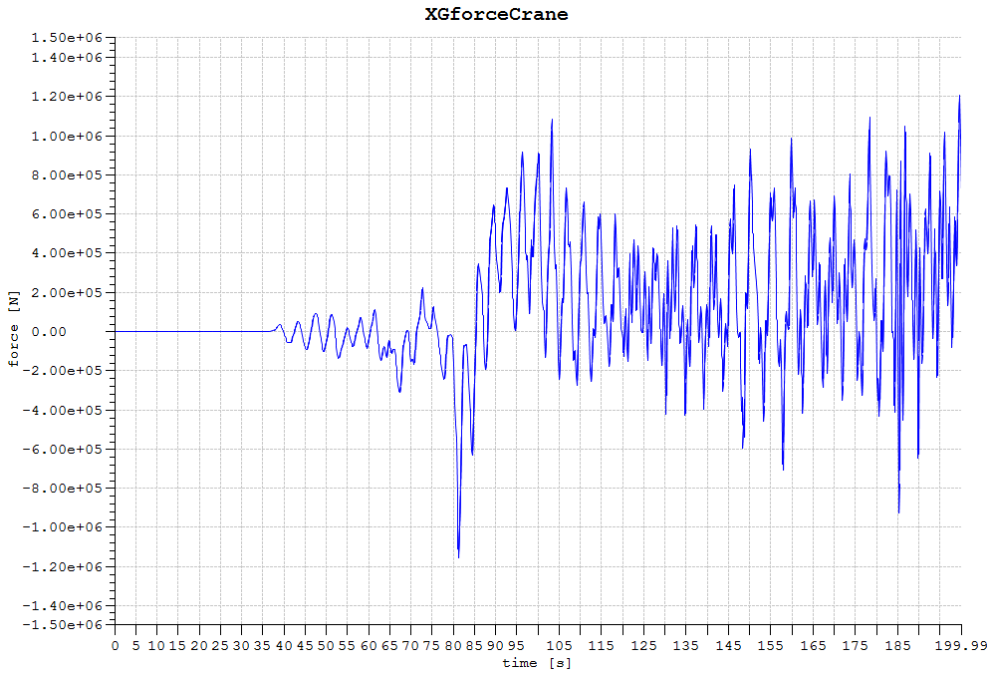

Figure 7.36 Local coupling force of the carne master, X-axis (max=1.207e+06, min=-1.160e+06, mean=1.157e+05, dev=3.002e+05)

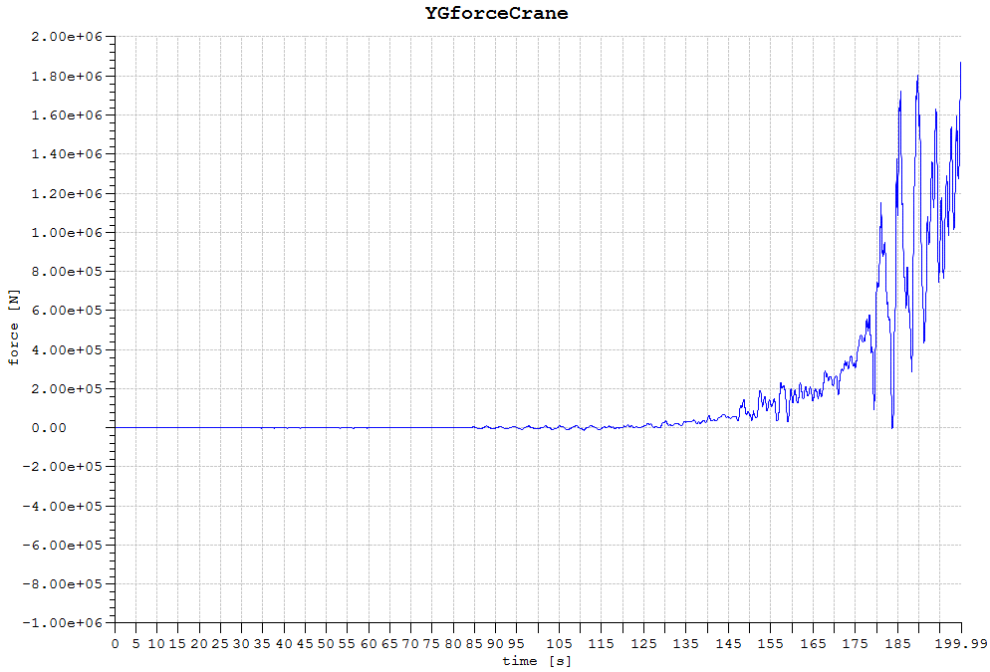

Figure 7.37 Local coupling force of the carne master, Y-axis (max=1.870e+06, min=-1.261e+04, mean=1.394e+05, dev=3.295e+05)

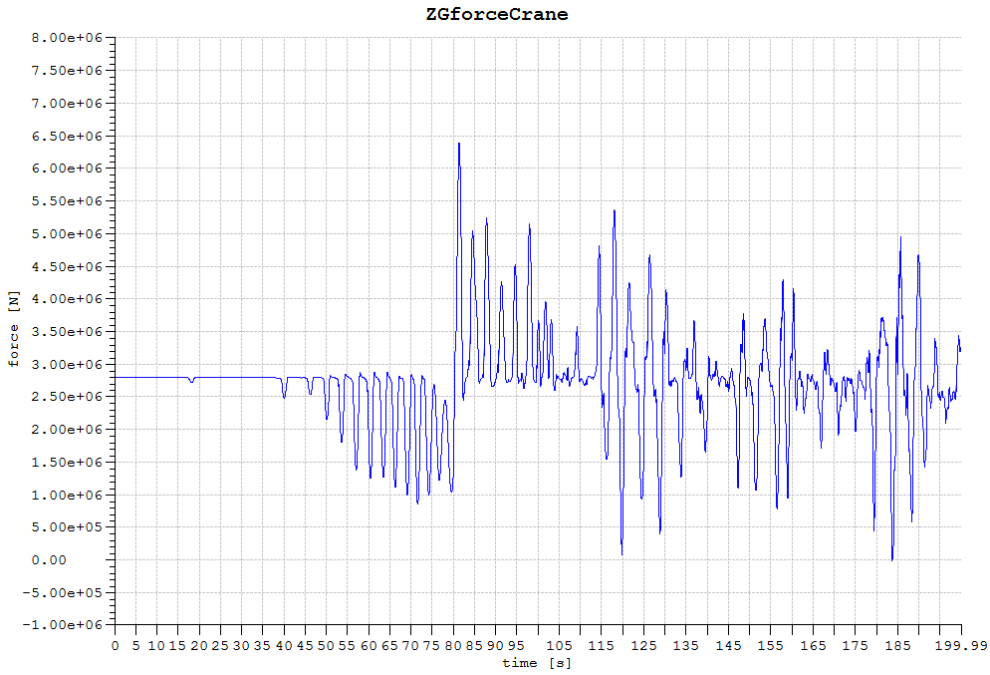

Figure 7.38 Local coupling force of the carne master, Z-axis (max=6.390e+06, min=0, mean=2.725e+06, dev=7.421e+05)

Take a further study on the vertical component of the local coupling force of the "crane" wire, this force component is a positive variable with the mean value of 2.725e+06. This value is slightly larger than the mean value of the total vertical coupling force on the template and this is mainly from the effect of the own weight of the crane master.

7.4 Dynamic analysis of the Hook

The mass of the hook is 8000kg in the model, and the hook is almost 40m higher than the template. This means that the motion of the template won't cause a significant influence on the load or motion of the hook. Thus only the result of the global position and the local coupling force will be discussed in this section.
The dynamic analysis results concerning the global acceleration, local velocity as well as the total force of the hook are also presented in Appendix A.

7.4.1 Analysis on Global Position

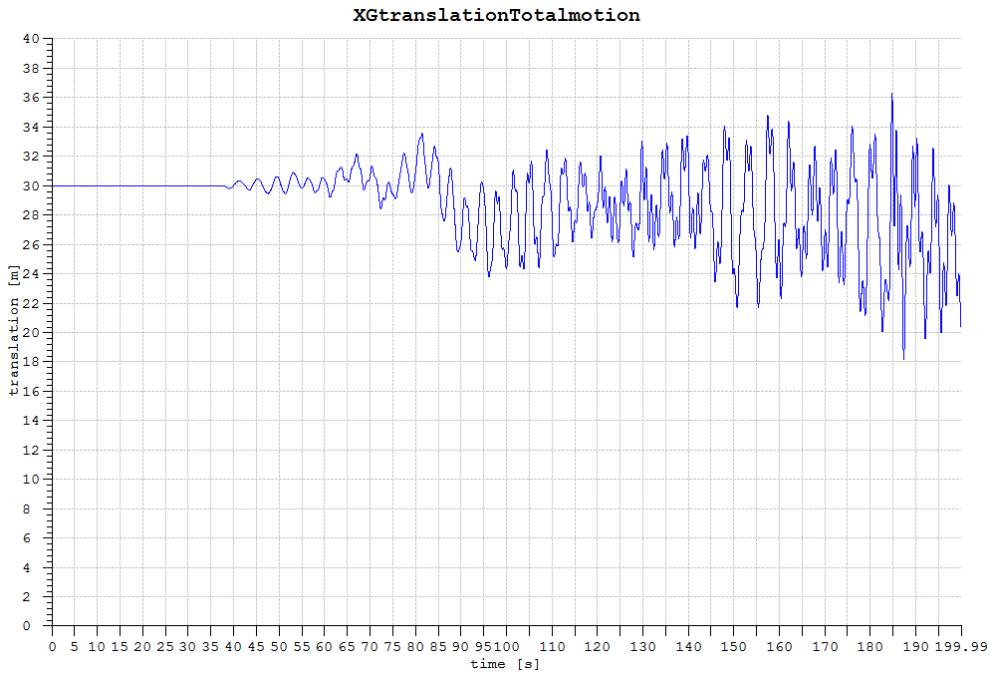

Figure 7.39 Global Position of the Hook, X-axis.
(max= 36.32, min= 18.18, mean= 28.90, dev= 2.604)

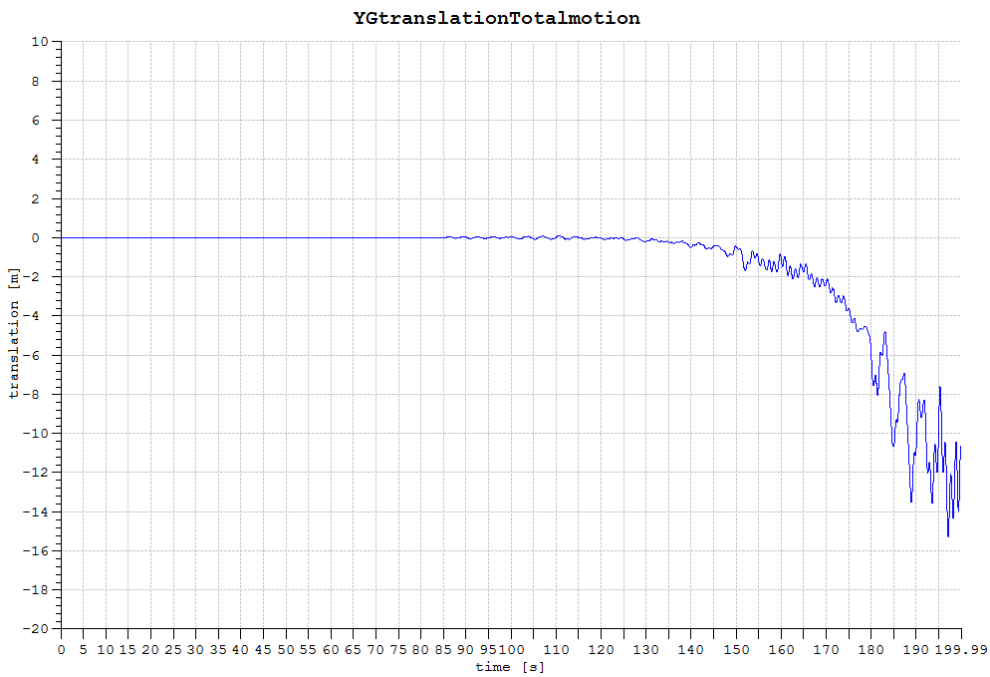

Figure 7.40 Global Position of the Hook, Y-axis.
(max=0.09853, min=-15.31, mean=-1.362, dev= 3.067)

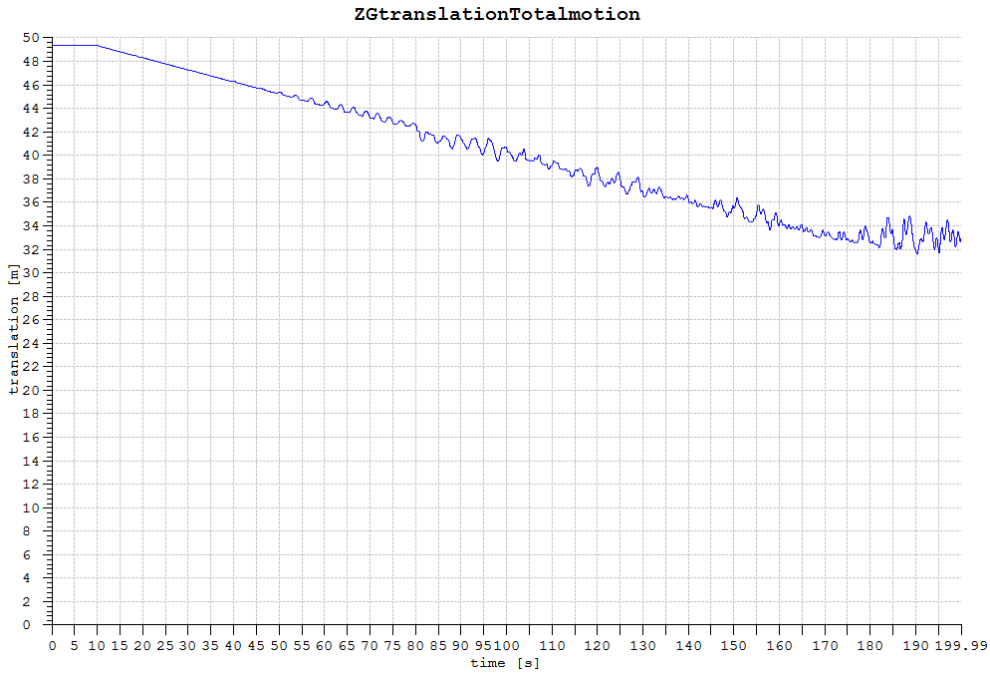

Figure 7.41 Global Position of the Hook, X-axis.
(max= 49.33, min= 31.57, mean= 40.41, dev= 5.491)

The disturbance of the vertical motion of the hook is much smaller than that of the crane master or the template. However, both of transversal and horizontal drift of the hook is quite significant.

7.4.2 Analysis on Local Coupling Force

The hook is connected to the crane and the crane master, respectively with the lifting line and the “crane” wire. The analysis on the coupling force of the “crane” has been presented in section 7.3, so only the analysis of the force components of the lifting line is involved in this section.
The results of the analysis are all presented in the following figures.

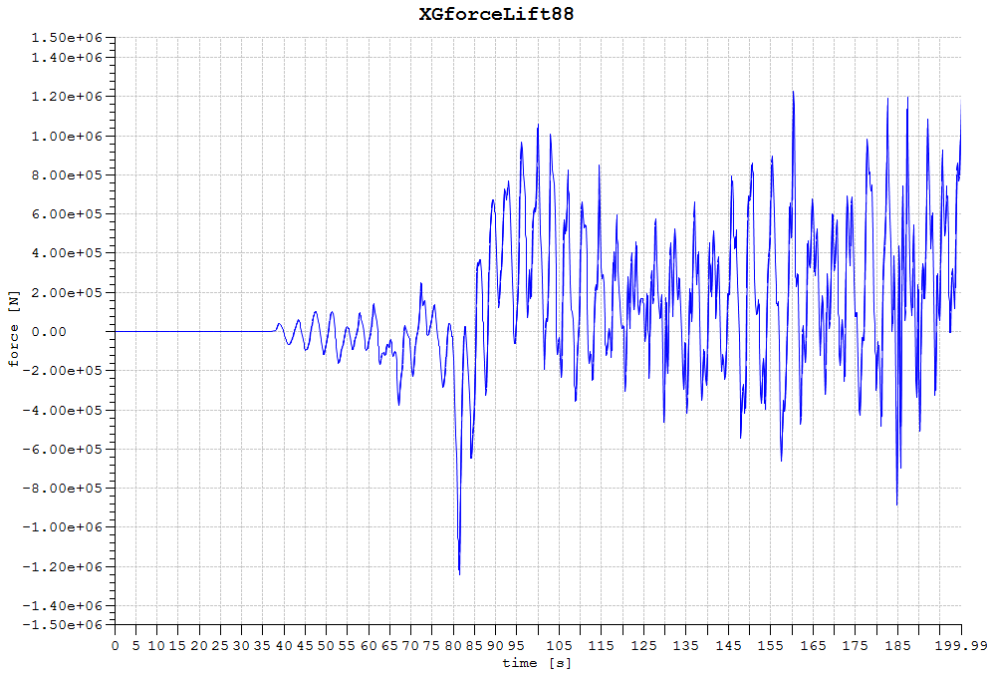

Figure 7.42 Local coupling force of the lifting line, X-axis (max=1.230e+06, min=-1.244e+06, mean=1.156e+05, dev=3.190e+05)

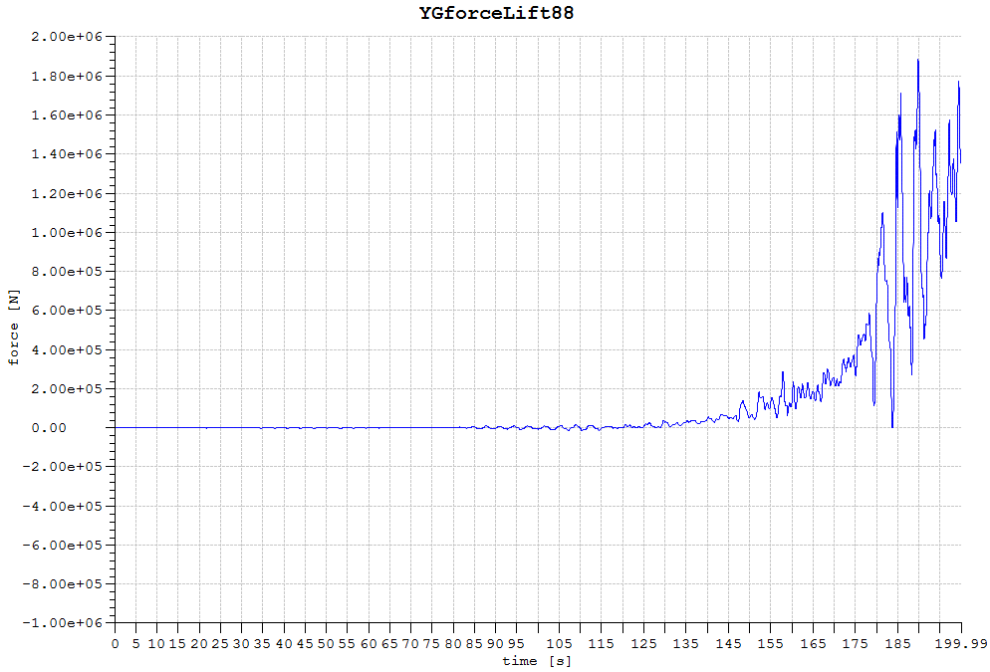

Figure 7.43 Local coupling force of the lifting line, Y-axis (max=1.888e+06, min=-1.507e+04, mean=1.392e+05, dev=3.300e+05)

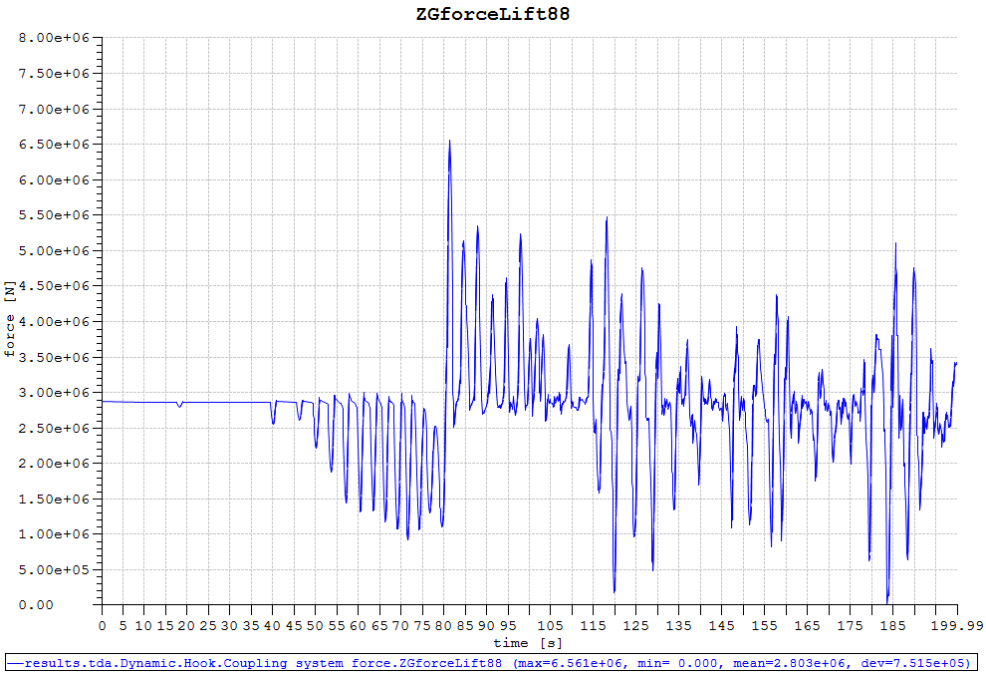

Figure 7.44 Local coupling force of the lifting line, Z-axis (max=6.561e+06, min= 0.000, mean=2.803e+06, dev=7.515e+05)

Most attention should be paid to the vertical component of the coupling force of the lifting line. The minimum force of the lifting line is zero, which is to say there is no compression in the wire during the whole operation. The maximum value is 6.561e+06(N), this can be used for selection of the lifting wires.

7.5 Analysis on the Global Position of the template under different sea-states

As discussed in section 7.2, the drift of the template in horizontal planes is sufficient large and this phenomenon may leads to potential danger to the lifting operation. So in this section a research concerning the dynamic performance of the template under different sea-states will take place.

State 1: Hs=4.5s&Tp=2.5s

State 2: Hs=4.5s&Tp=5s (This state has been discussed in section7.2)

State 3: Hs=4.5s&Tp=7.5s

Horizontal Motion

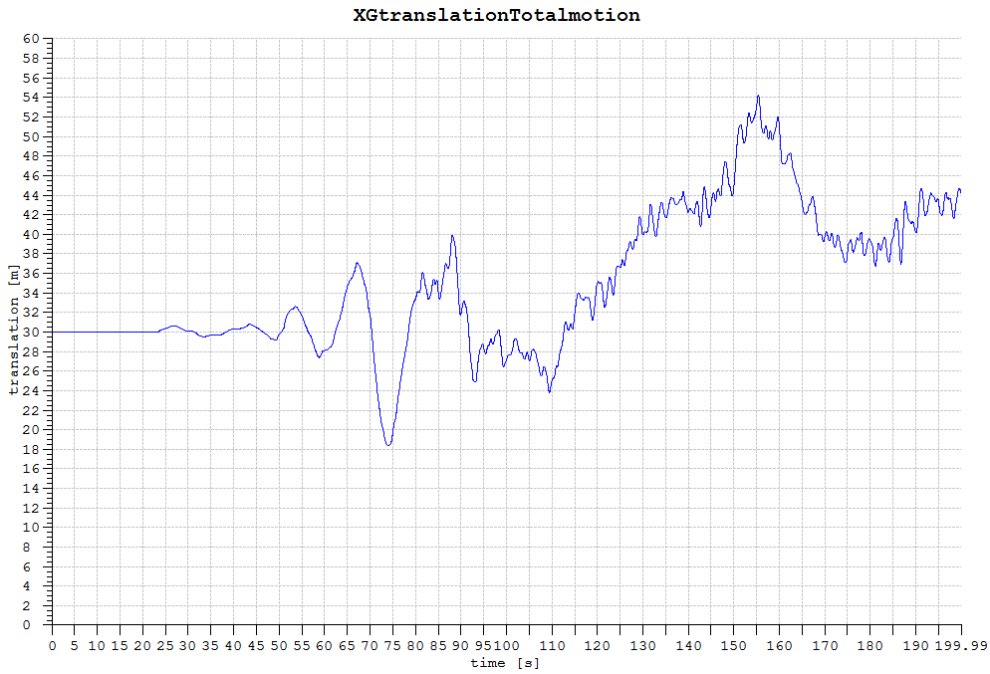

Figure 7.45 Horizontal displacement of the template, state 1 (max= 54.28, min= 18.38, mean= 35.02, dev= 7.160)

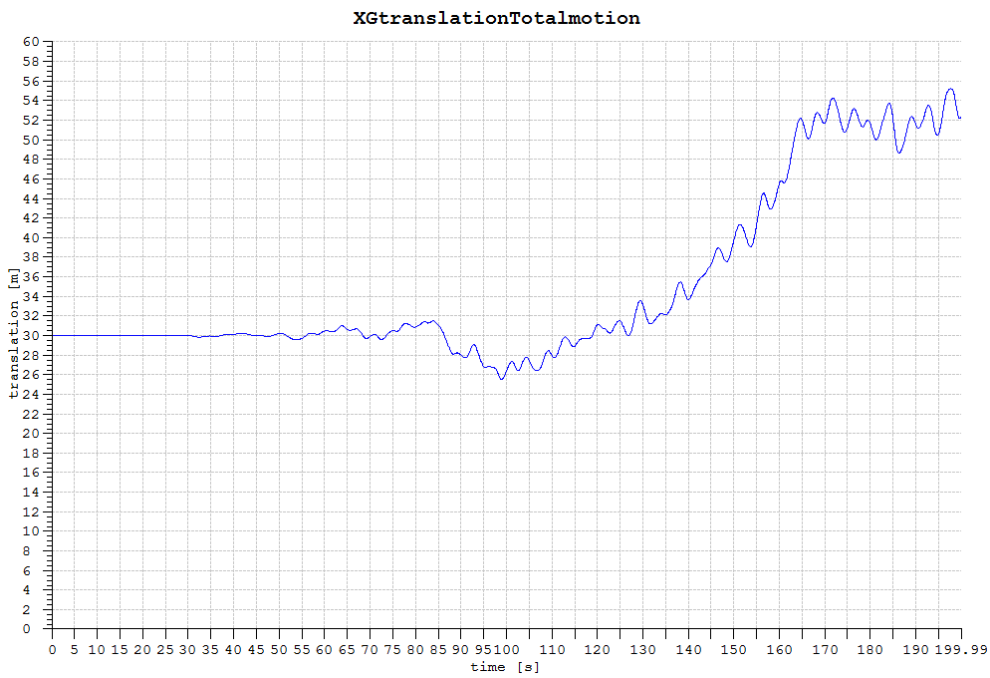

Figure 7.46 Horizontal displacement of the template, state 3 (max= 55.21, min= 25.51, mean= 35.21, dev= 8.844)

From the figures it is quite obvious that the template will experience a significant drift under each state. However, unlike state 2, the drift occurs in state 1 and state 3 trends to push the template to move away from the vessel, which will cause less risk or

danger to the lifting operation.

Transversal Motion

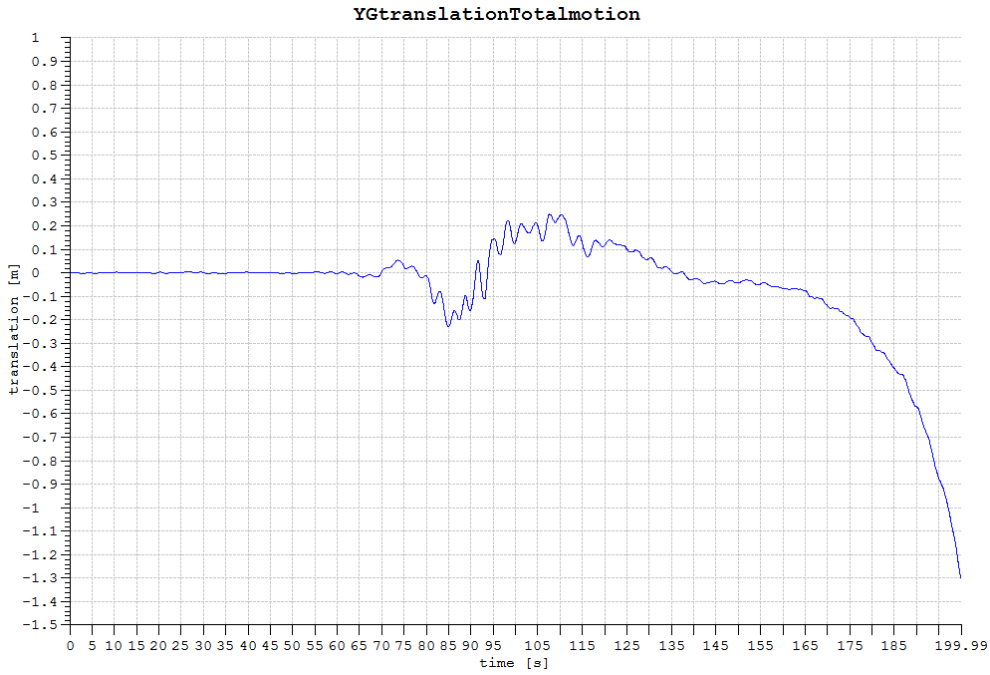

Figure 7.47 Transversal displacement of the template, state 1 (max=0.2500, min=-1.302, mean=-0.06401, dev=0.2322)

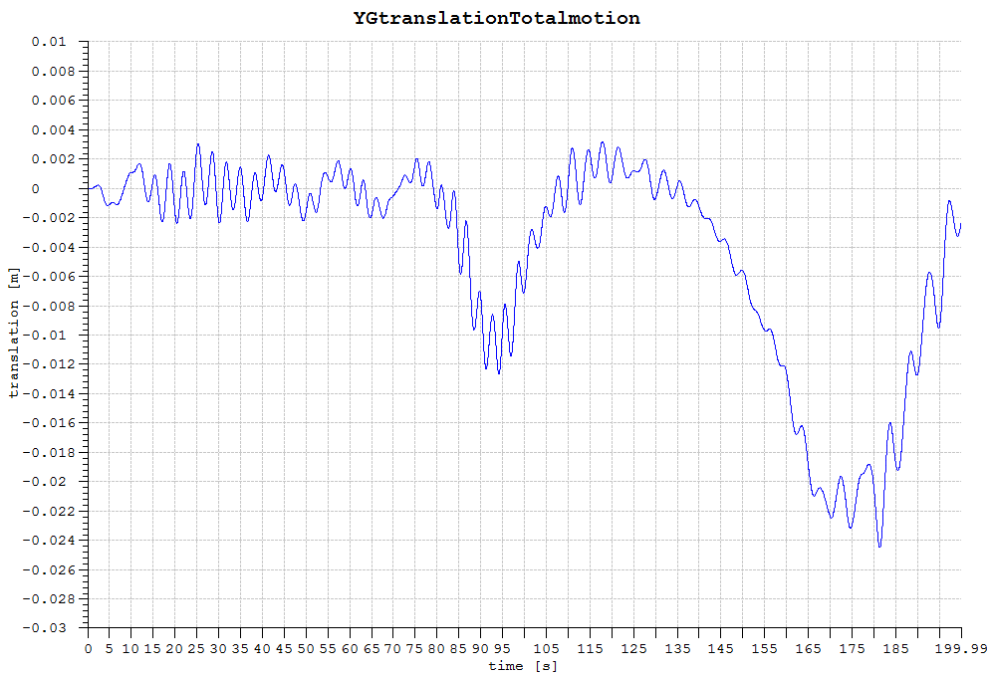

Figure 7.48 Transversal displacement of the template, state 3 (max=0.003209, min=-0.02449, mean=-0.004404, dev=0.007073)

The two figures illustrate that the maximum drift in Y-axis under state 1 and state 3 is below 2m, which is way smaller than that of state 2. Thus it is safer and more efficient

if the operation takes place under these two sea-states.

Combining the finding of this section with the former ones, it comes to the conclusion that the environmental conditions (it particularly refers to the wave states in this thesis) have significant influences on the lifting operation. Both of the wave height and the wave peak period will leave influences on the lifting structure. To sum up, the lifting operation should take place under a certain limiting wave height(4.5m) and the operation need to be paused when the wave peak period is approaching a certain value(5s).

8 Conclusion

The purpose of this thesis is to study the dynamic response of the template during the lowing operation through a splash-zone. The construction of a common lifting system is performed in the SIMA program in this thesis. Additionally, the static and dynamic analysis of each component under an extreme sea-state as well as the comparison of the global displacement of the template under different sea-states is presented. Based on this study, a more understanding of the dynamic performance of the lifting operation is obtained, therefore it will help shorten the operation time, improve the safety level as well as avoid the potential risk.

In order to carry out the dynamic analysis of the lifting system through the splash-zone, a parametric study is performed. The basic theories and guidelines involved in the lifting operation are introduced here and a lifting system is modeled in the SIMA program.

The simulation in SIMA shows some interesting results. First of all, the template experiences a significant drift in the wave induced direction for all sea-states, while the drift in the perpendicular direction can be eliminated by avoiding some certain sea-states. Secondary, the tension force in the lines under dynamic analysis can increase up to more than 2 times than that under the static analysis, which bring in a big challenge to ultimate stress of the lifting wires. There is no compression in the lifting wires during the analysis currently. However, there exist several points where the tension force trends to be 0, which leads to a critical situation where the lifting wires may experience compression if the wave height exceeds the critical value.
In addition, the vertical motion of the template is extremely strong, and may lead to potential risk. Thus, the operation should be paused once the wave peak period is approving the natural period of the template.

8.1 Recommendation for further work

This thesis has done a comprehensive analysis on the dynamic performance of the template during the lifting operation. However, due to some objective reasons, there are still a lot of problems and tasks remain unsolved. Therefore, there are still different kinds of work and new tasks can be added into this topic.

1. The Jack-up rig is finally applied in the analysis. However, in real situations, most of the lifting operations are carried out by crane vessels. So the first recommendation will be to replace the Jack-up rig with the crane vessel in SIMA program.
2. The template witnesses a significant drift, this might be caused by the wave drift force, which is not discussed in this thesis. Thus, in further work the wave drift force on the template can be introduced, especially the second-order forces.
3. Due to the lack of time and space, there isn't too much comparison among the dynamic results of different sea-states. So comparing the dynamic response of the template under more sea-states is strongly recommended.
4. Finally, there are many simplified and idealized assumptions in the modeling work. Therefore, to improve the modeling method for the template in SIMA can be also added in the future research.

Reference

[1] Finn Gunnar Nielsen: *Lecture Notes in Marine Operation*. Department of Marine Hydrodynamics, Faculty of Marine Technology, Norwegian University of Science and Technology, Trondheim/Bergen, January 2007, page 6-8, 126-135.
[2] P.O. Brinkmann, G.W. Barbier, and W. Rondriguez: *Design and Installation of a 20-Slot Template in the Gulf of Mexico in 760 ft of Water.* SPE Drilling Engineering, Volume 2, Number 2, June 1987, page 99-102.
[3] Tore Jacobsena, Bernt J. Leirab: *Numerical and experimental studies of submerged towing of a subsea template.* Ocean Engineering, Vol. 38, ISS. 1, January 2011, page 147-154.
[4] DetNorske Veritas (DNV): *Modeling and Analysis of Marine Operations*. Recommended Practice, DNV-RP-H103, April 2009.
[5] Dag Myrhaug/W.Lian: *Marine Dynamics, Lecture notes*. Department of Marine Technology-The Norwegian University of Science and Technology, Trondheim, 2009, page 11-21.
[6] Det Norske Veritas (DNV): *Environmental Conditions and Environmental Loads.* Recommended Practice, DNV-RP-C205, October 2010
[7] Larsen, C., M: *Lecture note for Special topic: Dynamic analysis of marine structures.* Department of marine technology, Norwegian University of Science and Technology, September 2005.
[8] Larsen, C., M: *TMR 4182Marine Dynamics.* Marine technology center, Department of Marine Technology, Trondheim, Norway, January 2012, page 14-19.
[10] Dag Myrhaug/W.Lian: *Marine Dynamics, Lecture notes*. Department of Marine Technology-The Norwegian University of Science and Technology, Trondheim, 2009, page 11-21.
[9] Min Wu: *Riser Angle Assessment*. Project Thesis, department of Marine Technology-The Norwegian University of Science and Technology, Trondheim, Norway, December 2012.
[10] Fossen T., I: *Marine Control Systems. Guidance, Navigation, and Control of Ships, Rigs and Underwater Vehicles.* Department of marine cybernetics – Norwegian University of Science and Technology, Trondheim, Norway, 2002
[11] MARINTEK: *SIMO-Theory Manual Version 4.0 rev.0.* Norwegian Marine Technology Research Institution, Trondheim, Norway, December 2012.
[12] Larsen, C., M: Dynamisk analyse av konstruksjoner. SINTEF, Department of constructions.

Appendix A

1. Summary of calculation options

Two parameters are used to define different calculation options:

IVOL = 0: Gravity force and buoyancy force are omitted
= 1: Gravity force and buoyancy force are included

IFOADD = 1: Forces integrated to wave surface: Z = ζ
= 0: Forces integrated to still water level: Z = 0

A summary of the different force components and how they are integrated, are given in the table below.

Force Component	IFOADD	
	1	0
Inertia: $F = (m + m_h)\ddot{x}$	a to z = ζ	a to z = ζ
Froude-Krylov: $F = (\rho V + m_h)\ddot{\xi}$ longitudinal transverse	a,V to $z = 0$ a,V to z = ζ	a,V to $z = 0$ a,V to z = ζ
Slamming: $F = v_r \, {dm_h}/{dt}$	a to z = ζ	a to z = ζ
Drag: $F = C_l v_r + C_q \lvert v_r \rvert v_r$	C_l, C_q to z = ζ	C_l, C_q to z = ζ
Froude-Krylov adjustment: $F = \rho g V$	V; z = 0 to ζ	V; z = 0 to ζ
Buoyancy: $F = \rho g V$	V to z = 0	V to z = 0

2. The comparison of the dynamic performance of the template under different water depth

Water Depth 400m

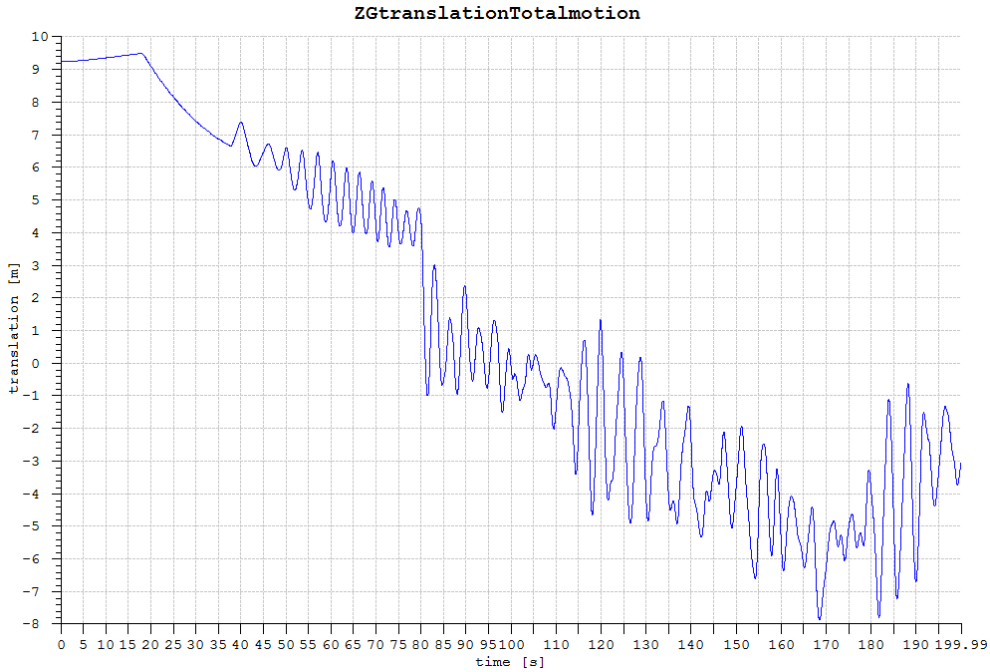

Global displacement of the template, Z-axis
(max= 9.489, min=-7.883, mean= 1.148, dev= 5.183)

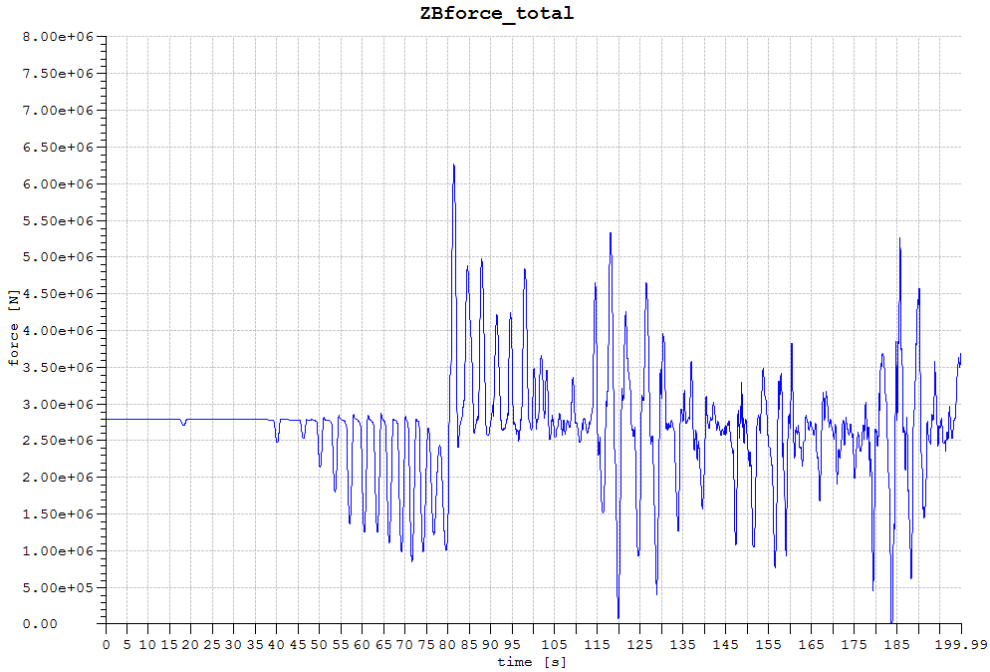

Total coupling force on the template, Z-axis
(max=6.278e+06, min= 0.000, mean=2.677e+06, dev=7.214e+05)

Water Depth 200m

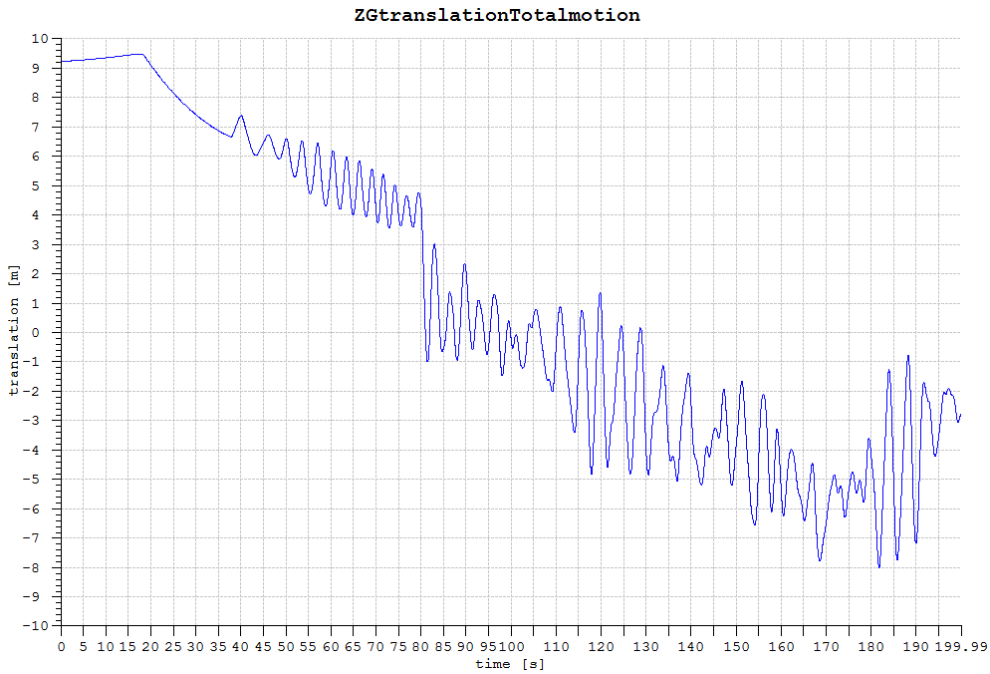

Global displacement of the template, Z-axis

(max= 9.489, min=-8.016, mean= 1.130, dev= 5.211)

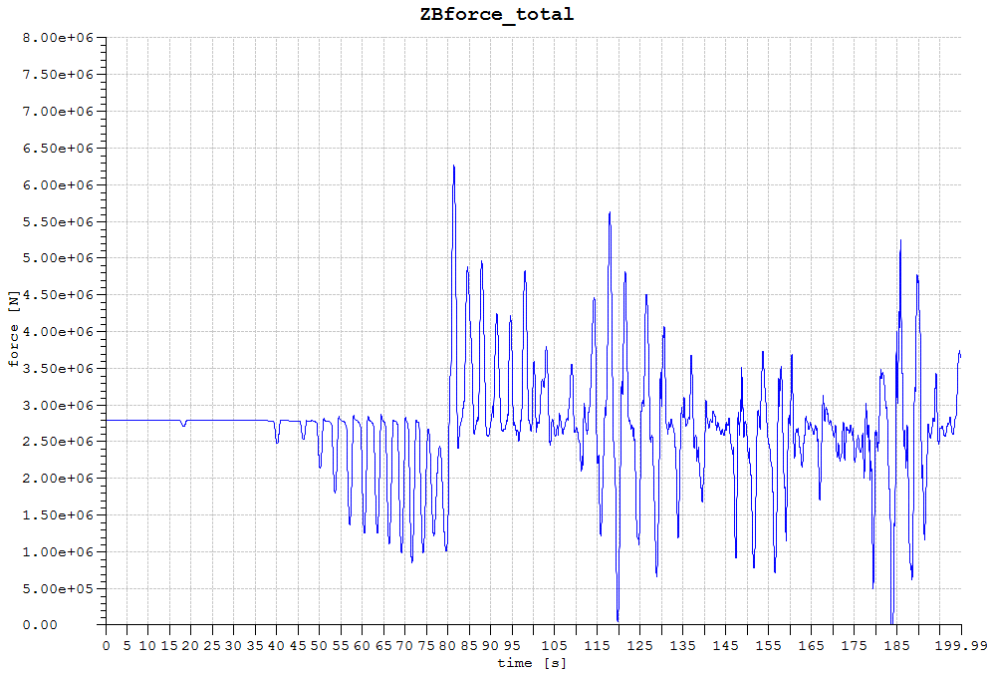

Total coupling force on the template, Z-axis
(max=6.278e+06, min= 0.000, mean=2.678e+06, dev=7.422e+05)

3. Dynamic result of the Hook in SIMA

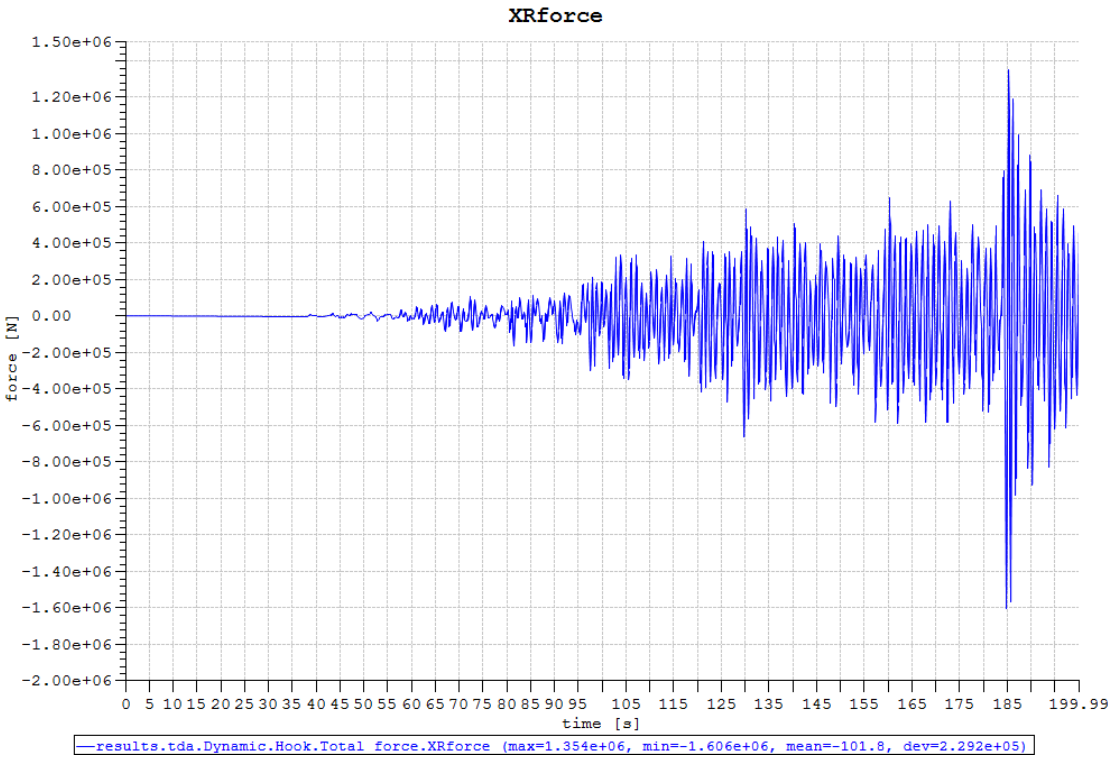

Total force of the Hook, X-axis

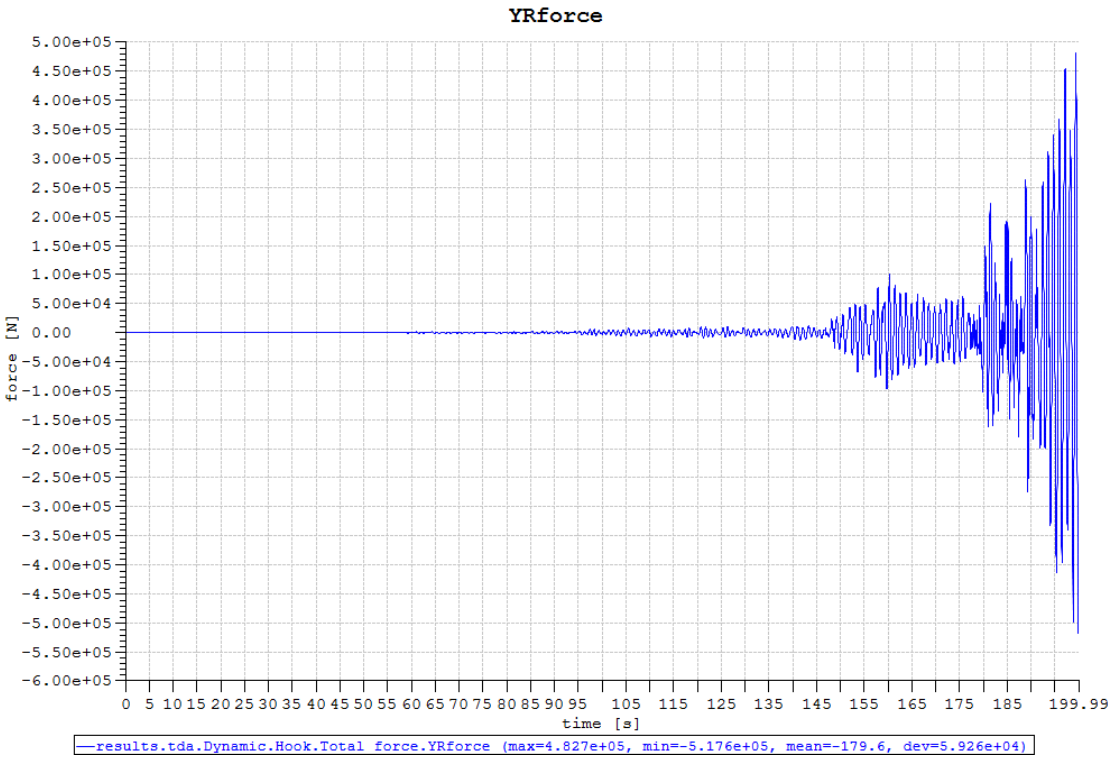

Total force of the Hook, Y-axis

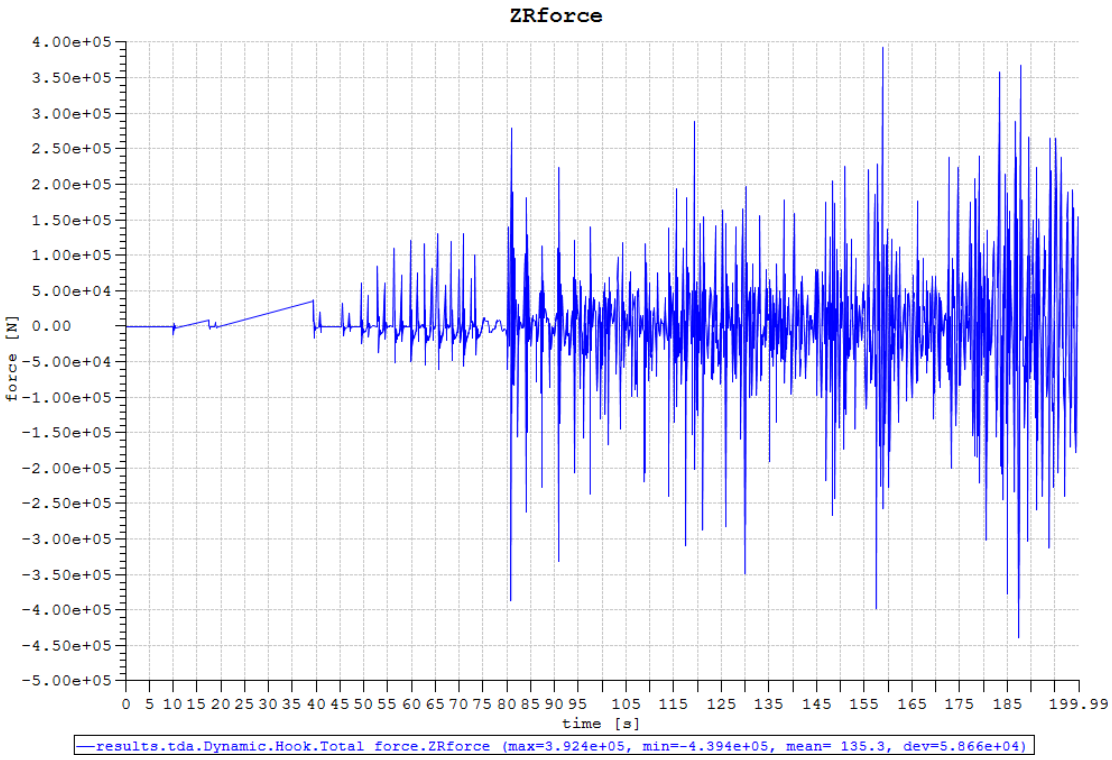

Total force of the Hook, Z-axis

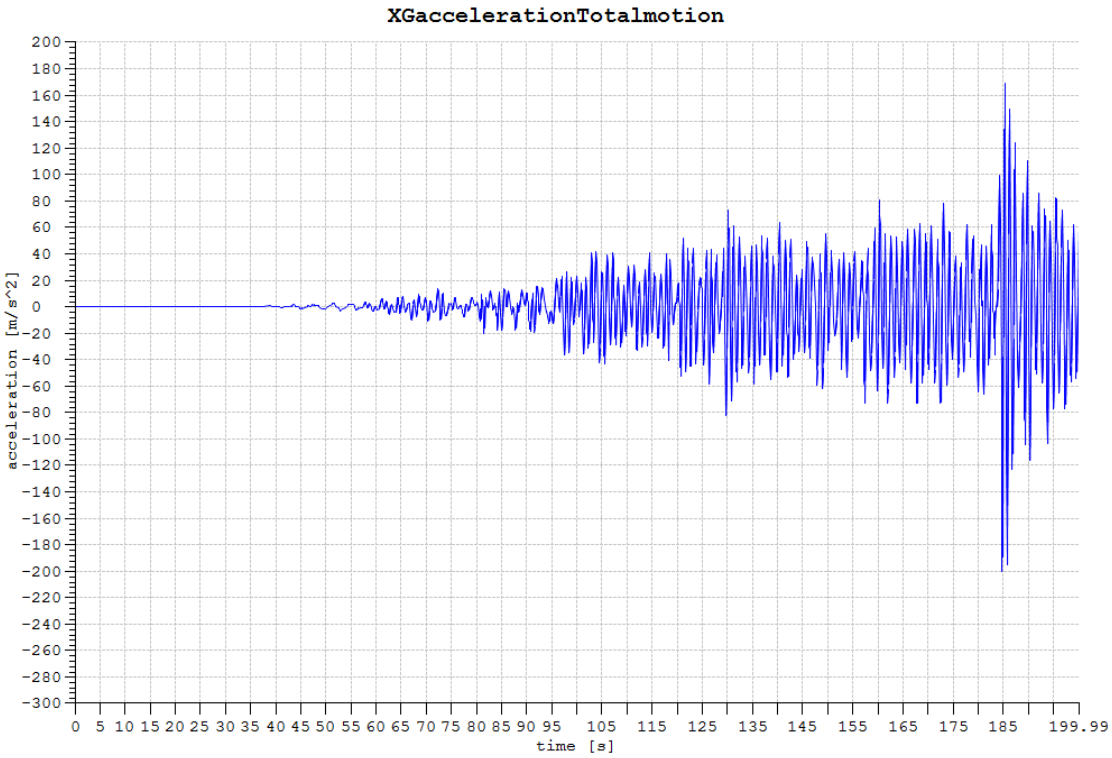

Global acceleration of the Hook, X-axis

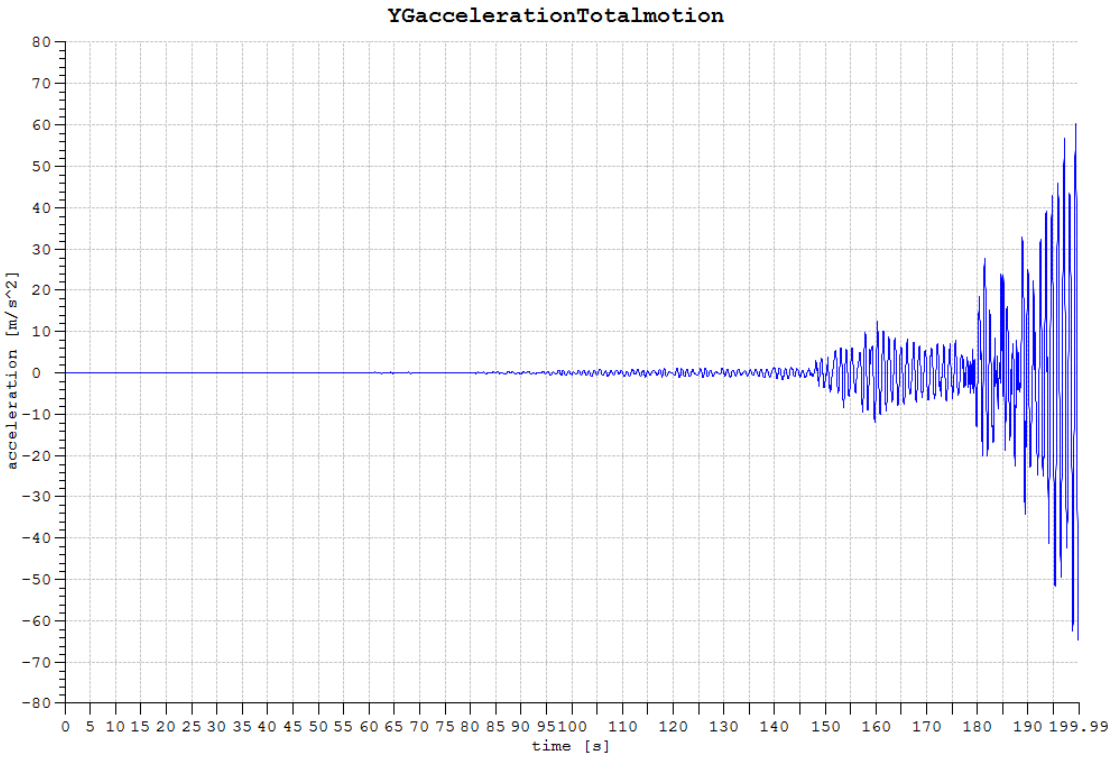

Global acceleration of the Hook, Y-axis

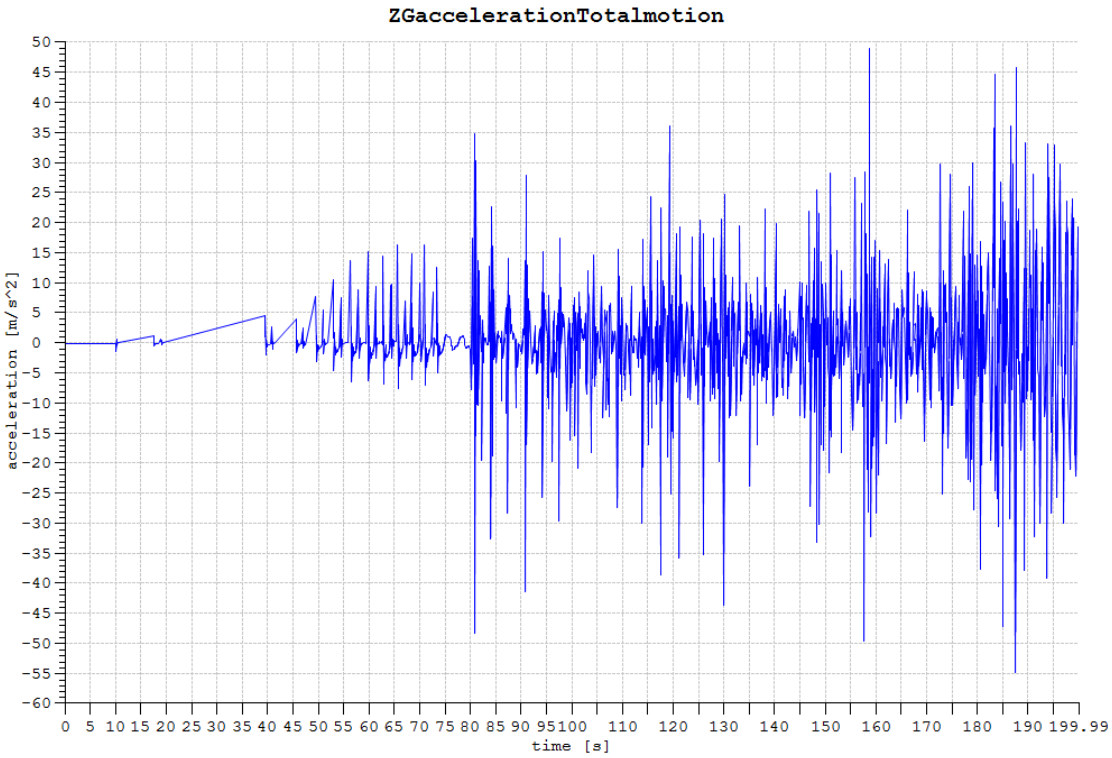

Global acceleration of the Hook, Z-axis

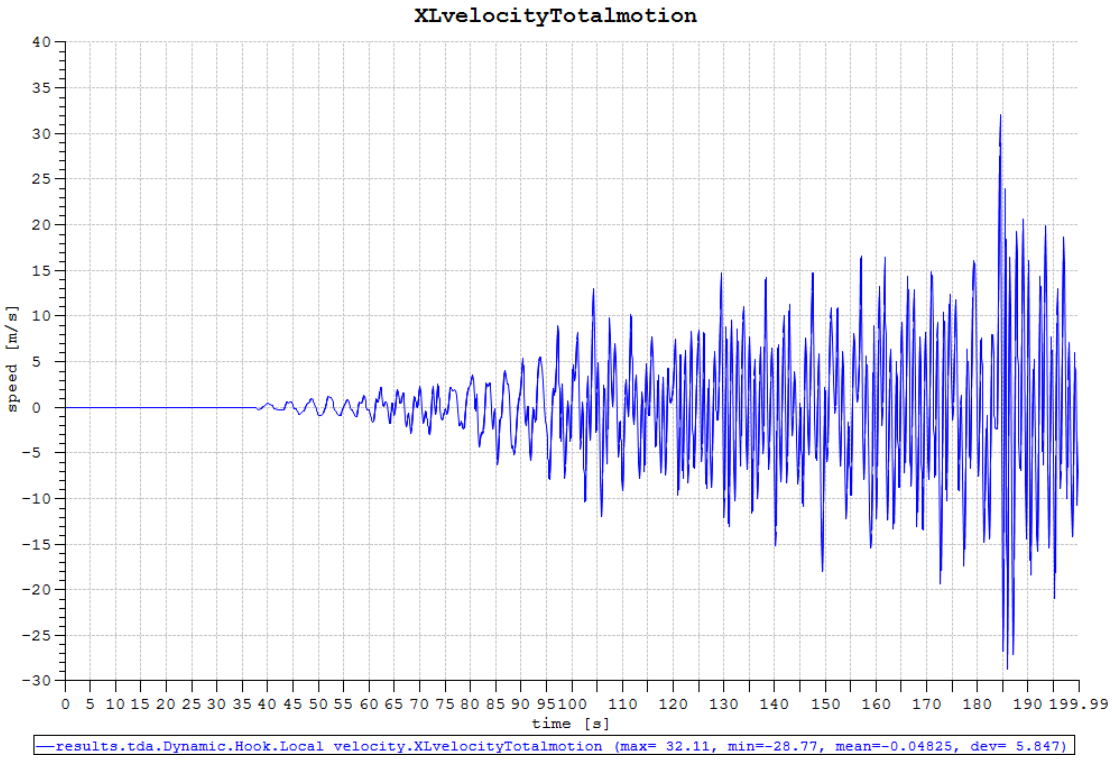

Local velocity of the Hook, X-axis

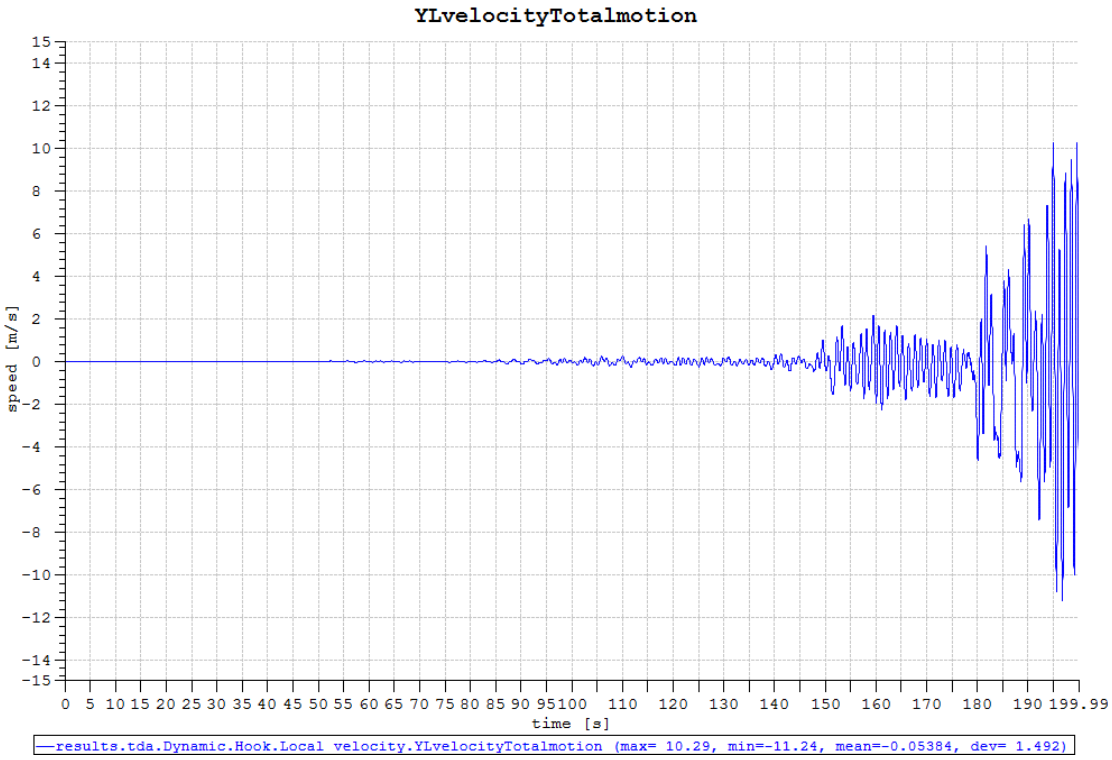

Local velocity of the Hook, Y-axis

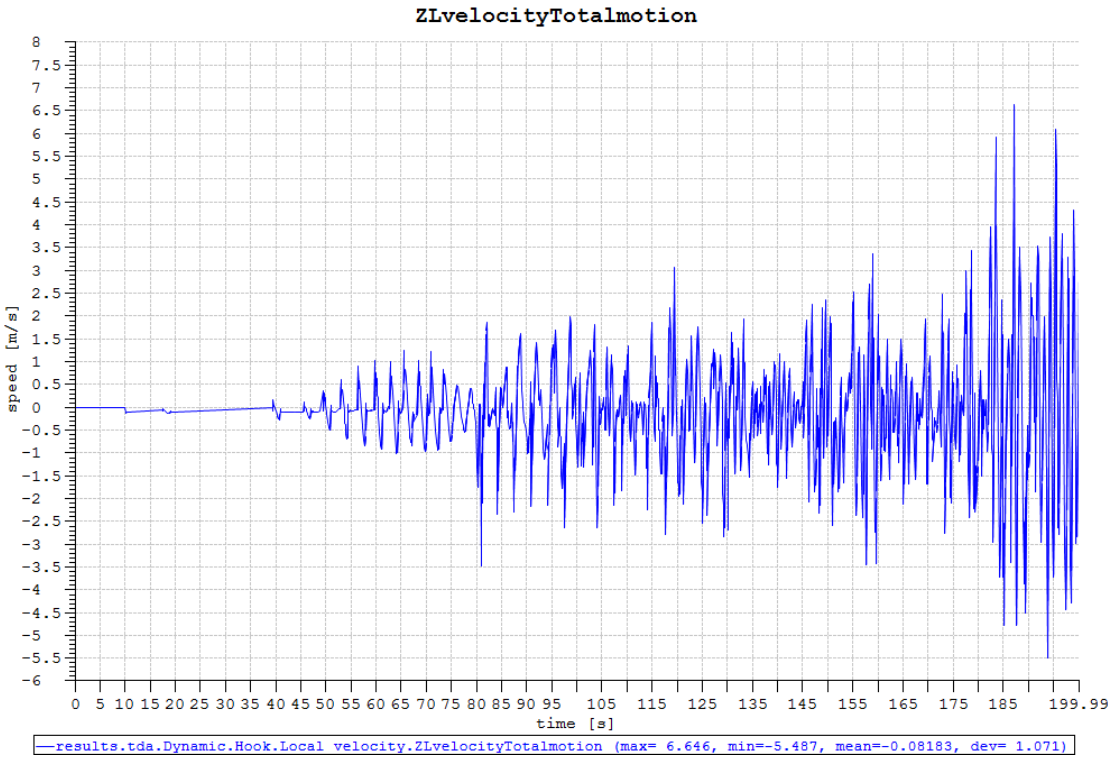

Local velocity of the Hook, Z-axis

4. Dynamic result of the Crane Master in SIMA

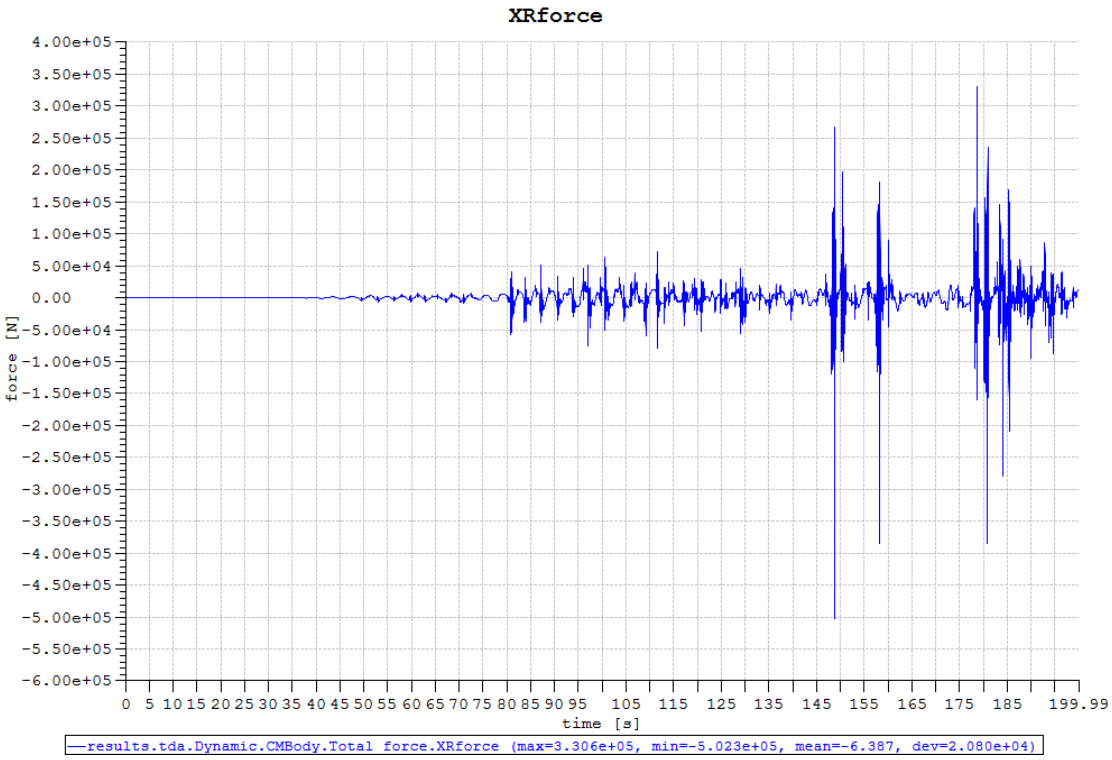

Total force of the Crane Master, X-axis

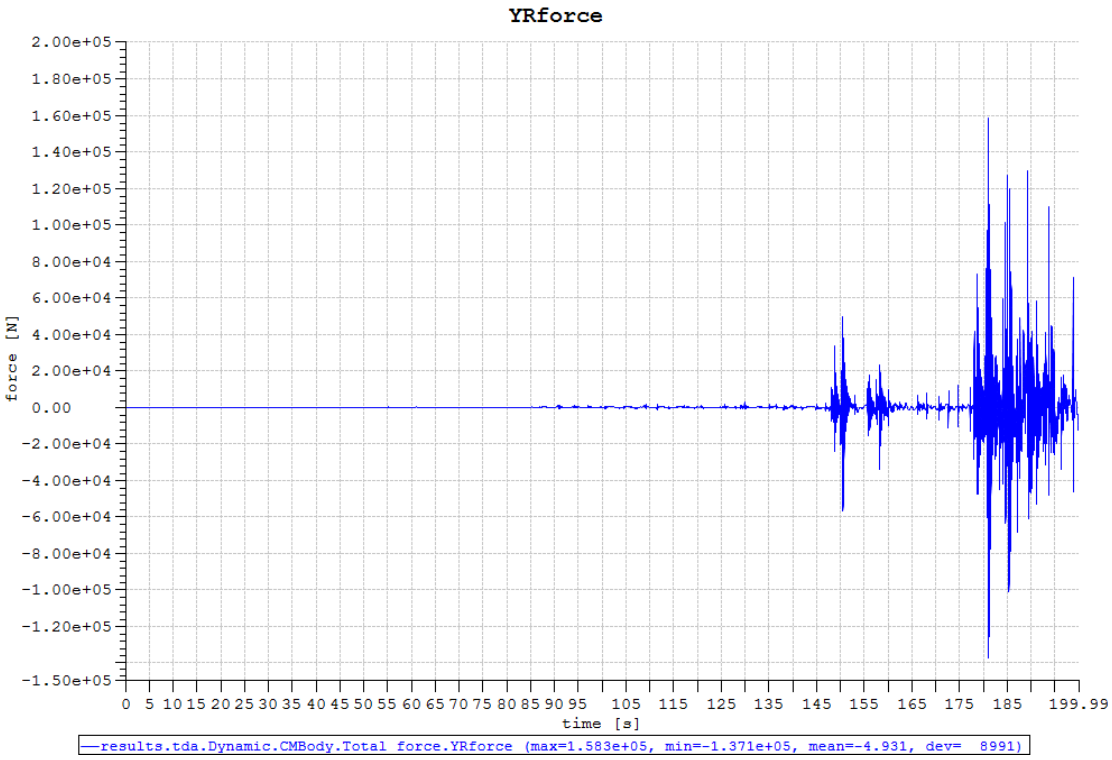

Total force of the Crane Master, Y-axis

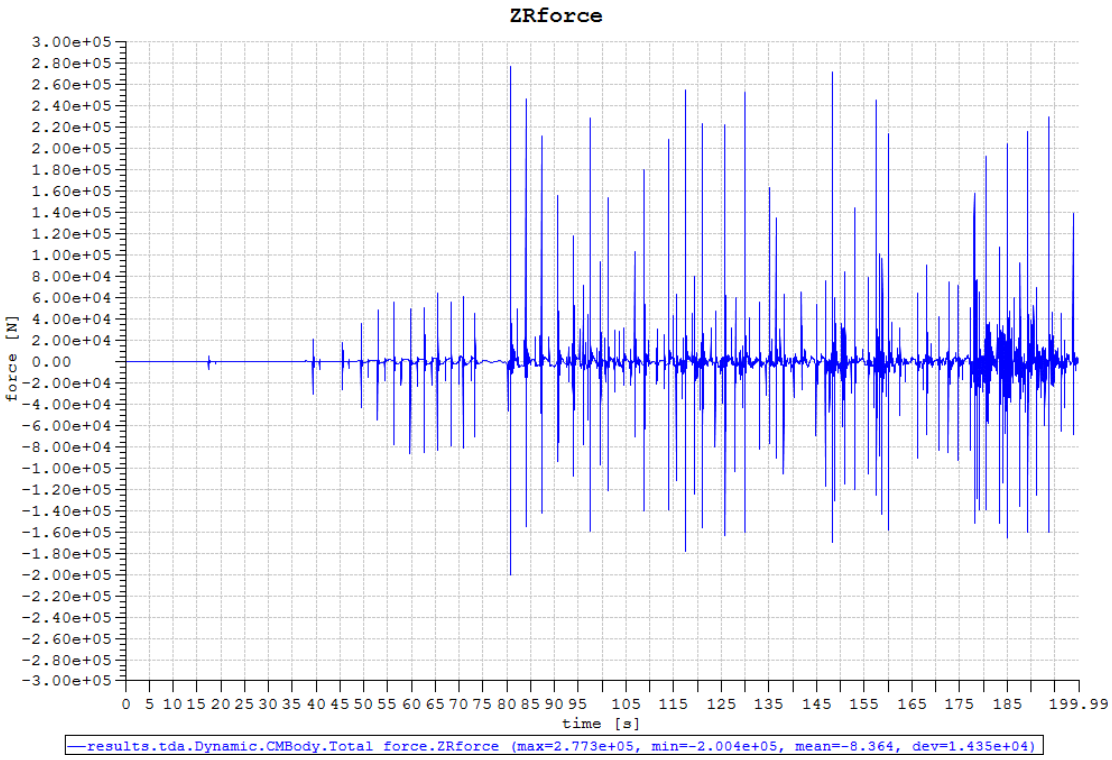

Total force of the Crane Master, Z-axis

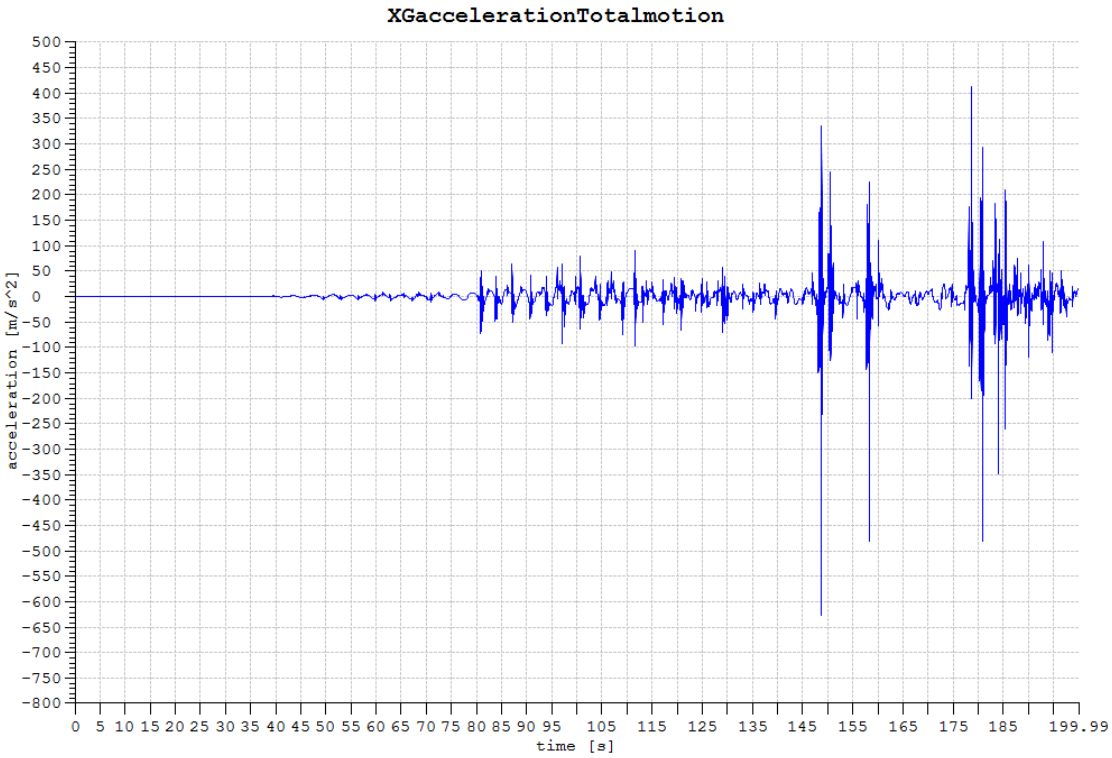

Global acceleration of the Crane Master, X-axis

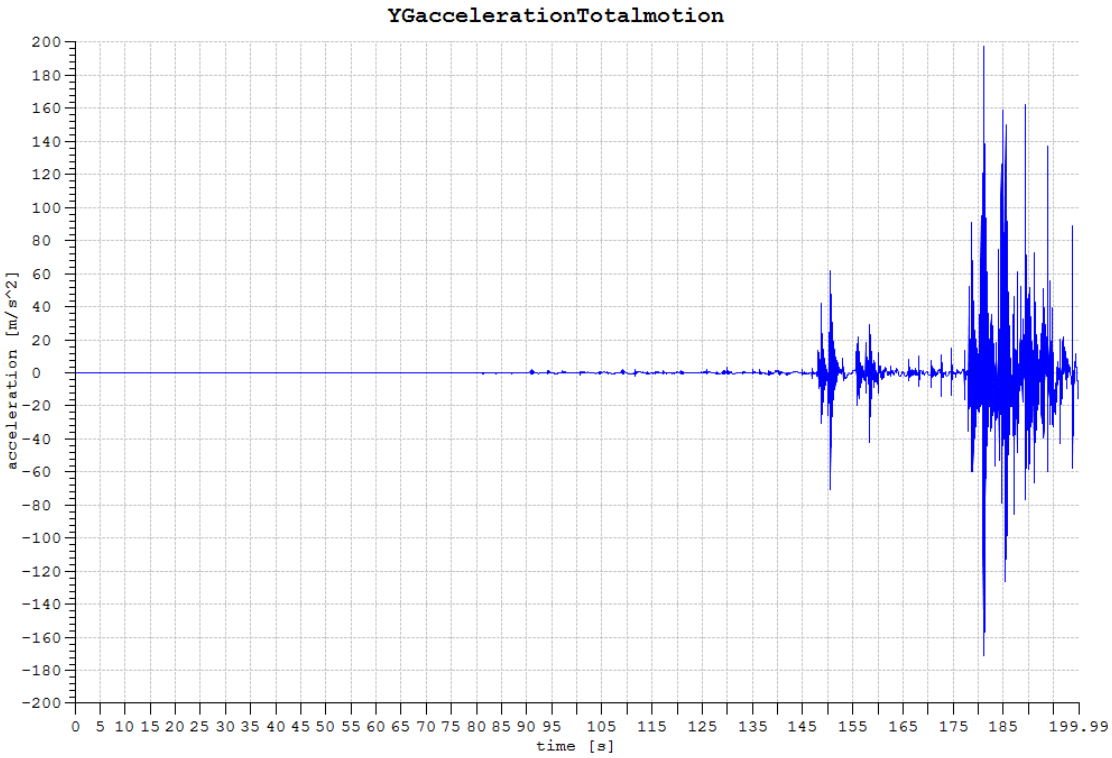

Global acceleration of the Crane Master, Y-axis

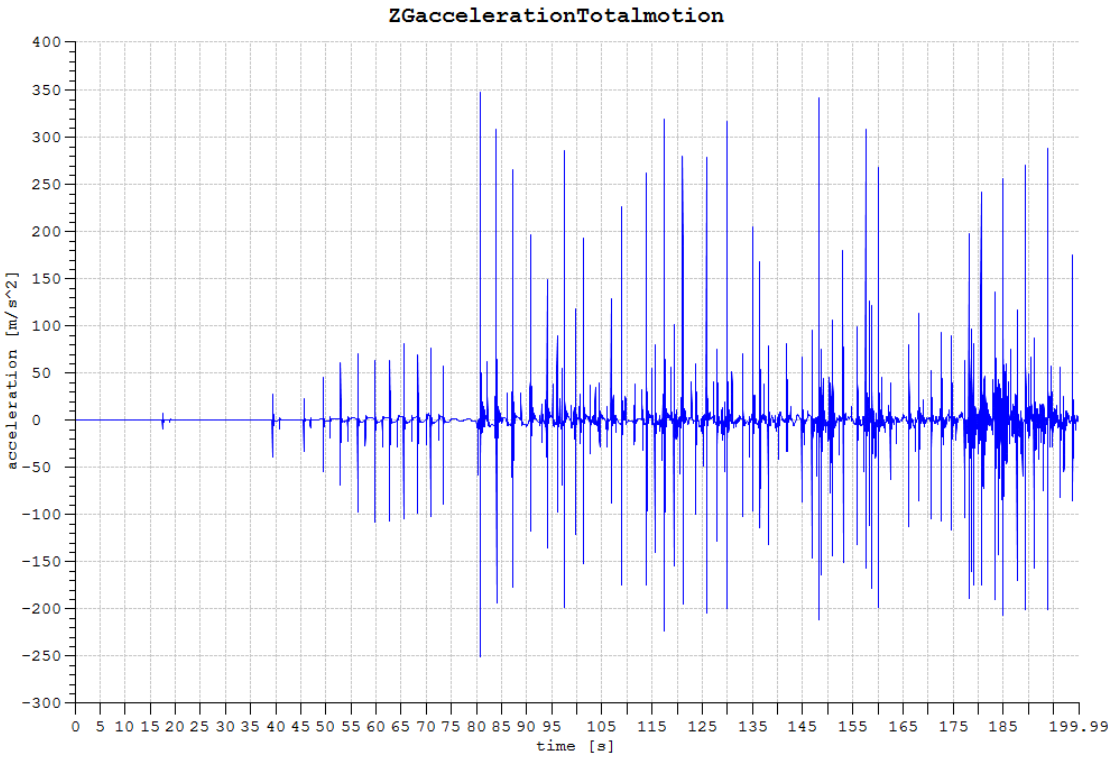

Global acceleration of the Crane Master, Z-axis

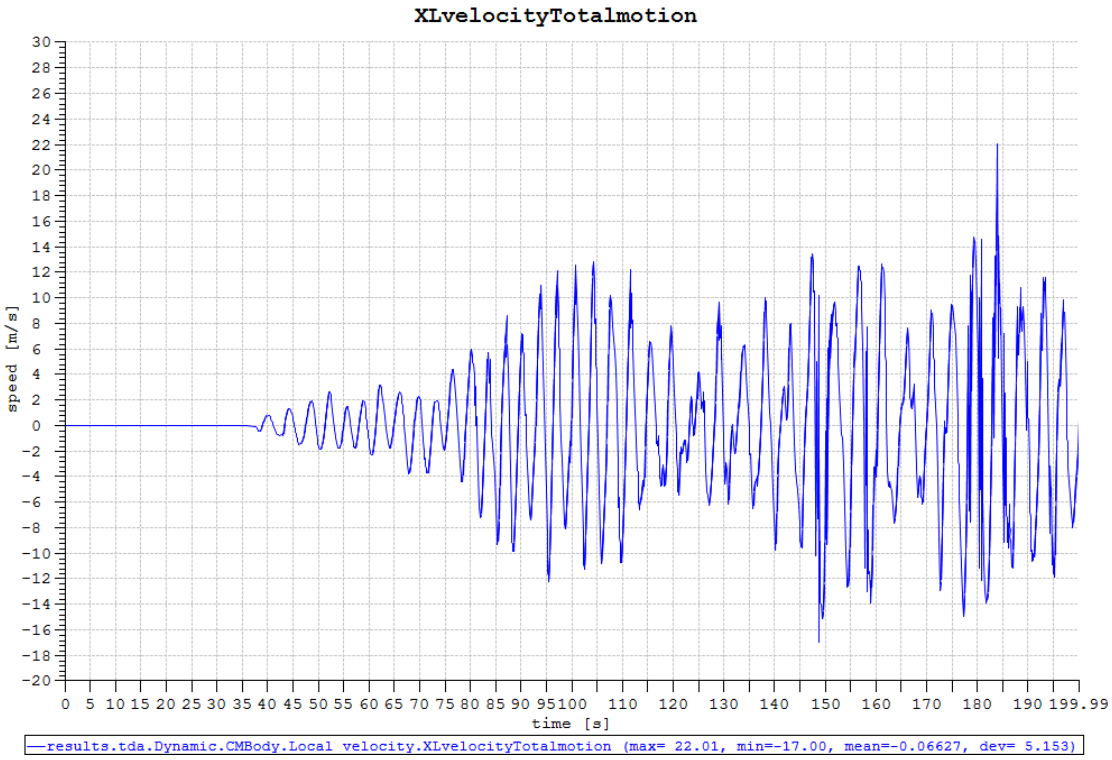

Local velocity of the Crane Master, X-axis

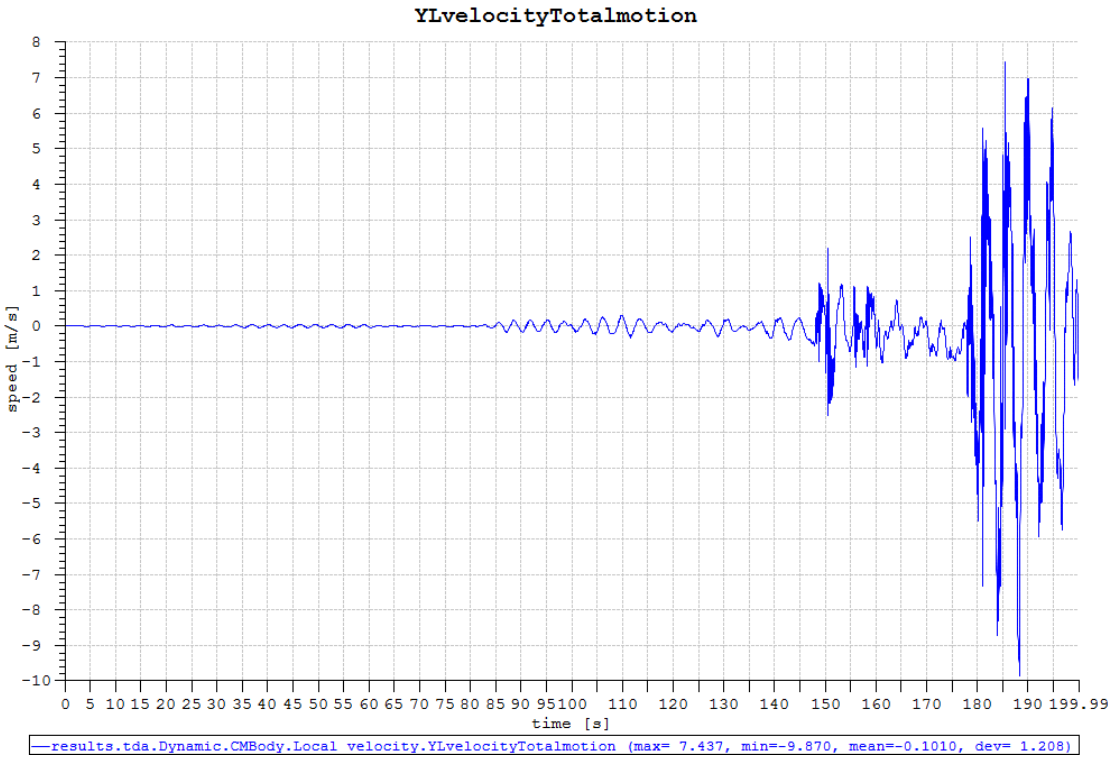

Local velocity of the Crane Master, Y-axis

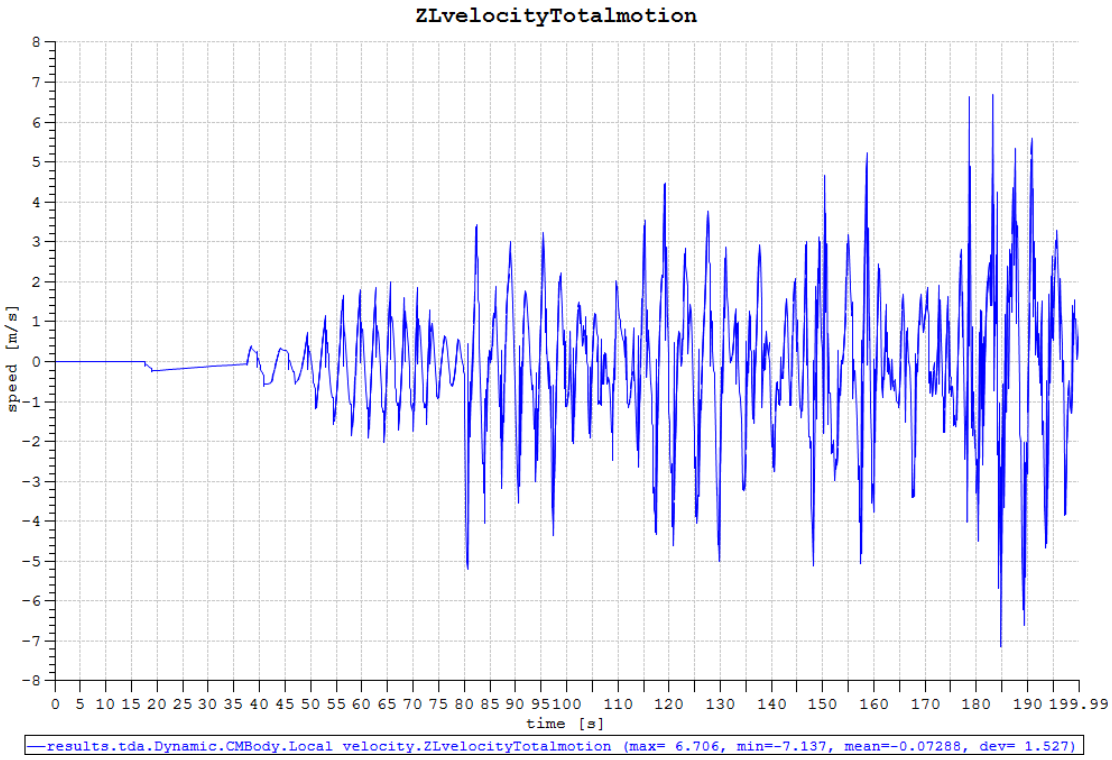

Local velocity of the Crane Master, Z-axis

Appendix B

Table B-1 Analytical added mass coefficient for two-dimensional bodies, i.e. long cylinders in infinite fluid (far from boundaries). Added mass (per unit length) is $A_{ij} = \rho C_A A_R$ [kg/m] where A_R [m2] is the reference area

Section through body	*Direction of motion*	C_A	A_R	*Added mass moment of inertia* [(kg/m)*m2]
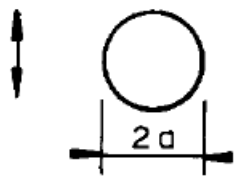		1.0	πa^2	0
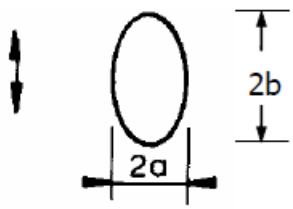	Vertical	1.0	πa^2	$\rho \frac{\pi}{8}(b^2 - a^2)^2$
	Horizontal	1.0	πb^2	
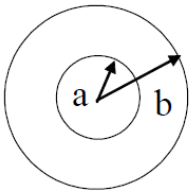 Cylinder within pipe		$\frac{b^2 + a^2}{b^2 - a^2}$	πa^2	
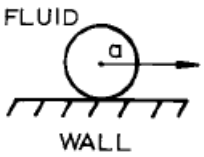	Horizontal	$\frac{\pi^2}{3} - 1$	πa^2	
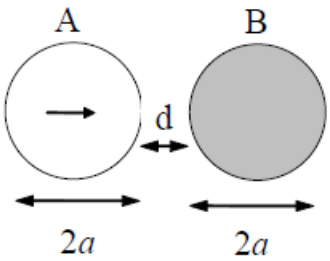 A moving B fixed	Horizontal	d/a = ∞ 1.000 d/a = 1.2 1.024 d/a = 0.8 1.044 d/a = 0.4 1.096 d/a = 0.2 1.160 d/a = 0.1 1.224	πa^2	

Table B-2 Analytical added mass coefficient for three-dimensional bodies in infinite fluid (far from boundaries). Added mass is Aij=ρ$C_A V_R$ [kg] where V_R [m3] is reference volume

Body shape		Direction of motion	C_A		V_R
			b/2a	C_A	
Right circular cylinder	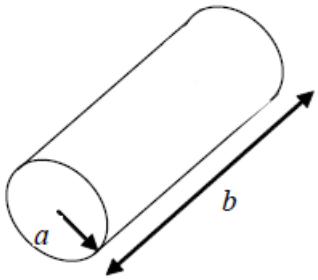	Vertical	1.2 2.5 5.0 9.0 ∞	0.62 0.78 0.90 0.96 1.00	$\pi a^2 b$

Appendix C

Table C-1 Drag coefficient on three-dimensional objects for steady flow CDS. Drag force is defined as $F_D = \frac{1}{2}\rho C_{DS} S u^2$. S = projected area normal to flow direction [m2]. Re = uD/ν = Reynolds number where D = characteristic dimension.

Geometry	Dimensions	C_{DS}	
Rectangular plate normal to flow direction 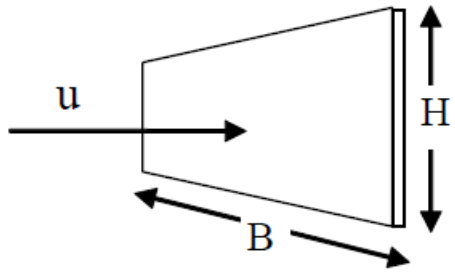	B/H 1 5 10 ∞	1.16 1.20 1.50 1.90 $R_e > 10^3$	
Circular cylinder. Axis parallel to flow 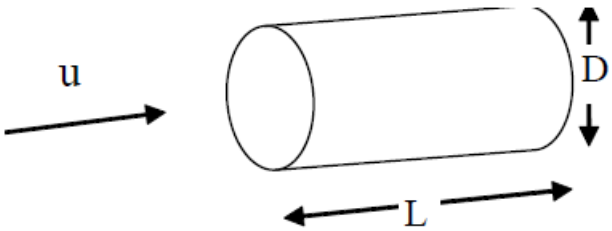	L/D 0 1 2 4 7	1.12 0.91 0.85 0.87 0.99 $R_e > 10^3$	
Circular cylinder normal to flow 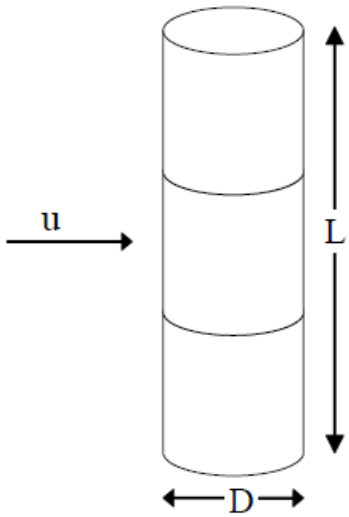	L/D	Sub critical flow $Re < 10^5$	Supercritical flow $R_e > 5 \cdot 10^5$
		κ	κ
	2	0.58	0.80
	5	0.62	0.80
	10	0.68	0.82
	20	0.74	0.90
	40	0.82	0.98
	50	0.87	0.99
	100	0.98	1.00
	$C_{DS} = \kappa C_{DS}^{\infty}$ κ is the reduction factor due to finite length. C_{DS}^{∞} is the 2D steady drag coefficient.		